**Stretto di Messina**

Concessionaria per la progettazione, realizzazione e gestione del collegamento stabile tra la Sicilia e il Continente Organismo di Diritto Pubblico
(Legge n° 1158 del 17 dicembre 1971, modificata dal D.Lgs. n°114 del 24 aprile 2003)

EurolinK

# PONTE SULLO STRETTO DI MESSINA

# PROGETTO DEFINITIVO

## EUROLINK S.C.p.A.

IMPREGILO S.p.A. (MANDATARIA)
SOCIETÀ ITALIANA PER CONDOTTE D'ACQUA S.p.A. (MANDANTE)
COOPERATIVA MURATORI E CEMENTISTI - C.M.C. DI RAVENNA SOC. COOP. A.R.L. (MANDANTE)
SACYR S.A.U. (MANDANTE)
ISHIKAWAJIMA - HARIMA HEAVY INDUSTRIES CO. LTD (MANDANTE)
A.C.I. S.C.P.A. - CONSORZIO STABILE (MANDANTE)

| IL PROGETTISTA | IL CONTRAENTE GENERALE | STRETTO DI MESSINA | STRETTO DI MESSINA |
|---|---|---|---|
| Ing E.M.Veje<br>COWI<br>EurolinK<br>Dott. Ing. E. Pagani<br>Ordine Ingegneri Milano<br>n° 15408 | Project Manager<br>(Ing. P.P. Marcheselli) | Direttore Generale e<br>RUP Validazione<br>(Ing. G. Fiammenghi) | Amministratore Delegato<br>(Dott. P. Ciucci) |

PS0079_F0

| | |
|---|---|
| *Unità Funzionale* | OPERA D'ATTRAVERSAMENTO |
| *Tipo di sistema* | SOVRASTRUTTURE |
| *Raggruppamento di opere/attività* | Impalcato |
| *Opera - tratto d'opera - parte d'opera* | Generale |
| *Titolo del documento* | Design Report - Local FE-models for Suspended Deck |

CODICE: C G 1 0 0 0 P C L D P S V I 3 0 0 0 0 0 0 0 0 0 3 F0

| REV | DATA | DESCRIZIONE | REDATTO | VERIFICATO | APPROVATO |
|---|---|---|---|---|---|
| F0 | 20-06-2011 | EMISSIONE FINALE | MLSA/AMOL/HEAE | JESO/HPO | HPO/LSJ |
| | | | | | |
| | | | | | |
| | | | | | |

NOME DEL FILE: PS0079_F0.docx

# INDICE

# 1 Introduction

## 1.1 Scope of Works

The local FE-models for suspended deck are performed in the computer program Robot Millennium 2010 an integrated graphic program used for modeling, analysing and designing various types of structures. A detailed description of the local FE-models can be found in the report "General Design Principles for Suspended Deck" including the boundary conditions, global- and local coordinate systems, geometry, supports, loads and load combinations. The boundary conditions applied on the local FE-models are taken from the global IBDAS model. The most critical load cases used in the local ROBOT FE-models are determined based on influence line plots from the global IBDAS model.

In total four different models have been developed for the verification of the suspended deck:

- **<u>Bridge deck local FE-model:</u>** Describing the cross girder and the longitudinal railway and roadway girders determining the stress level in the plate elements with special regards to stresses in the cross girder outer plates, diaphragms and at the intersection between girders. A plot of the bridge deck local FE-model is shown in Figure 1-1.

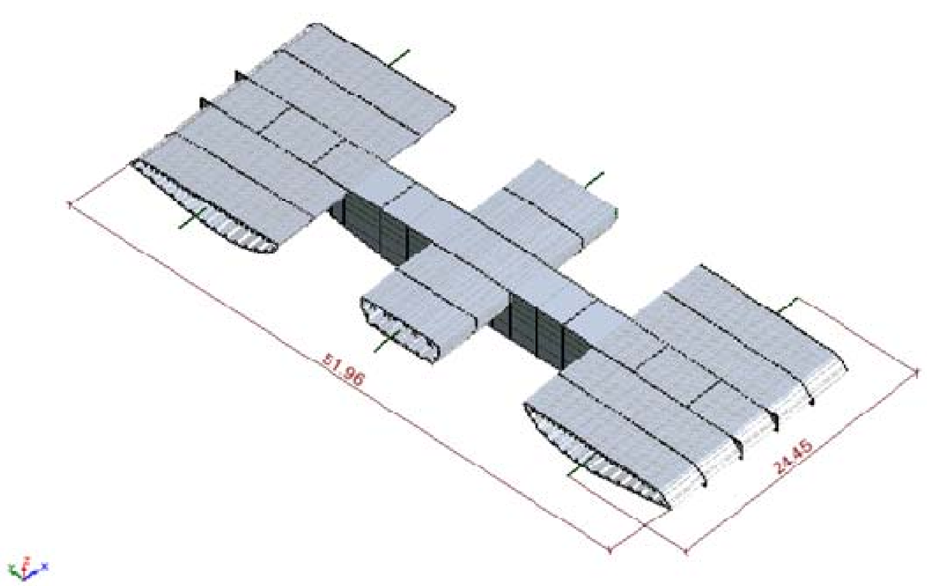


*Figure 1-1 Overall geometry of bridge deck FE-model*

- **Roadway local FE-model**: Describing the stress level in the diaphragm of the roadway girder with regards to the stress concentration at the troughs, cope holes, diaphragm stiffeners and openings and further more to determine von Mises stresses in skin plates including local loading effect from wheel loads. The longitudinal stresses from local loading effect are a result of the roadway troughs spanning between transverse diaphragms. The stresses are calculated for both the top plate and top plate stiffeners and both minimum and maximum stresses are considered. A plot of the bridge deck local FE-model is shown on Figure 1-2.

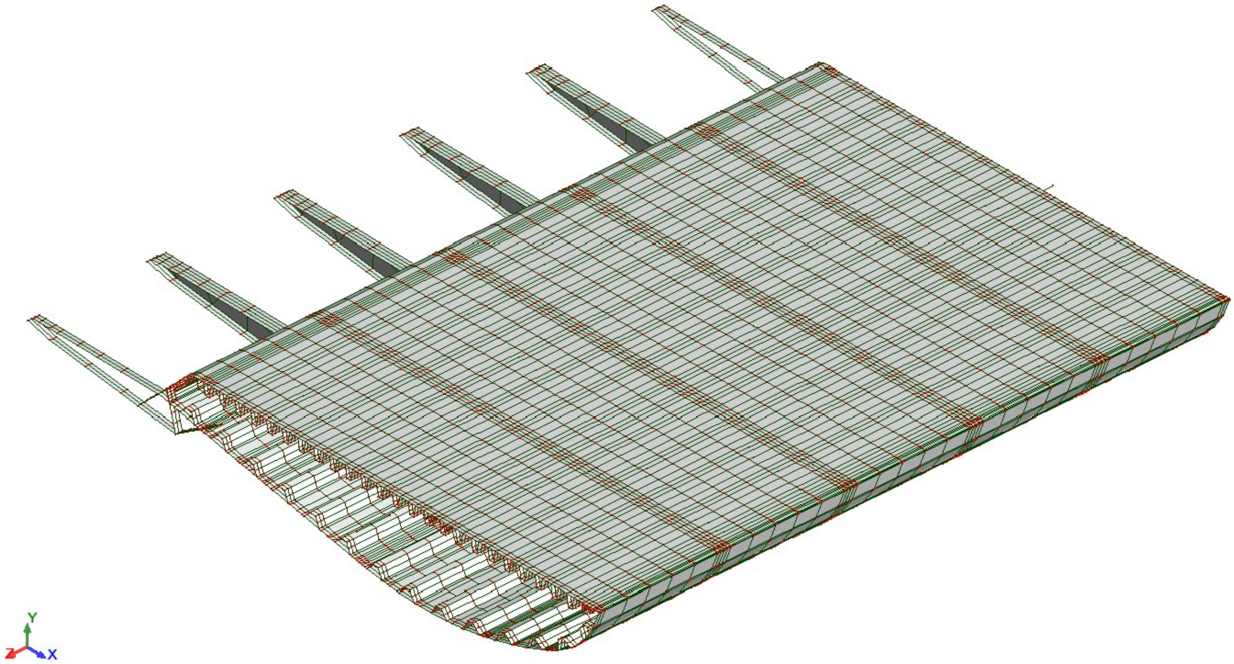


*Figure 1-2 Overall geometry of roadway girder FE-model*

**Railway local FE-model:** Describing the stress level in the diaphragm of the railway girder with regards to the stress concentration at the troughs, diaphragm stiffeners and openings and further more to determine von Mises stresses in skin plates and top plate stiffeners including local loading effect from wheel loads. In calculating stresses in the top plate and top plate stiffeners, both minimum and maximum stresses are considered. A plot of the bridge deck local FE-model is shown on Figure 1-3.

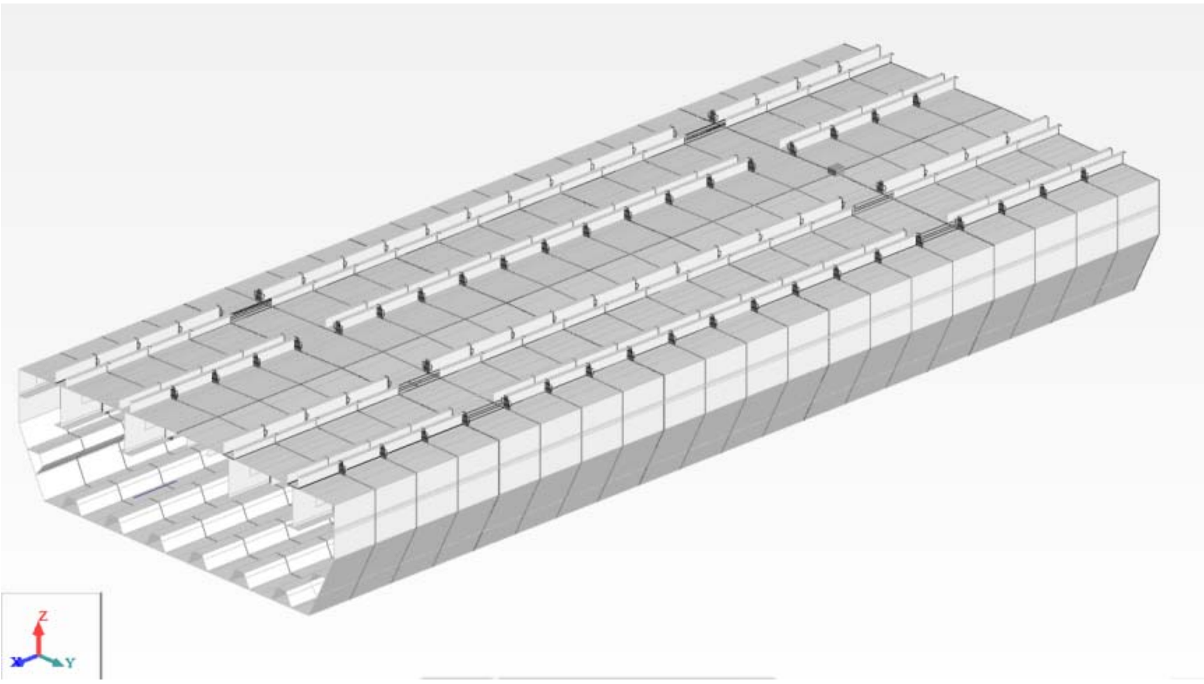

*Figure 1-3 Overall geometry of railway girder FE-model*

- **<u>Hanger anchorage local FE-model:</u>** Describing the stress level in the plates related to the hanger anchorages. A plot of the bridge deck local FE-model is shown on Figure 1-4.

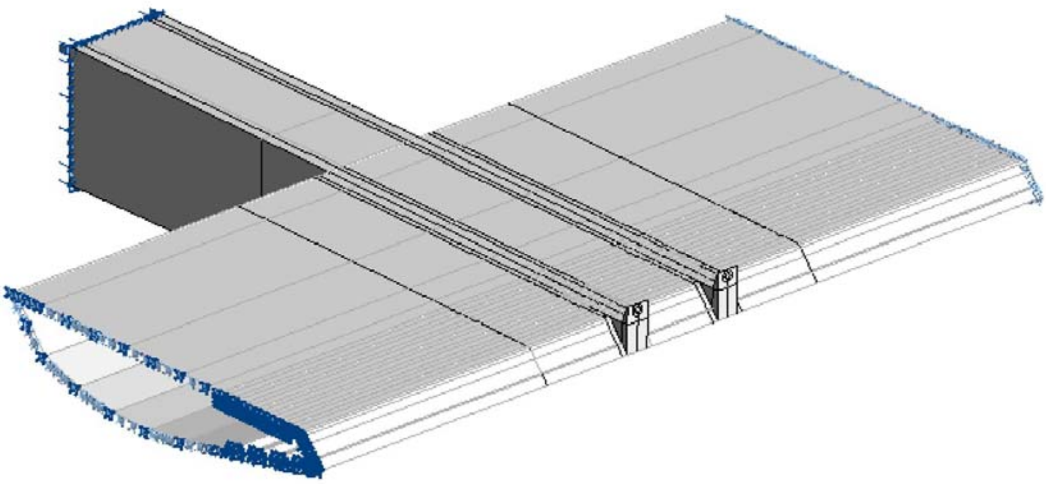

*Figure 1-4 Overall geometry of hanger anchorage local FE-model*

The purpose of the local FE-models is to verify that the local design and verify the stress level is acceptable for applied ULS load combinations. As shown in the following chapters this criteria is fulfilled with some local areas where stresses are within an acceptable yielding range. In these cases it has been verified that yielding areas and the peak stresses are acceptable.

Further more a semi-local IBDAS FE-model has been developed within the global analysis model enabling a more detailed modeling with shell elements and diaphragms to be used for selected parts. Only a local part of the main span is modeled with shell elements whereas the rest of the suspended deck is modeled with beam elements, see Figure 1-5. A detailed description of the model can be found in the report “Semi-local IBDAS Model, Suspended Deck”.

As a verification of the local FE-models, axial stress values in the stress plots from the local FE-models is compared with the results from the semi-local IBDAS model.

## 1.2 Semi-local IBDAS model

The location and geometry of the semi-local IBDAS model is shown in Figure 1-5.

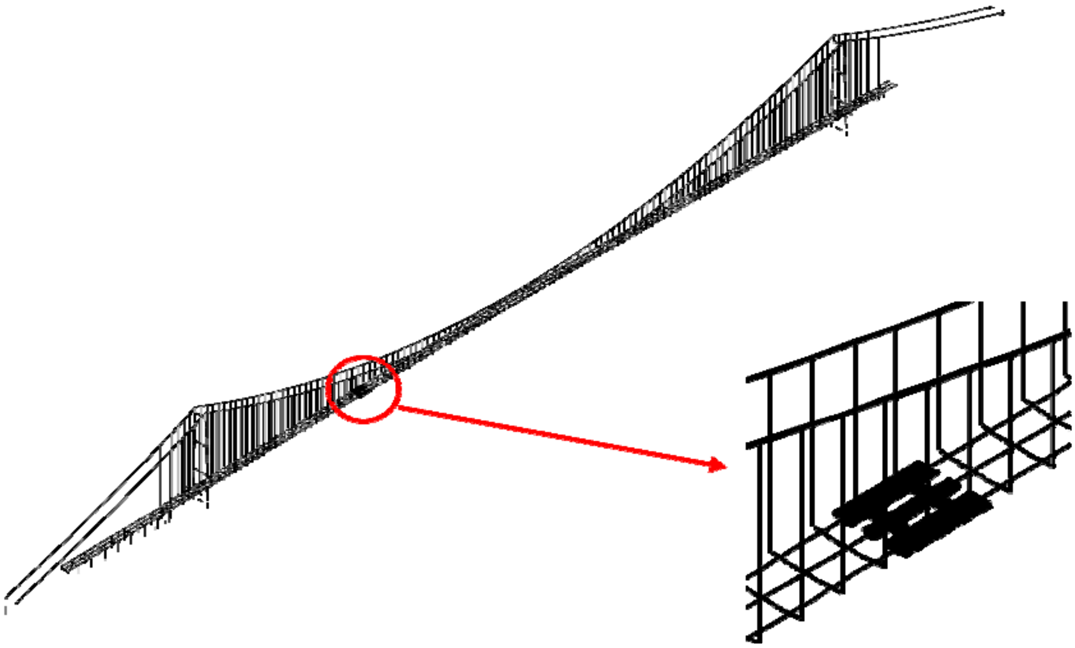

*Figure 1-5 Location of the semi-local IBDAS model within the global analysis model, (Centre of semi-local model: s=-825)*

The shell model consists of 3 individual longitudinal girders connected by two cross girders. A rendered view of the model is shown in Figure 1-6.

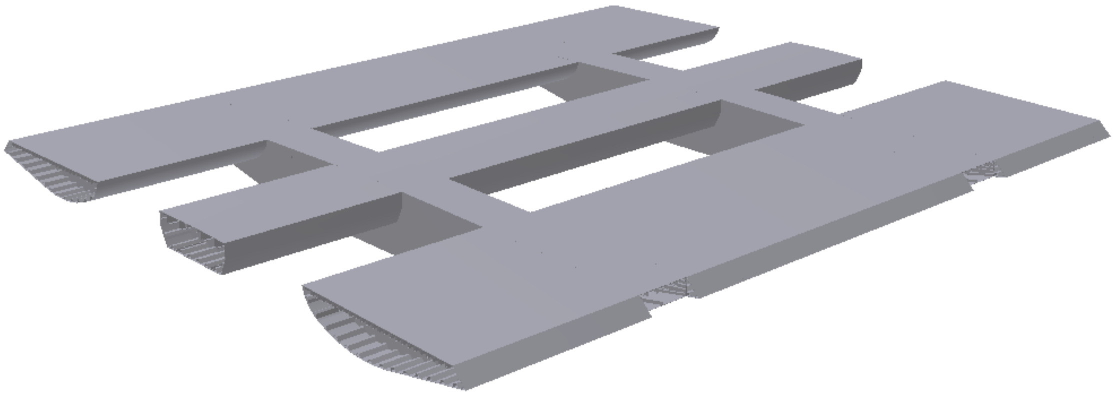

*Figure 1-6 Rendered image of the suspended deck, semi local IBDAS-model*

All the longitudinal steel skin plates of the girders including stiffeners is modeled with their exact geometry and plate thicknesses.

The above mentioned stress comparisons as well as other relevant contour plots of stresses of relevant details modeled by the local FE-models can be found in the following.

Further comparison with stress values given by the verification of the cross sections done by ADVERS has been performed and can be found in document "Design Report - Roadway, Railway and Cross Girders".

# 2 Results of the Local FE-Models

## 2.1 Local FE-model of Suspended Deck

### 2.1.1 Local coordinate system for bridge deck local FE-model

The local coordinate system for the shell elements in the cross girder model are illustrated in Figure 2-1 and Figure 2-2.

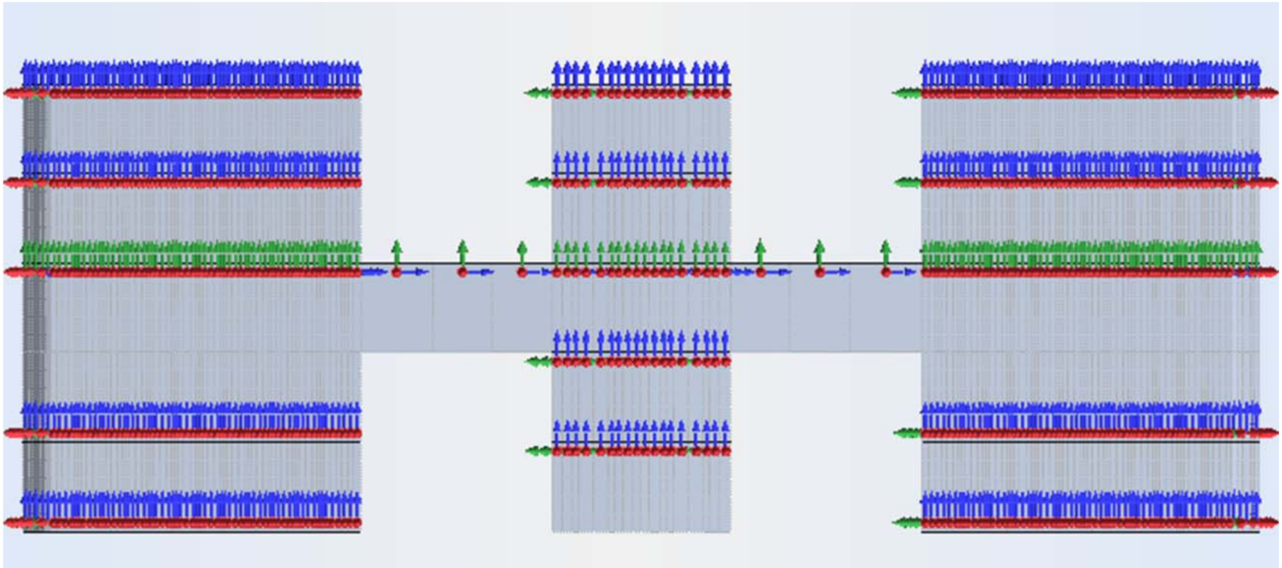

*Figure 2-1 Local coordinate system top plate*

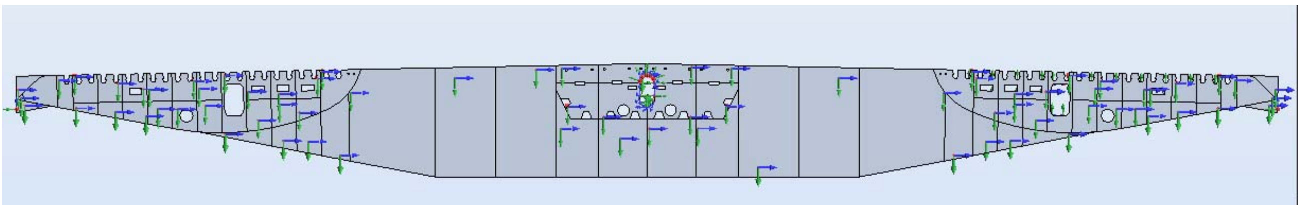

*Figure 2-2 Local coordinate system cross girder web plate*

#### 2.1.2 Stress Comparison with semi-local IBDAS Model

In the following contour plots and stress values of both the bridge deck local FE-model and the semi-local IBDAS model are presented.

The scope has been to verify that the stress distribution throughout the deck and further to check whether the stress magnitude in three characteristic locations of the bridge elements is comparable with stresses from the semi-local IBDAS model.

For the correct interpretation and comparison of the contour plots the orientation of the panels (local x and y coordinate axis of the ROBOT model) has been aligned with the ones set in the IBDAS model.

The comparison has been performed for the following combination numbers refer to IBDAS load cases:

- Reference condition case (dead load combination)
- Load combination 6542 (max tension in hanger)
- Load combination 6532 (Max bending in roadway girder at intersection with cross girder)

Detailed description of the mentioned load cases can be found in the document "General Design Principles for Suspended Deck". The different loads included in the combinations are also given in Table 2-1.

*Table 2-1 Load combination for comparison*

| **Load Case** | **LC 6532** | **LC 6542** |
|---|---|---|
| PP | 1.35 | 1.35 |
| PN | 1.5 | 1.5 |
| Boundary conditions | 1.0 | 1.0 |
| QL: Road load LM1 | 1.01 (TS)<br>0.54 (UDL) | 1.35 |
| QL: Rail load SW/2 | 1.45 | 1.16 |
| QL: Rail load LM71 | 1.45 | 1.16 |
| QL: Braking Rail force | 1.45 | 0.58 |
| QL: Nosing Rail force | 0.73 | 1.16 |
| VV: Wind | 0.6 | 0.6 |
| Calibration load | 1.45 | 1.45 |

The structural elements investigated are the deck plates, the bottom plates and the webs of the cross girder and a summary of the stress elements compared can be found in Table 2-2. The load combinations and the layer where the stresses have been calculated are also presented.

*Table 2-2 Stresses used for comparison*

| | Element | Stress | Panel layer | Stress | Panel layer |
|---|---|---|---|---|---|
| **Reference condition** | Deck plates | sXX, sYY | Middle | von Mises | top |
| | Bottom plates | sXX, sYY | Middle | von Mises | bottom |
| | Web (cross girder) | sXX, sYY | Middle | von Mises | bottom |
| **Case 6532** | Deck plates | sXX, sXY | Middle | von Mises | top |
| | Bottom plates | sXX, sXY | Middle | von Mises | bottom |
| | Web (cross girder) | sXX, sXY | Middle | von Mises | bottom |
| **Case 6542** | Deck plates | sXX, sXY | Middle | von Mises | top |
| | Bottom plates | sXX, sXY | Middle | von Mises | bottom |
| | Web (cross girder) | sXX, sXY | Middle | von Mises | bottom |

In the following figures a full set of results of the above mentioned stresses are presented showing the IBDAS plot on the top and the ROBOT plot in the bottom. A differences in the stress color can be noticed, however this does not represent a relevant difference of the stress level; a color chart of the stress magnitude is also shown in the plots. The results of the main stress direction sXX are highlighted for both models in three characteristic points for the top and bottom plates along the cross girder and two point in the upper and lower edge of the web.

A summary of the results including the deviation of stresses between the models can be seen in Table 2-3. The results shows that the two models are comparable as discrepancies can be justified by the following reasons:

- A different location of the two models, namely s= -420 for the ROBOT model and s= -810 for the semi-local IBDAS model with the consequence of not fully comparable boundary conditions.
- The IBDAS semi-local model is not developed to be moved to the same location at the ROBOT bridge deck FE-model at the current design stage. Since the general purpose of the local models is to verify the proposed element solutions and to document that the stress flow is acceptable with respect to ULS load combinations. Therefore, it is considered acceptable that the location of bridge stationing is not identical for the two models. The

overall geometry of the structural parts is exactly the same; however the steel quality differs for the roadway and railway girder at these locations.

- In order to make a conservative design, the modeled cross girder is in correspondence of the cross over location which leads to an increment of the self weight and therefore some difference in loading compared to the IBDAS semi-local model. This variation is in the order of 13,2kN/m per side.
- Variation of stresses in the top and bottom plates due to a slight different location of the neutral axis due to the different modeling approach (equivalent thickness of the stiffeners for the IBDAS model and actual geometry in the ROBOT model).

*Table 2-3 Stresses on elements comparison*

| | Element | Section | Stress | IBDAS [MPa] | ROBOT [MPa] | Deviation from IBDAS |
|---|---|---|---|---|---|---|
| **Reference condition** | Deck plates | 1 | sXX | -62.43 | -69.91 | 11.98% |
| | | 2 | sXX | -73.15 | -74.56 | 1.93% |
| | | 3 | sXX | -39.78 | -31.65 | -20.44% |
| | Bottom plates | 1 | sXX | 63.81 | 69.07 | 8.24% |
| | | 2 | sXX | 73.15 | 79.08 | 8.11% |
| | | 3 | sXX | 40.26 | 49.26 | 22.35% |
| | Web (cross girder) | 1 | sXX | 73.53 | 68.38 | -7.00% |
| | | 2 | sXX | -63.18 | -64.17 | 1.57% |
| **LC6532** | Deck plates | 1 | sXX | -244.65 | -265.44 | 8.50% |
| | | 2 | sXX | -259.98 | -270.70 | 4.12% |
| | | 3 | sXX | -117.49 | -101.01 | -14.03% |
| | Bottom plates | 1 | sXX | 325.89 | 263.61 | -19.11% |
| | | 2 | sXX | 270.49 | 271.81 | 0.49% |
| | | 3 | sXX | 163.31 | 134.30 | -17.76% |
| | Web (cross girder) | 1 | sXX | 284.36 | 253.93 | -10.70% |
| | | 2 | sXX | -228.85 | -247.03 | 7.94% |
| **LC6542** | Deck plates | 1 | sXX | -229.33 | -242.31 | 5.66% |
| | | 2 | sXX | -245.56 | -250.89 | 2.17% |
| | | 3 | sXX | -134.34 | -110.21 | -17.96% |
| | Bottom plates | 1 | sXX | 287.07 | 237.58 | -17.24% |
| | | 2 | sXX | 247.73 | 255.58 | 3.17% |
| | | 3 | sXX | 170.69 | 146.92 | -13.93% |
| | Web (cross girder) | 1 | sXX | 249.84 | 228.63 | -8.49% |
| | | 2 | sXX | -205.11 | -230.76 | 12.51% |

The above mentioned stresses of both models can be seen in Figure 2-3 to Figure 2-29. Besides the comparable stress ranges it can also be seen from the plots that the stress distribution is similar for the two models indicating similar loading arrangement and structural behavior of the two.

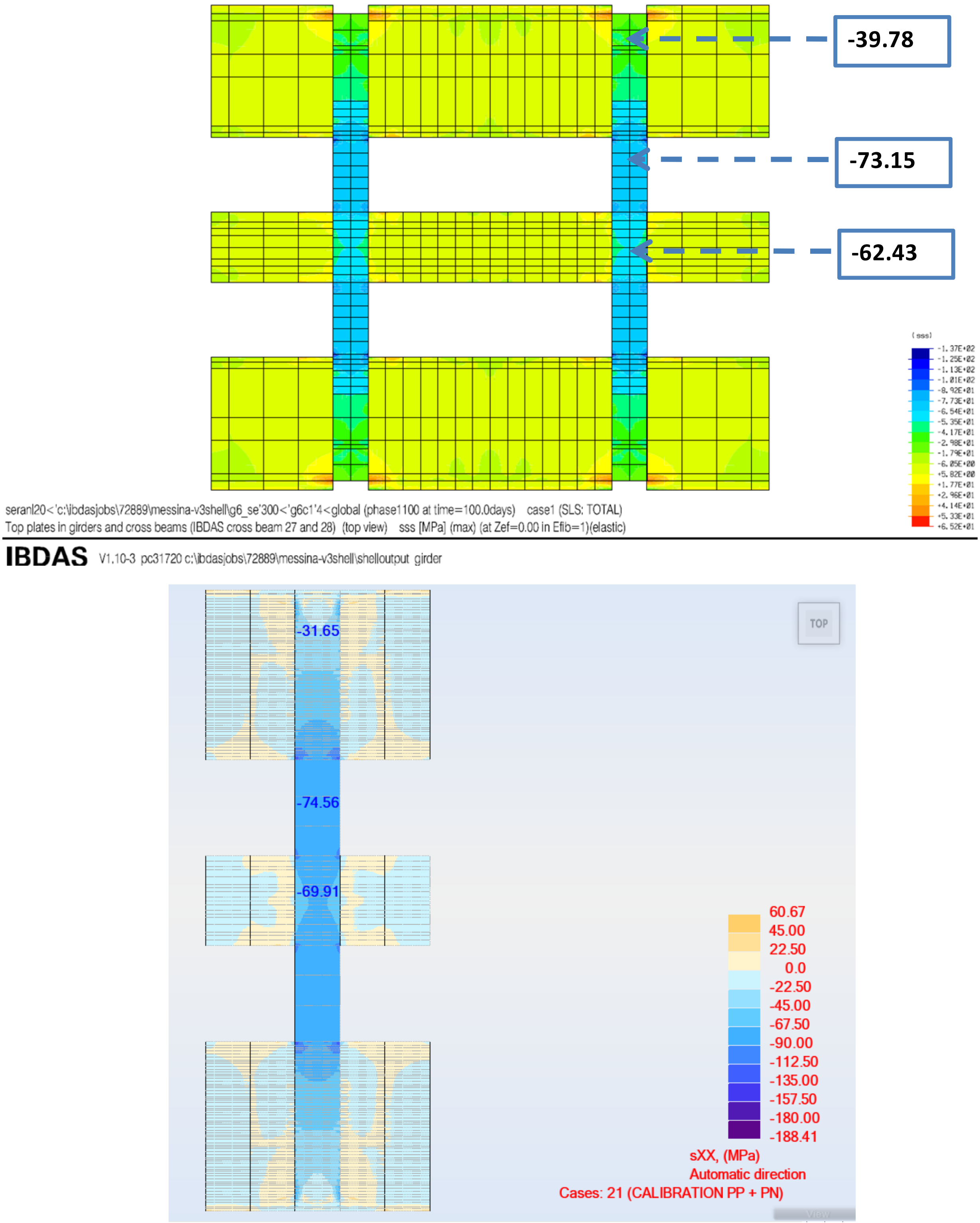


*Figure 2-3 Deck plates, Reference condition load case – stress sXX*

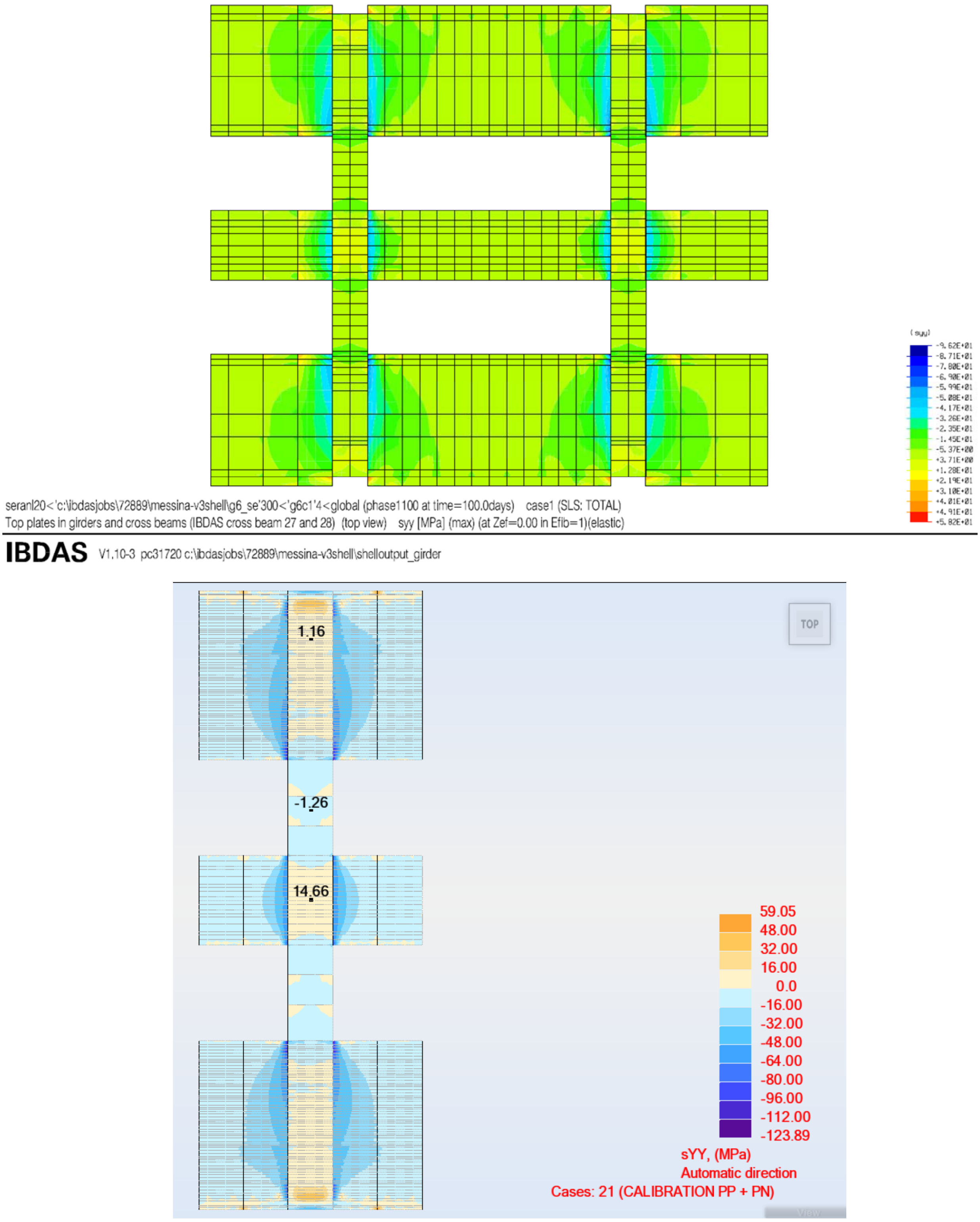


*Figure 2-4 Deck plates, Reference condition load case – stress sYY*

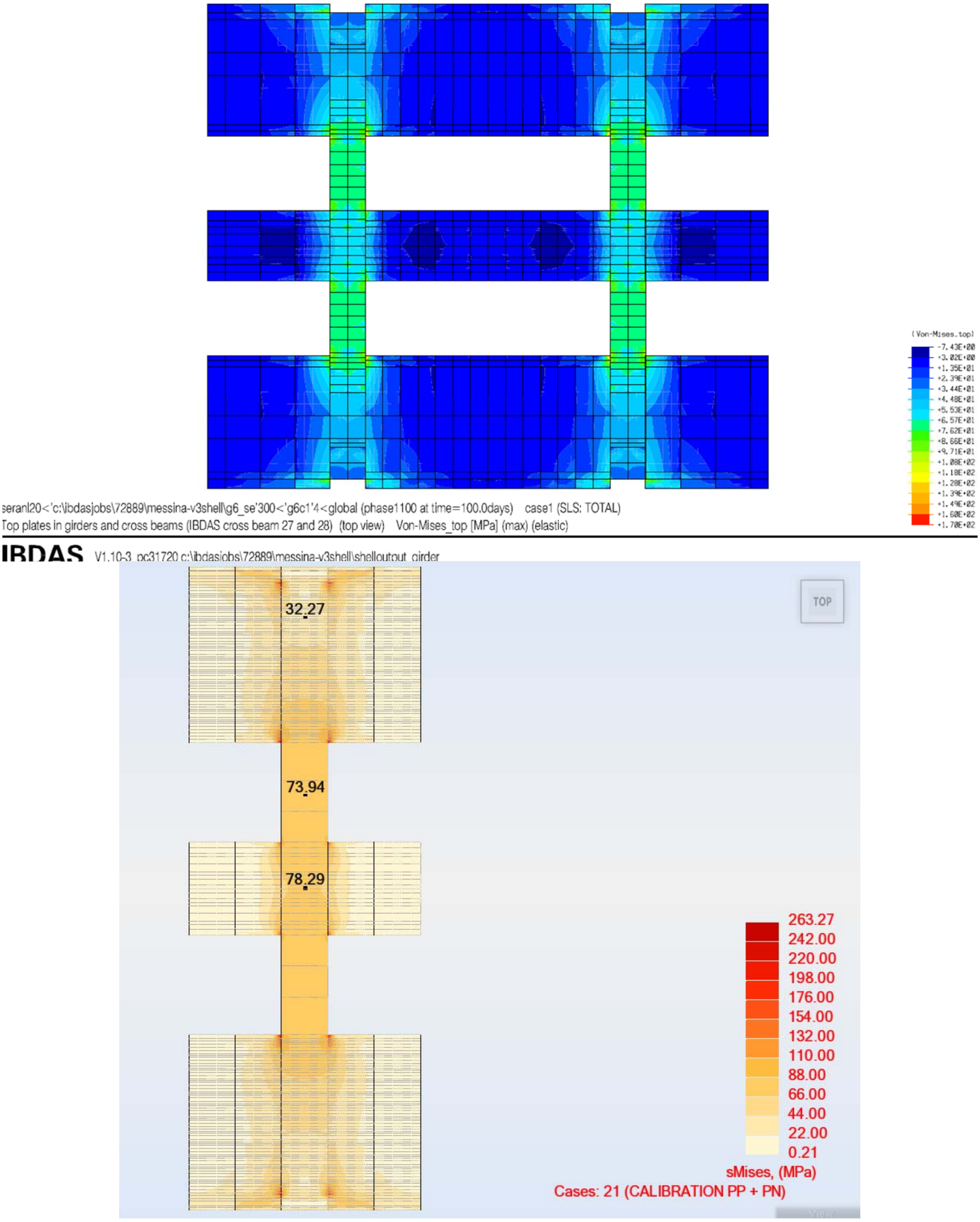


*Figure 2-5 Deck plates, Reference condition load case – von Mises*

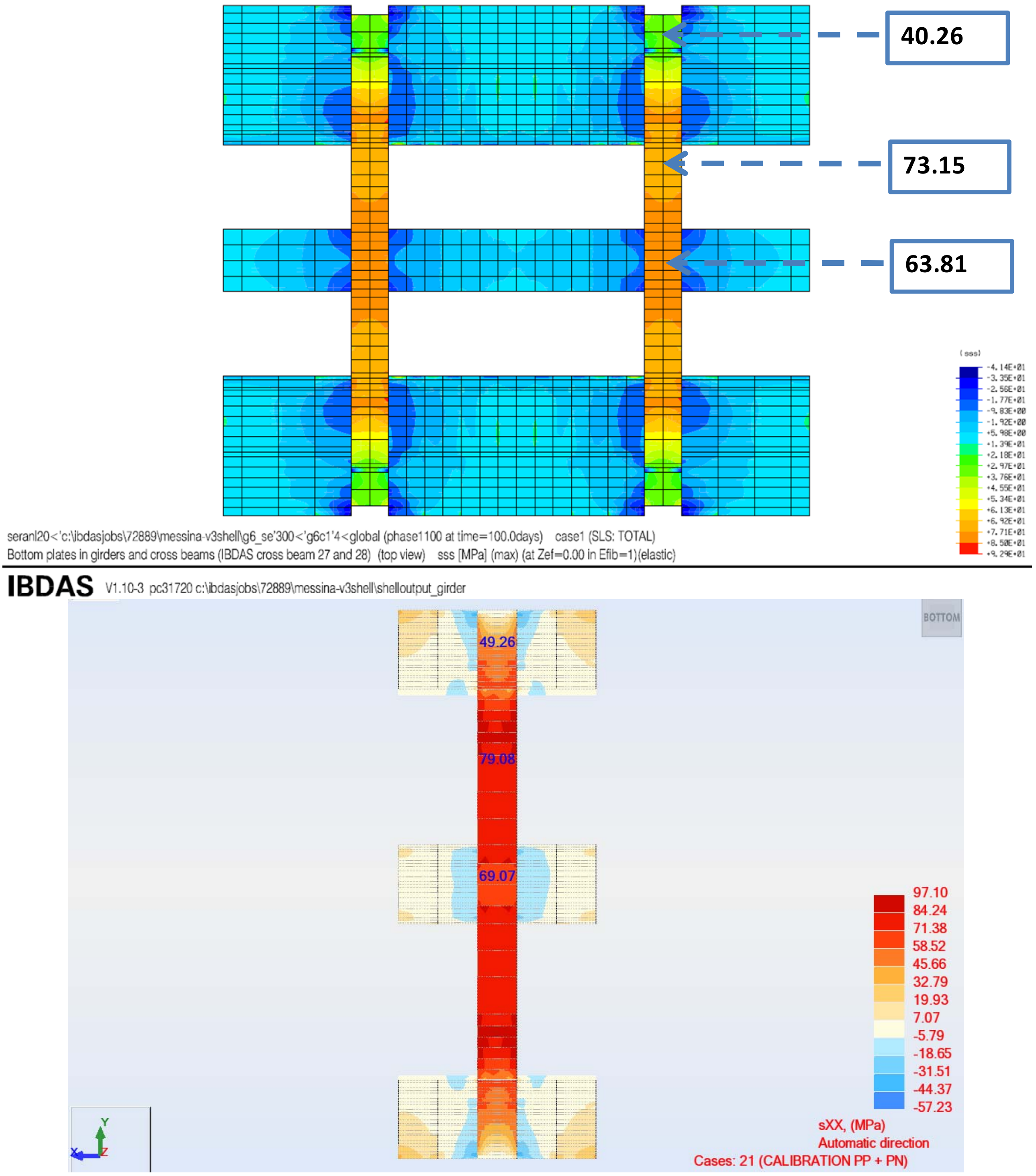


*Figure 2-6 Bottom plates, Reference condition load case – stress sXX*

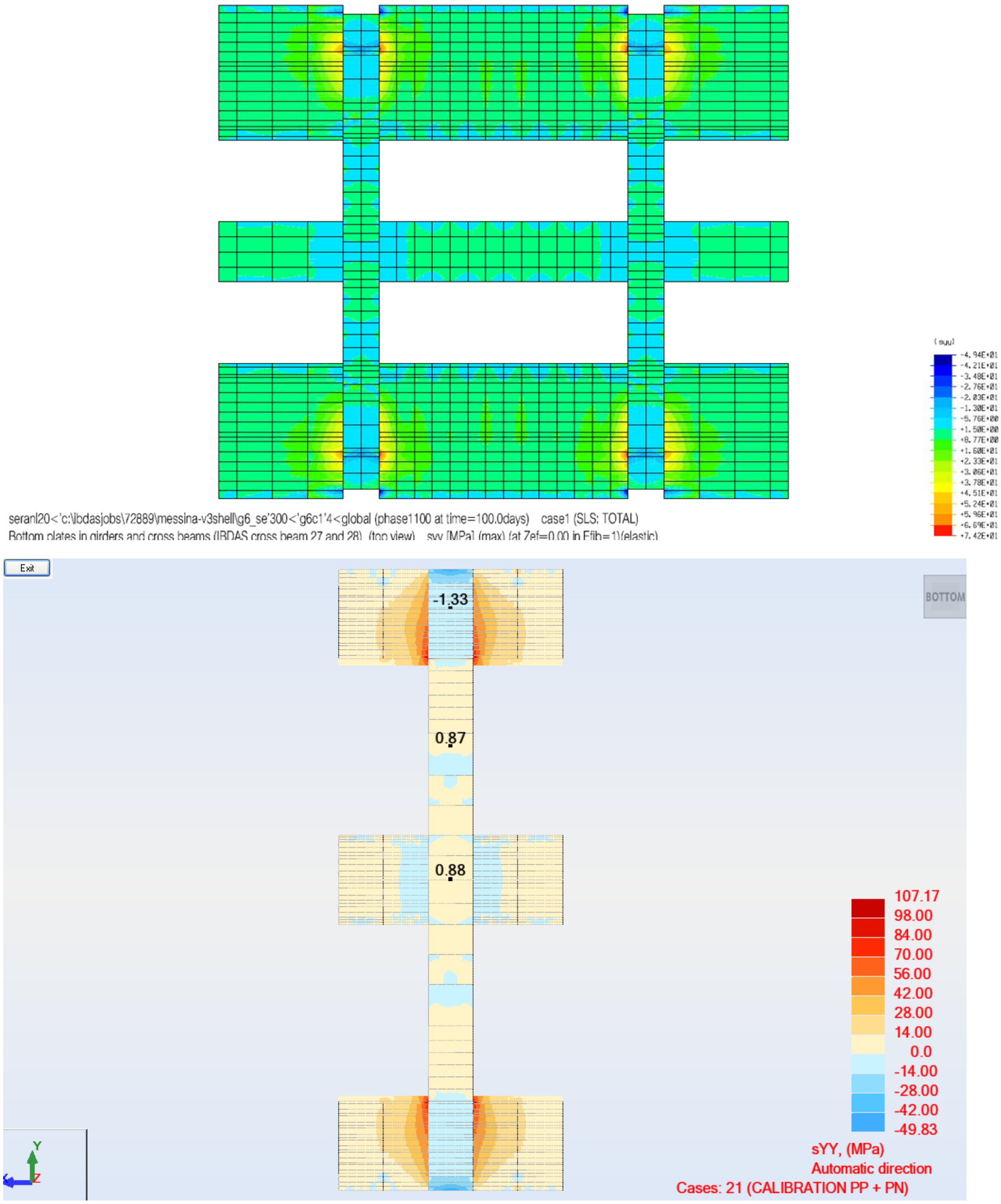


*Figure 2-7 Bottom plates, Reference condition load case – stress sYY*

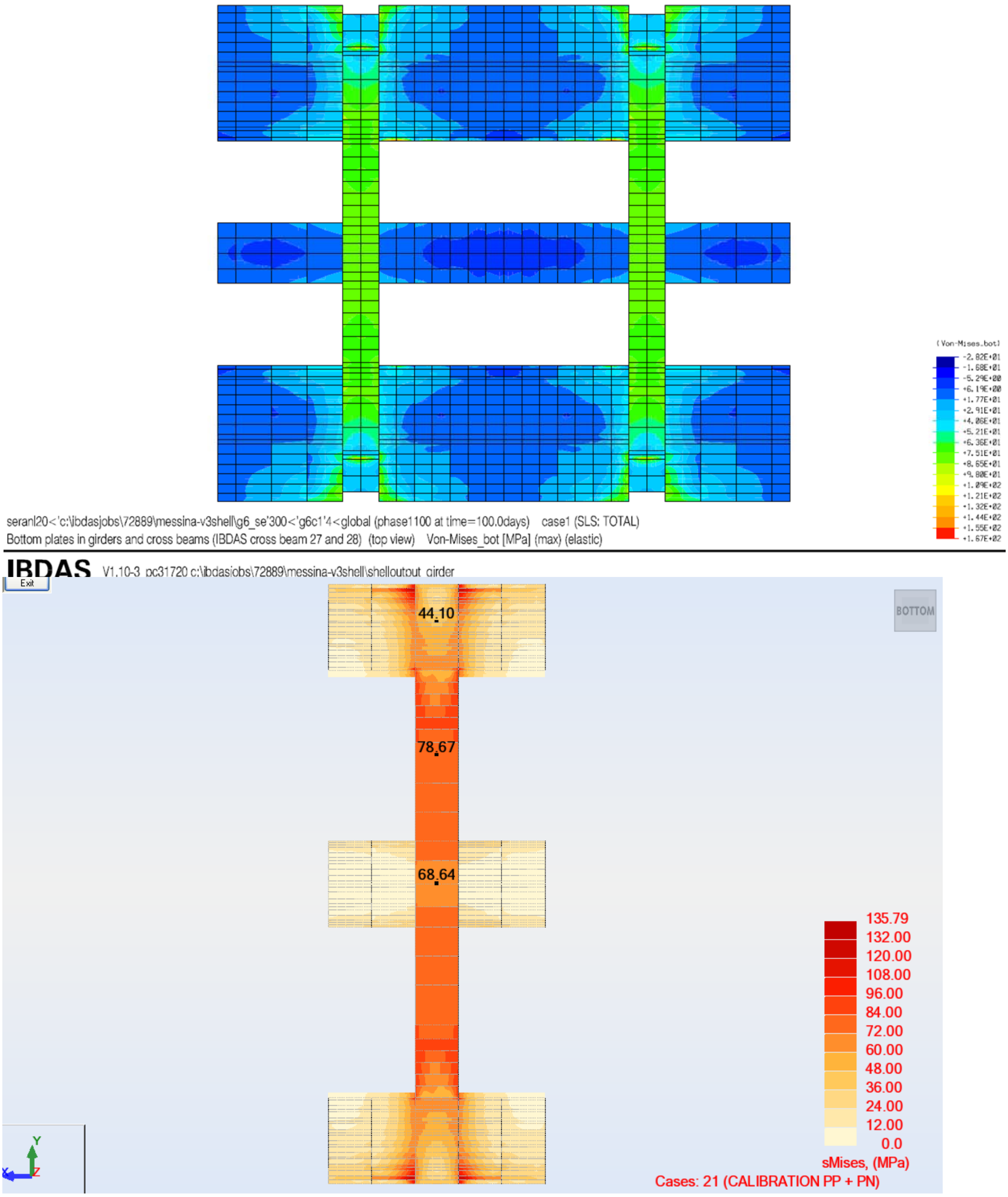


*Figure 2-8 Bottom plates, Reference condition load case – von Mises*

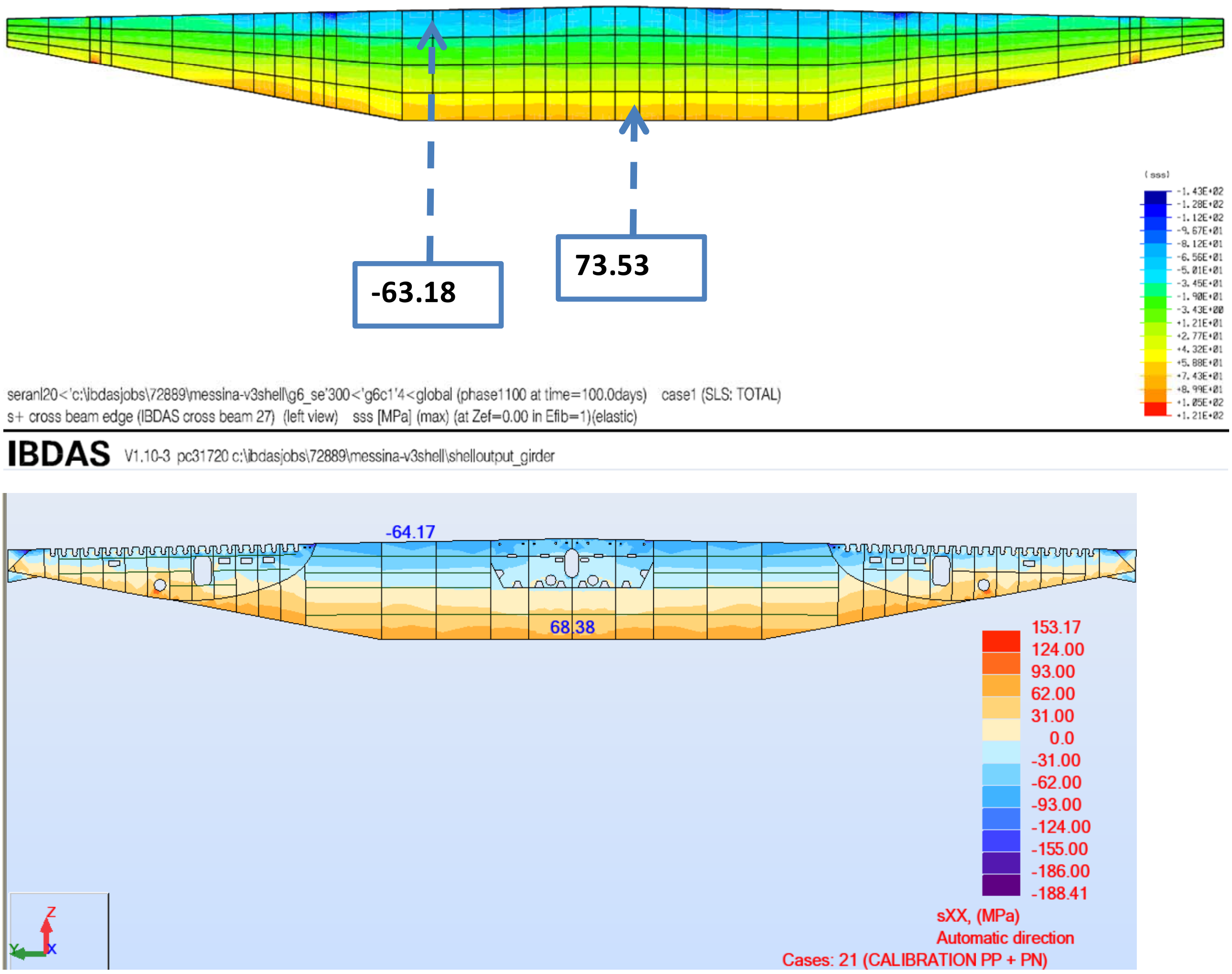


*Figure 2-9 Cross girder web, Reference condition load case – stress sXX*

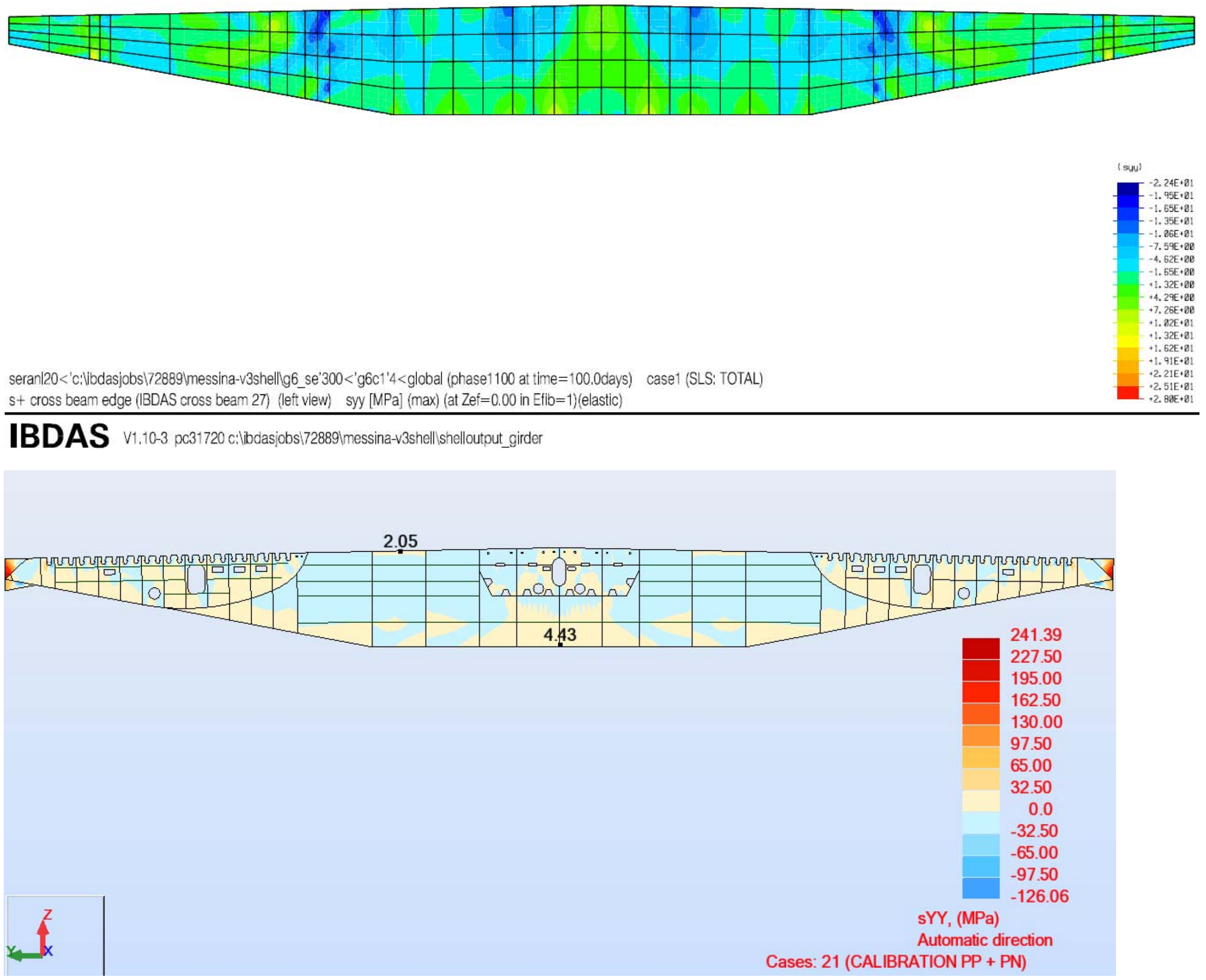


*Figure 2-10 Cross girder web, Reference condition load case – stress sYY*

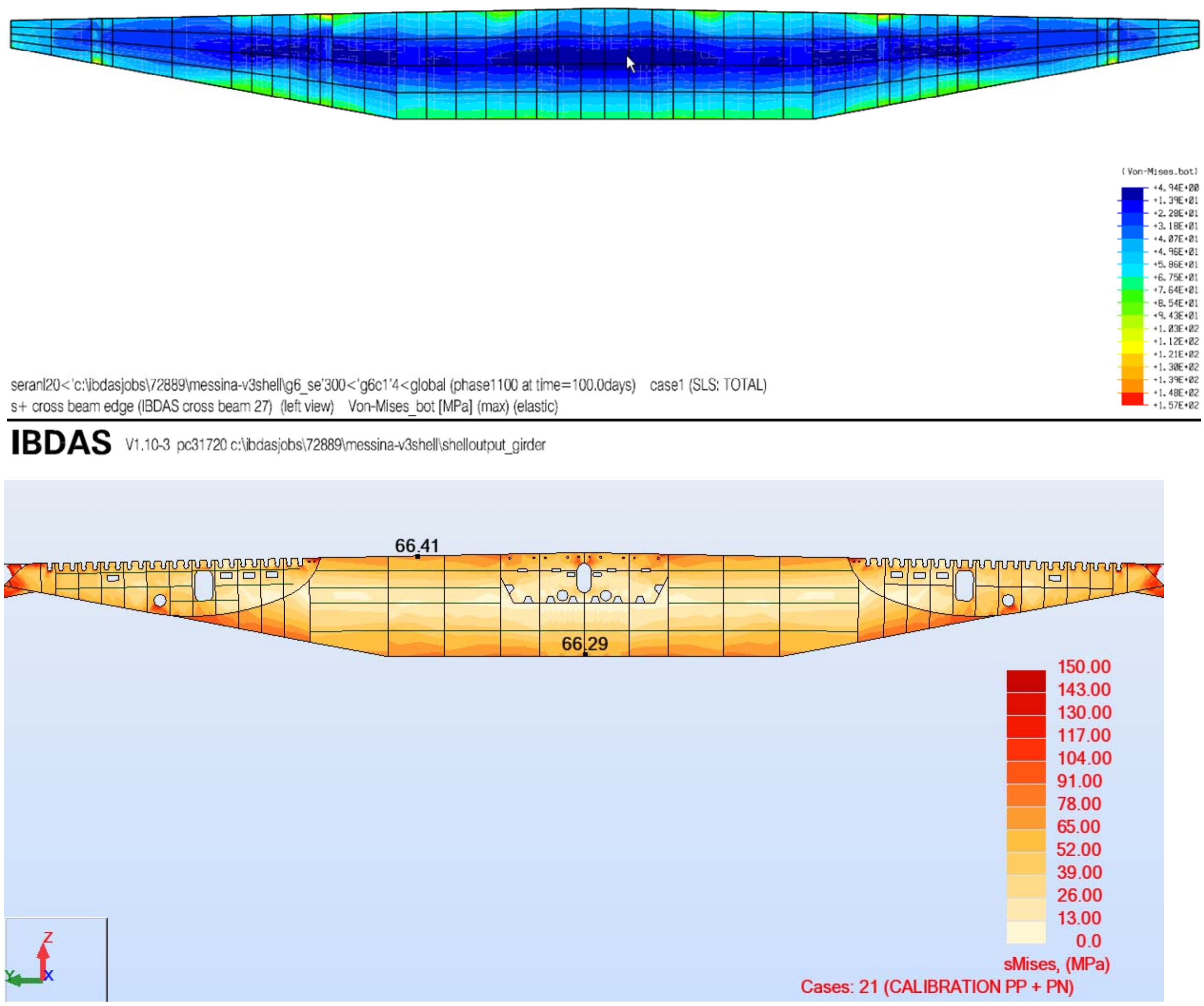


*Figure 2-11 Cross girder web, Reference condition load case – von Mises*

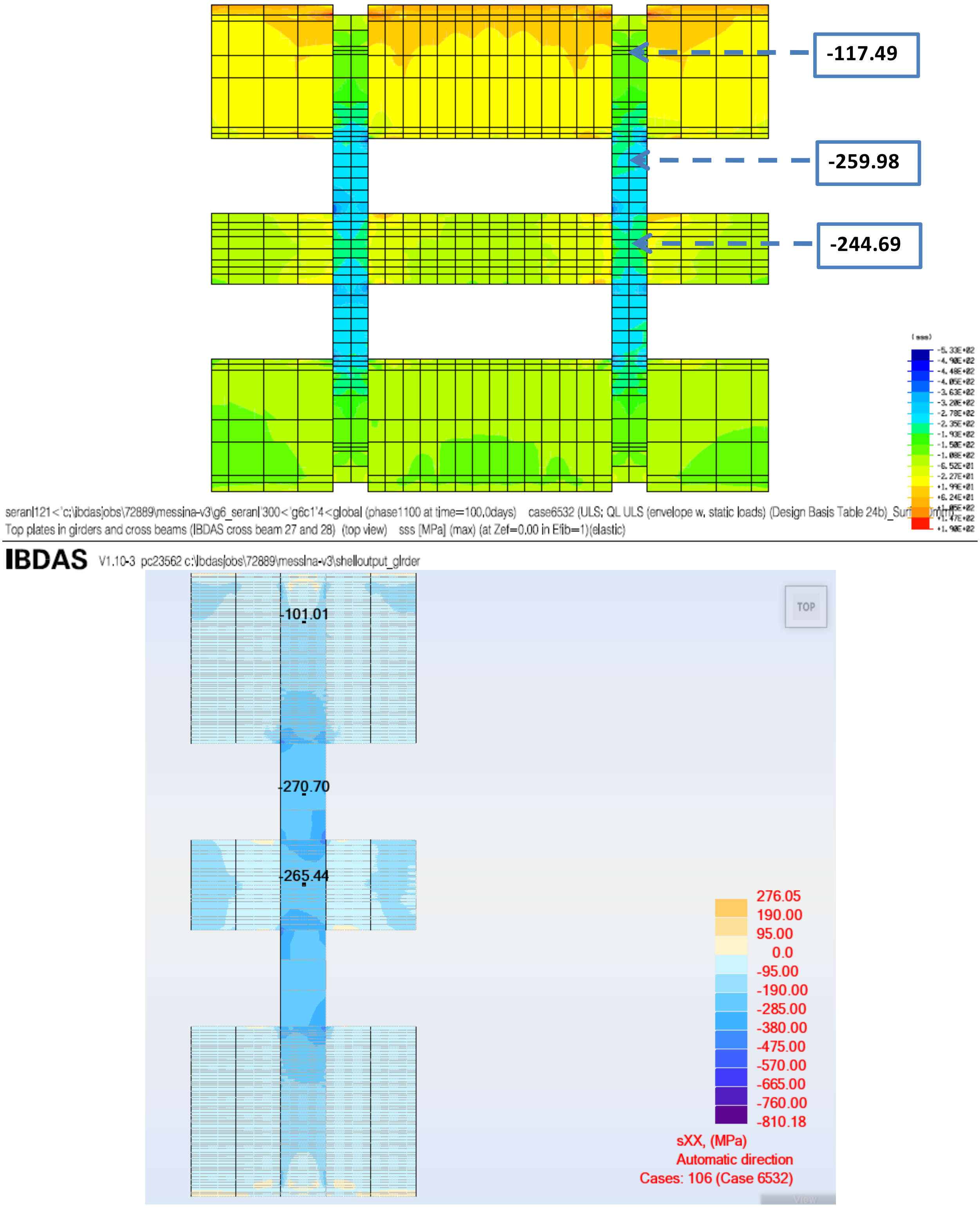


*Figure 2-12 Deck plates, 6532 load case – stress sXX*

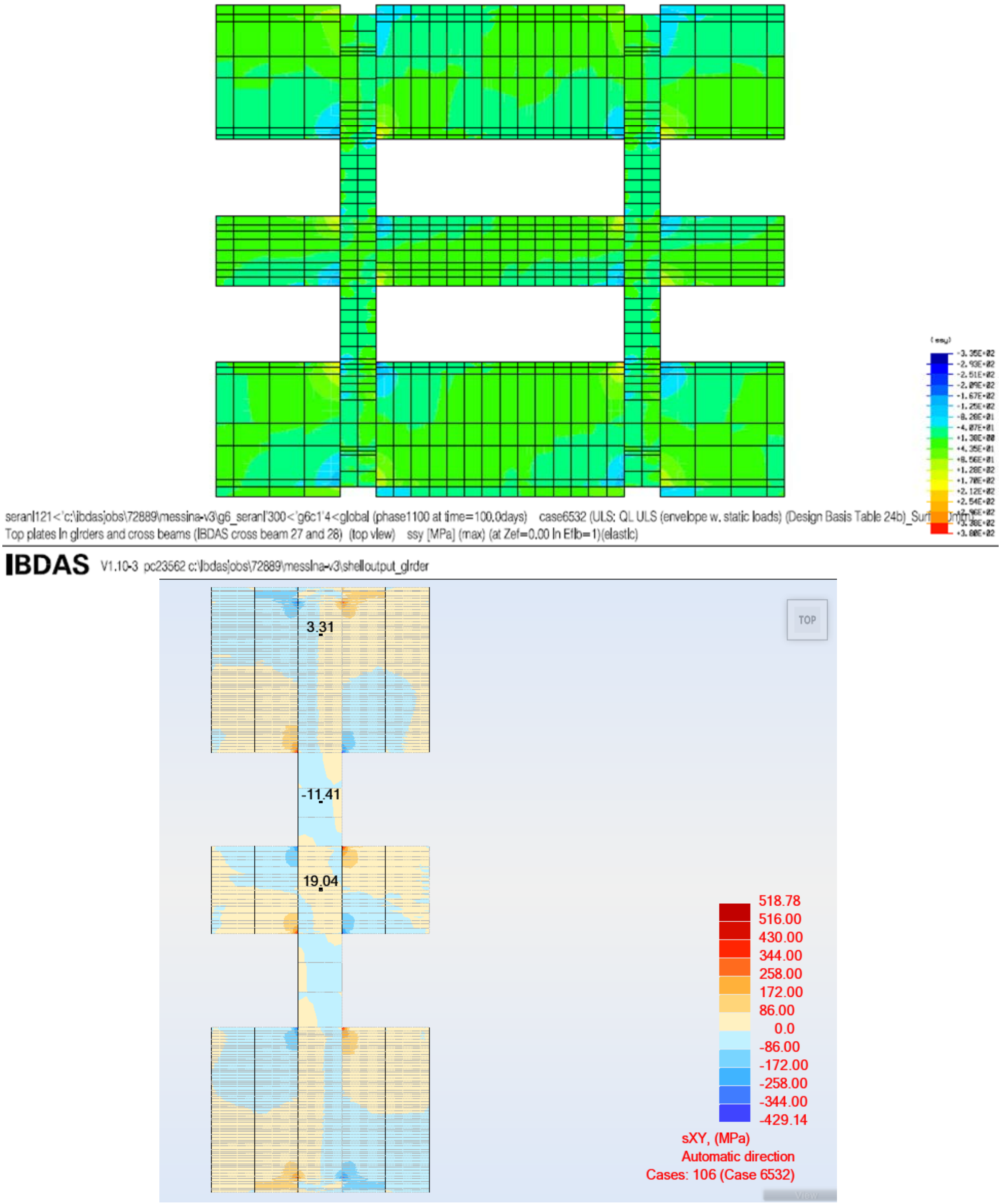


*Figure 2-13 Deck plates, 6532 load case – stress sXY*

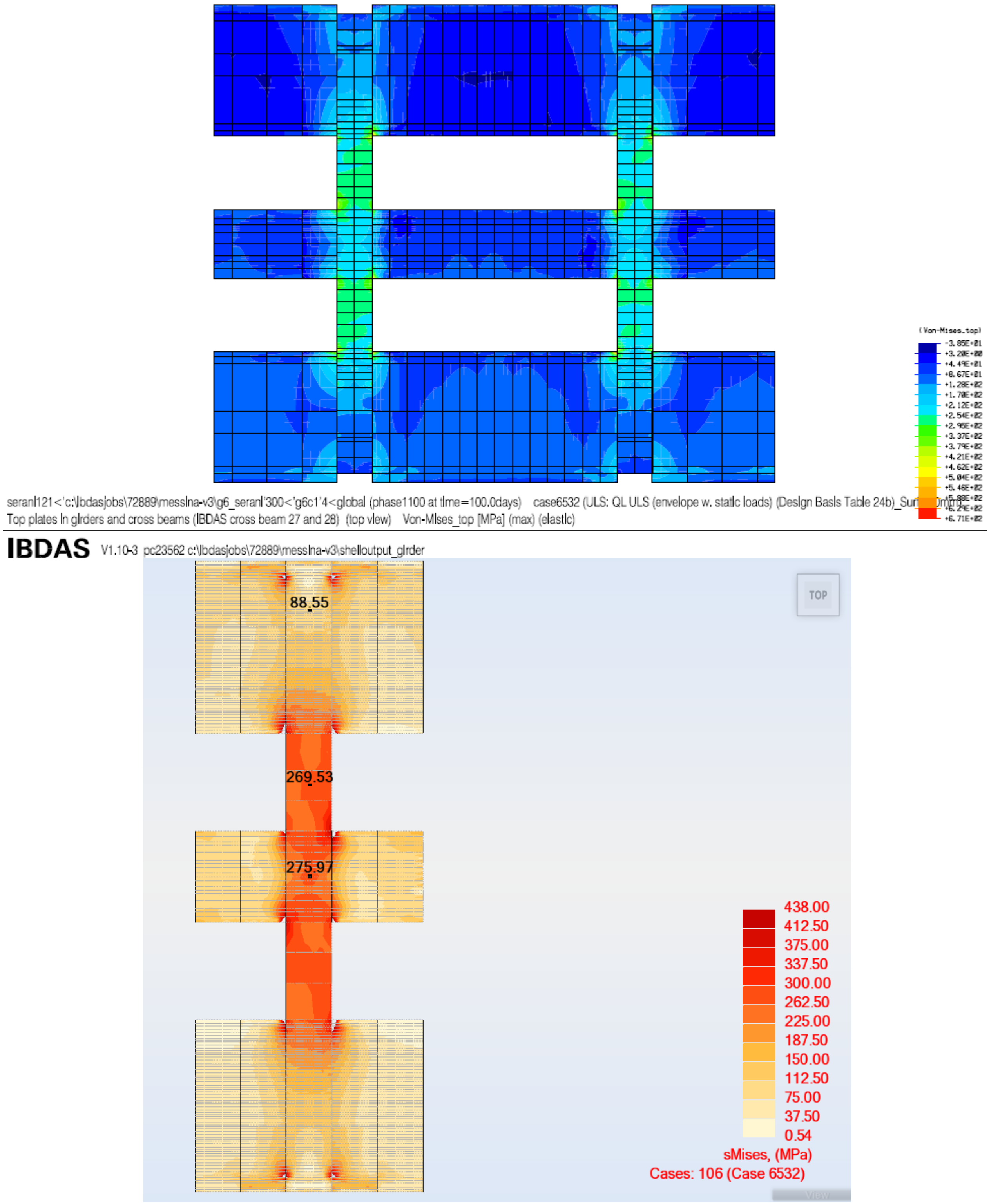


*Figure 2-14 Deck plates, 6532 load case – stress von Mises*

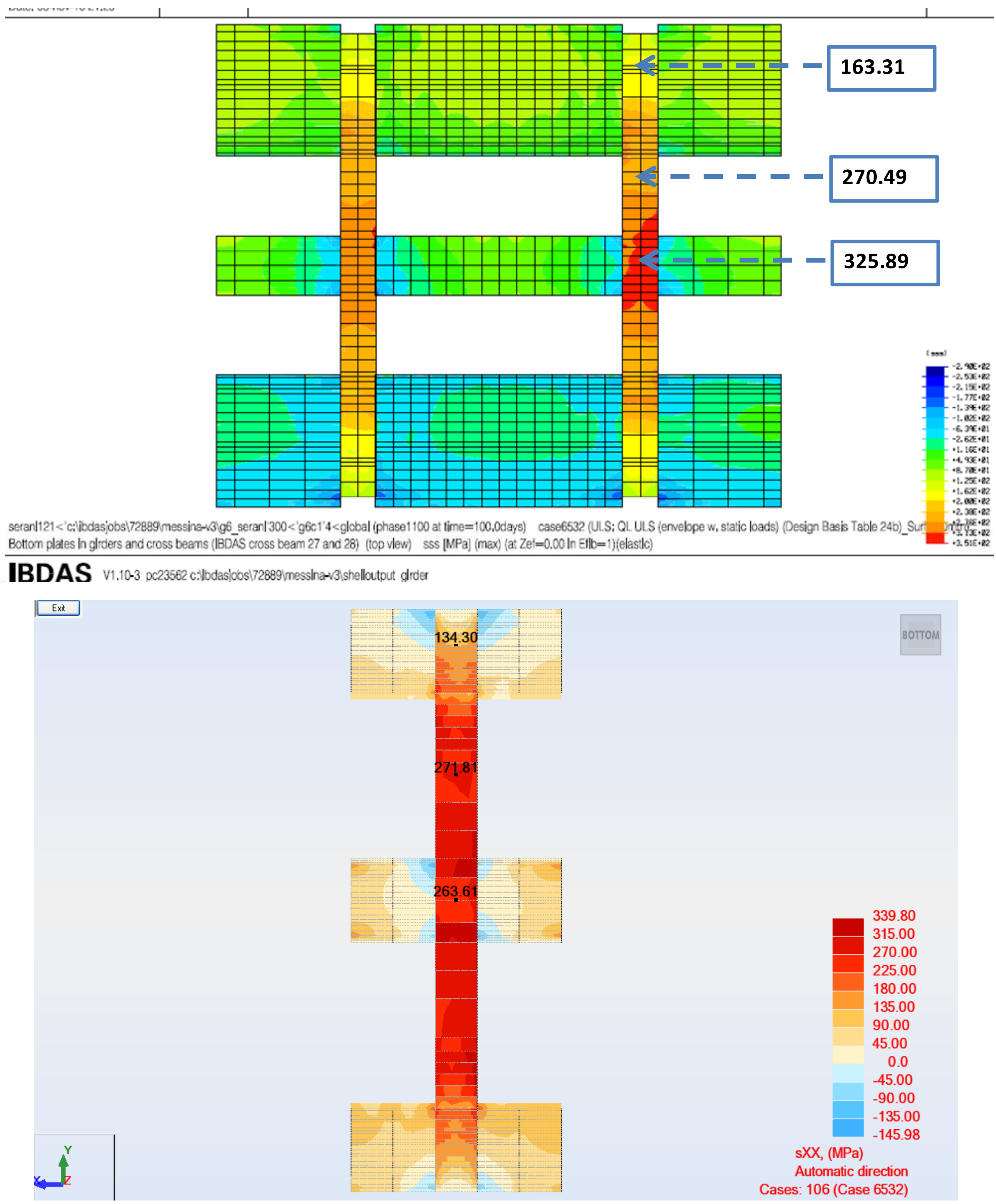


*Figure 2-15 Bottom plates, 6532 – stress sXX*

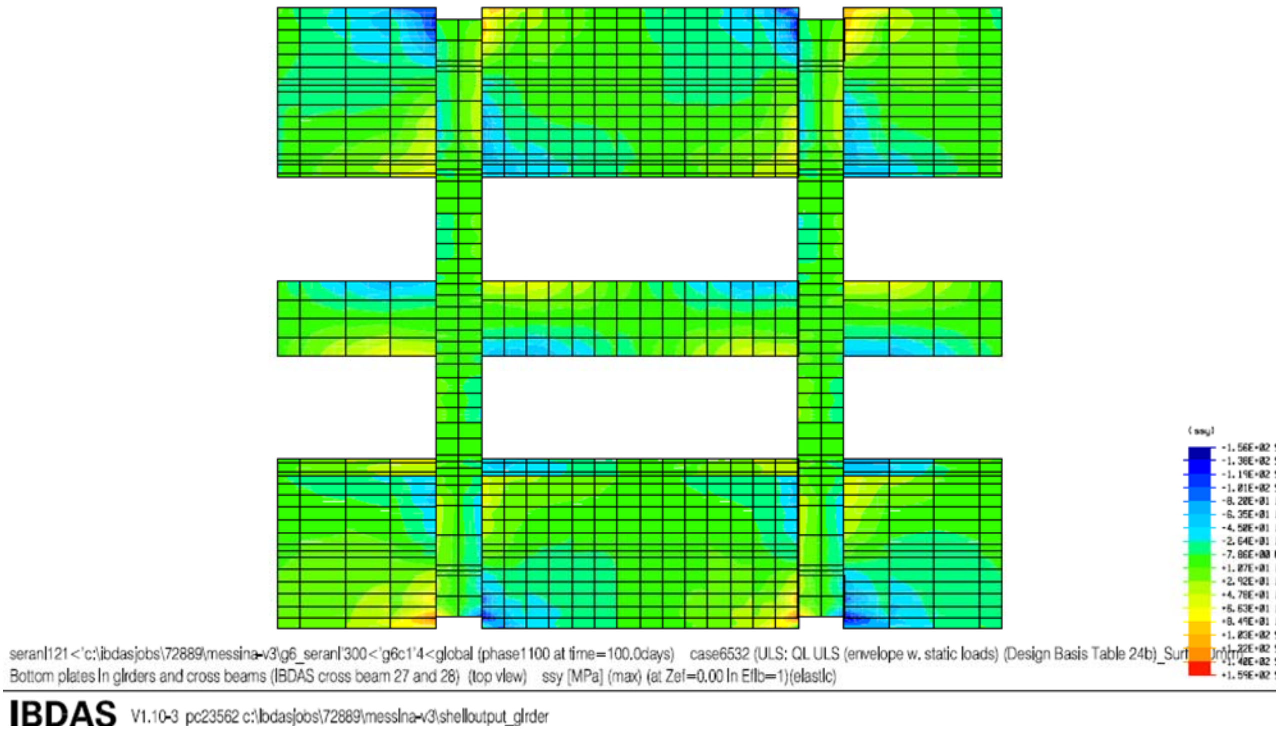


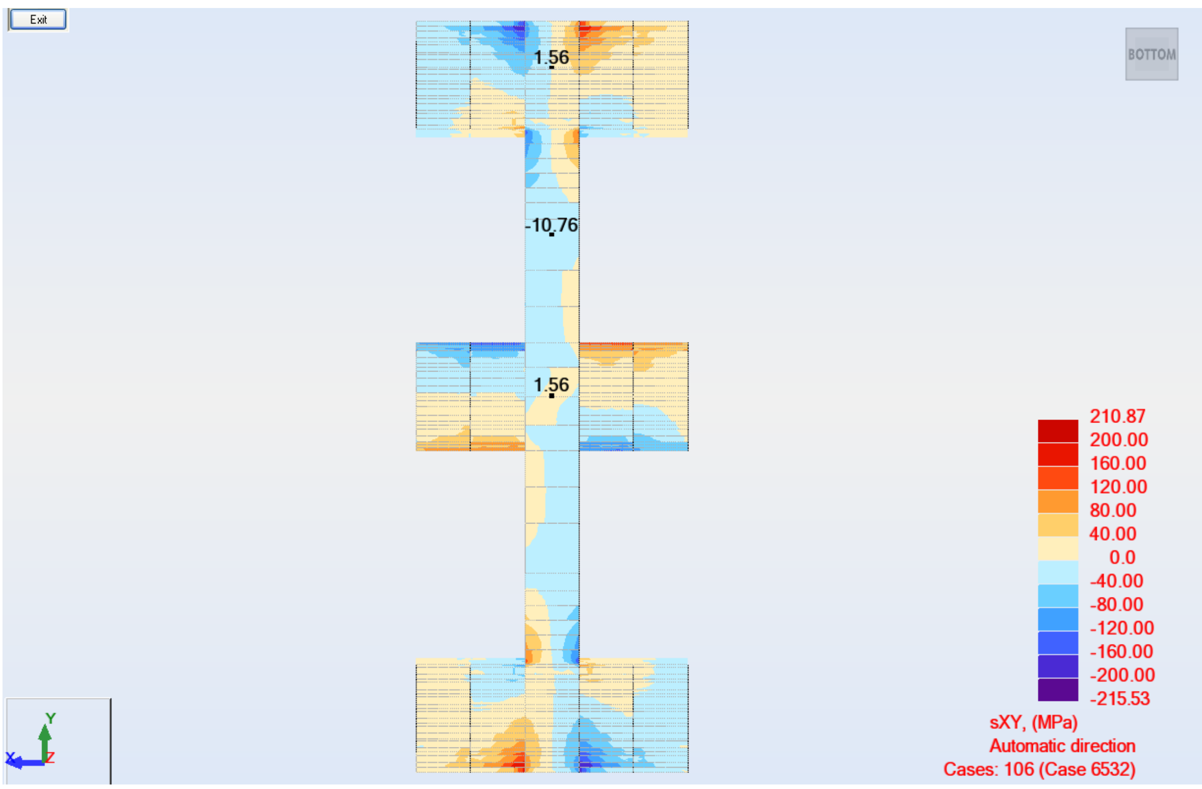


*Figure 2-16 Bottom plates, 6532 – stress sXY*

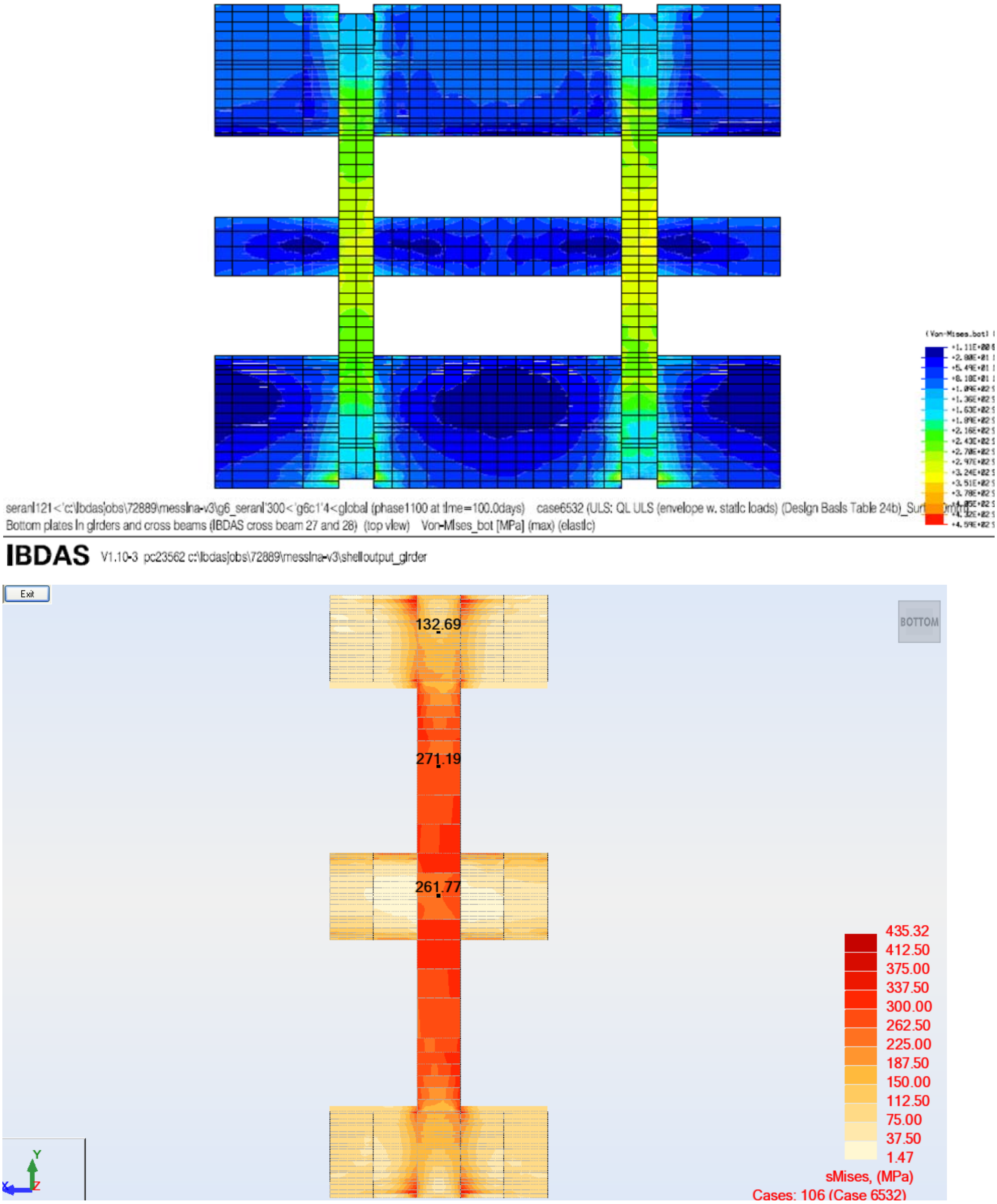


*Figure 2-17 Bottom plates, 6532 – stress von Mises*

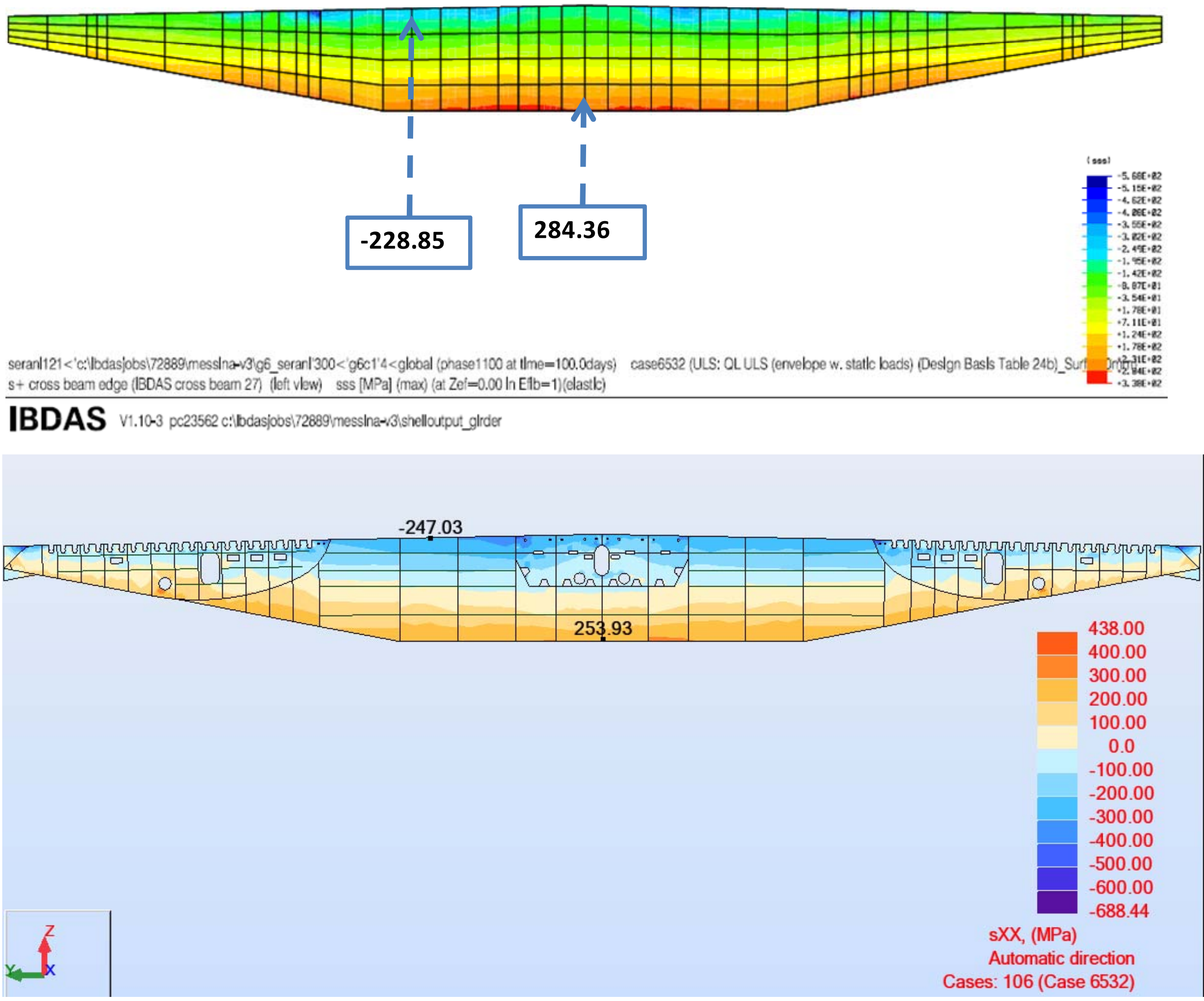


*Figure 2-18 Cross girder web, 6532 – stress sXX*

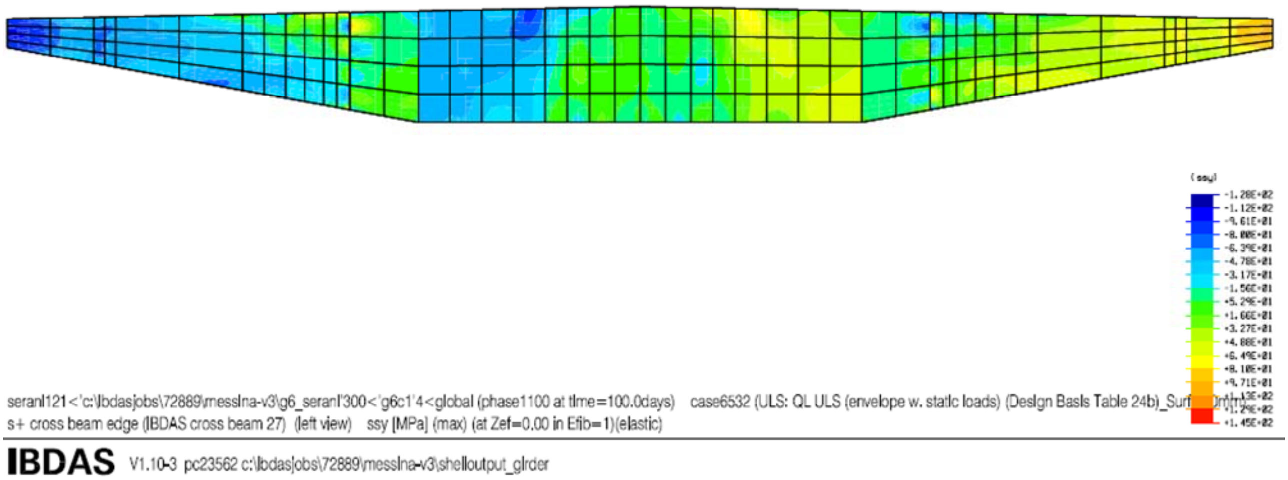


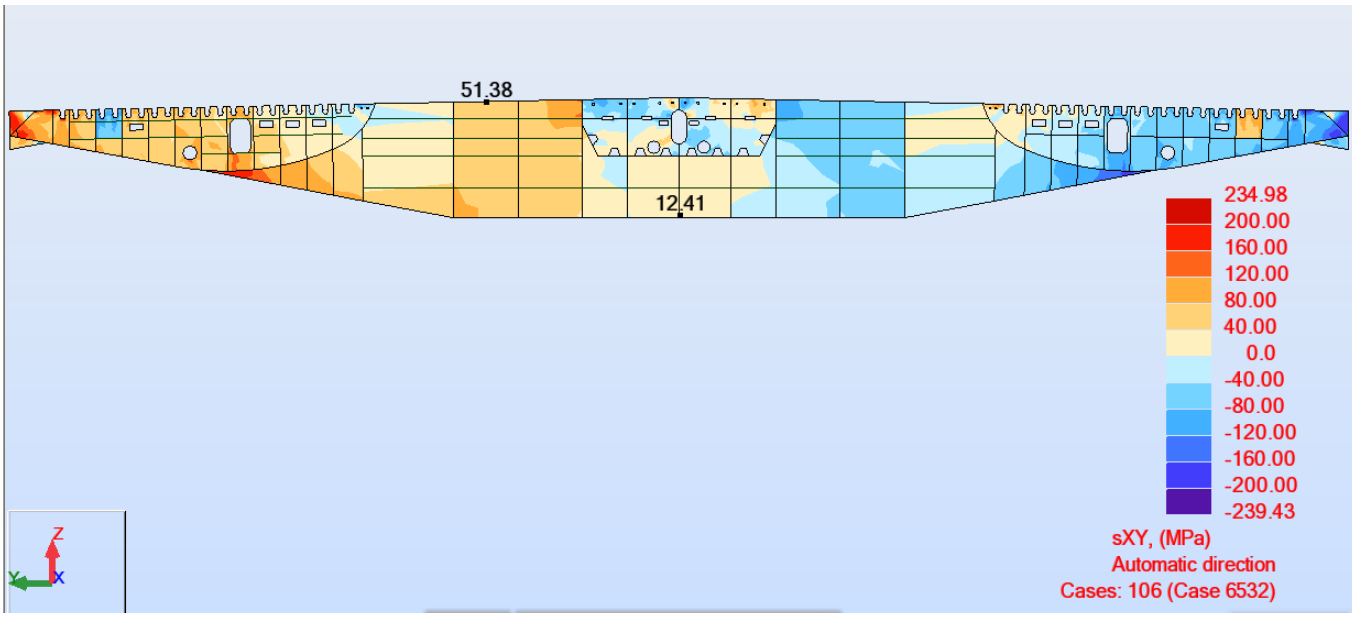


*Figure 2-19 Cross girder web, 6532 – stress sXY*

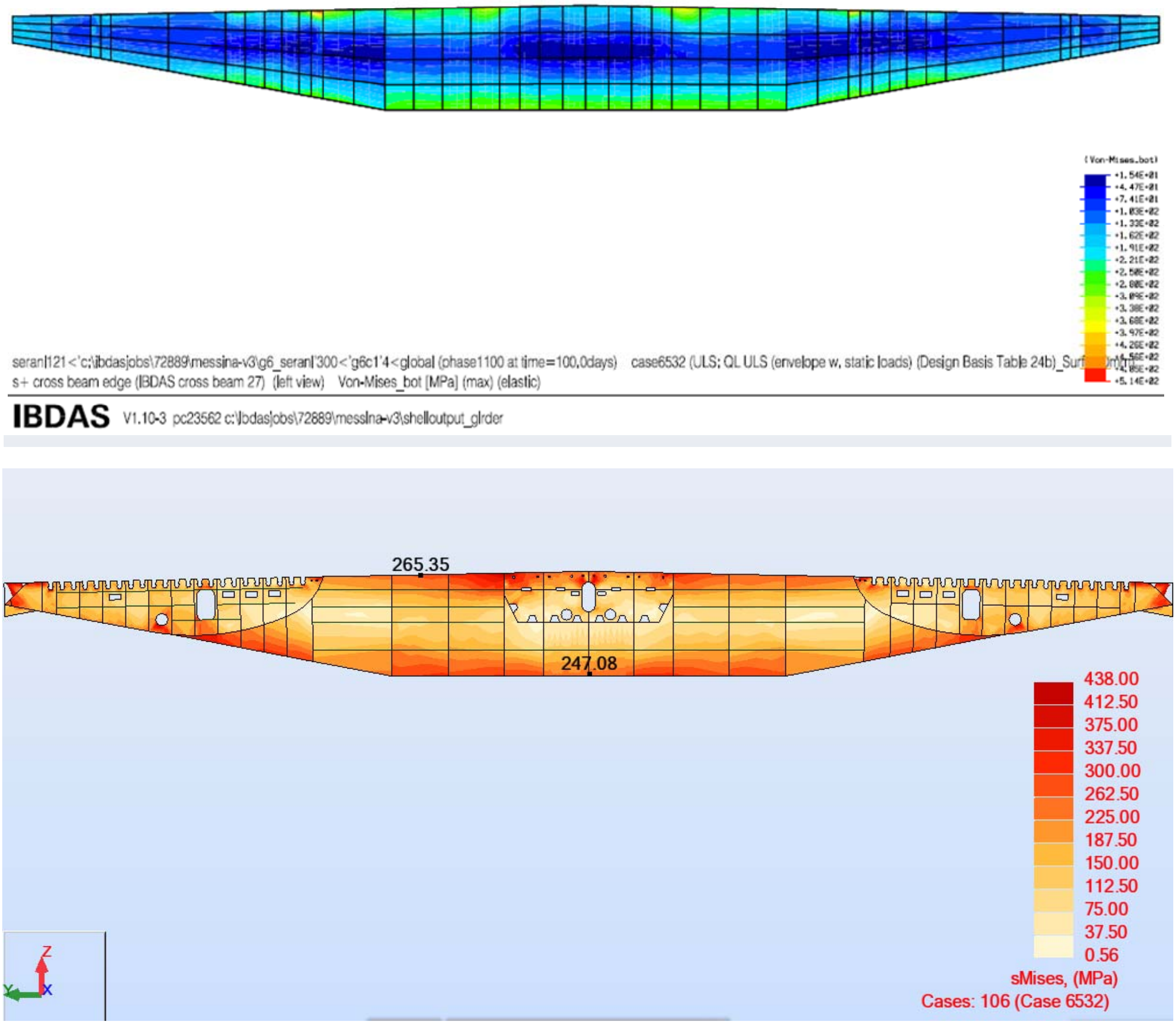


*Figure 2-20 Cross girder web, 6532 – stress von Mises*

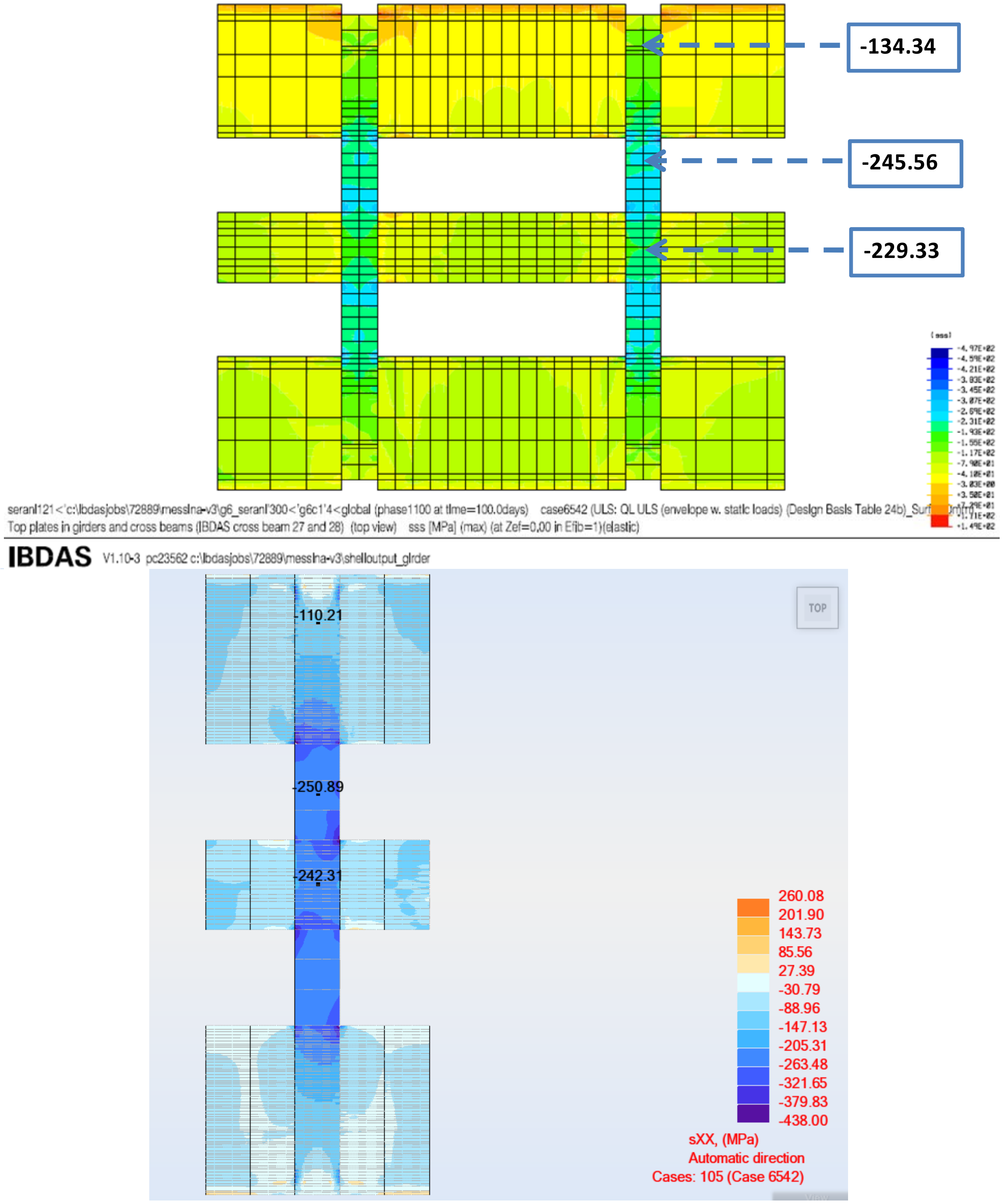


*Figure 2-21 Deck plates, 6542 load case – stress sXX*

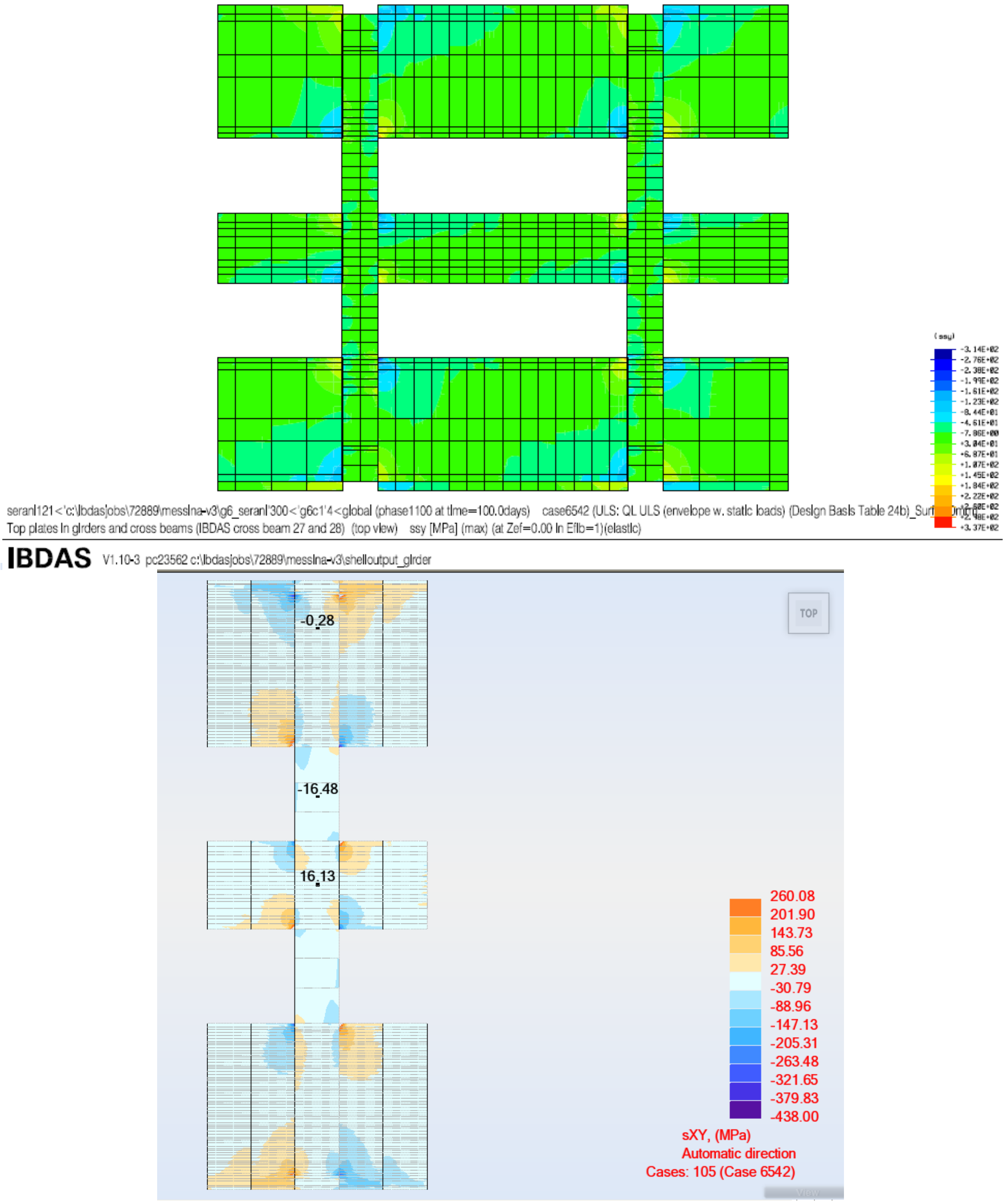


*Figure 2-22 Deck plates, 6542 load case – stress sXY*

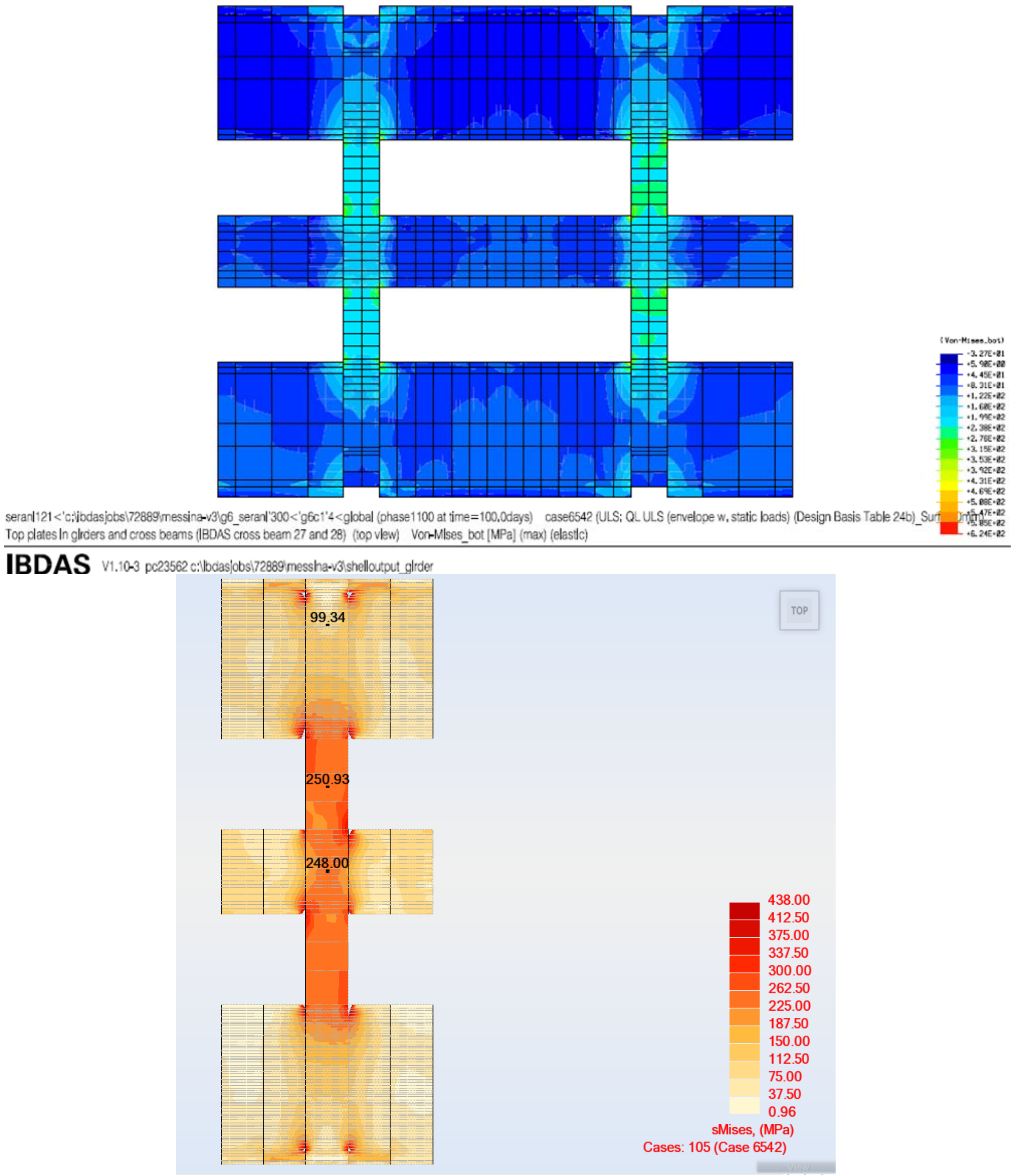


*Figure 2-23 Deck plates, 6542 load case – stress von Mises*

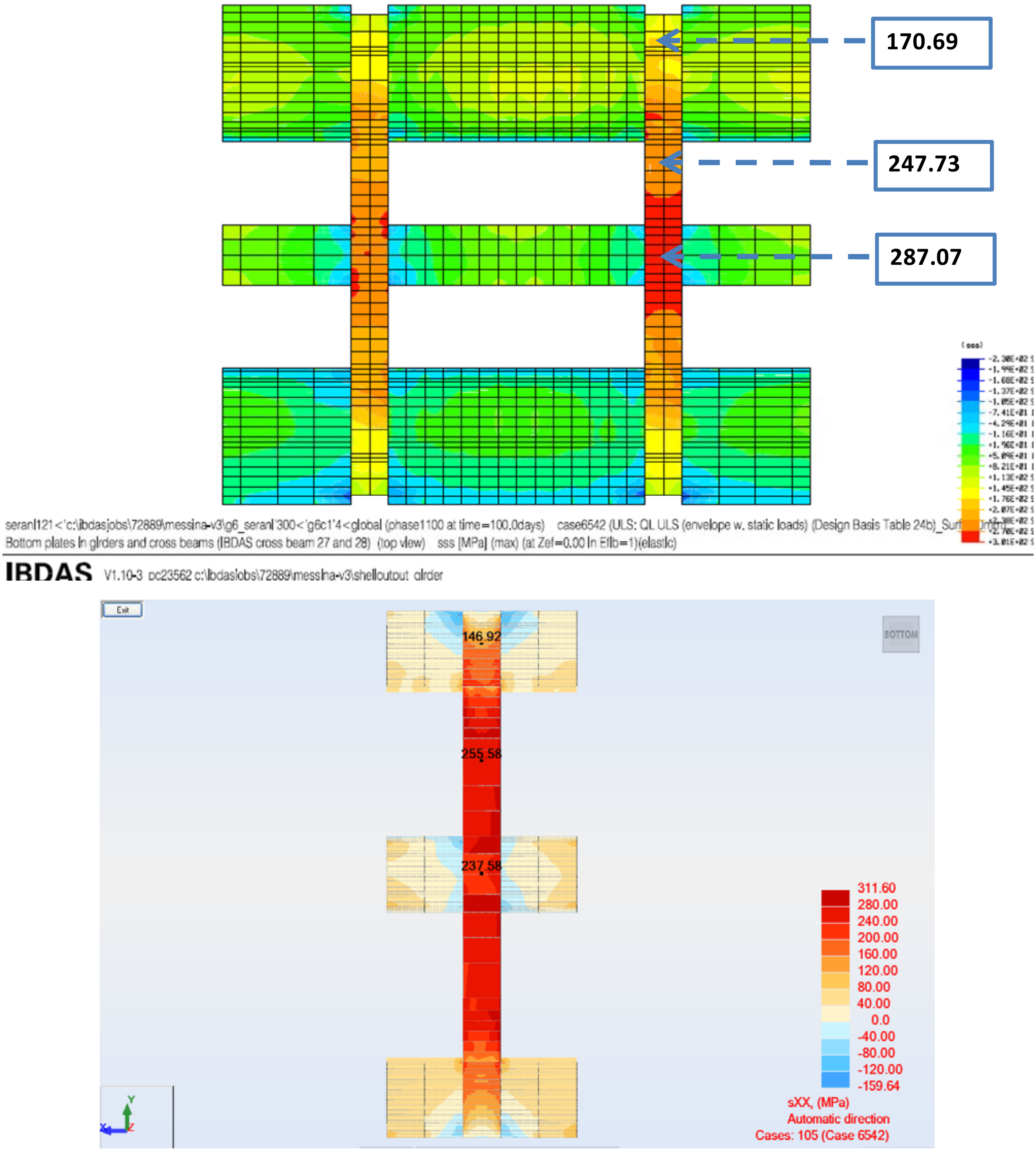


*Figure 2-24 Bottom plates, 6542 – stress sXX*

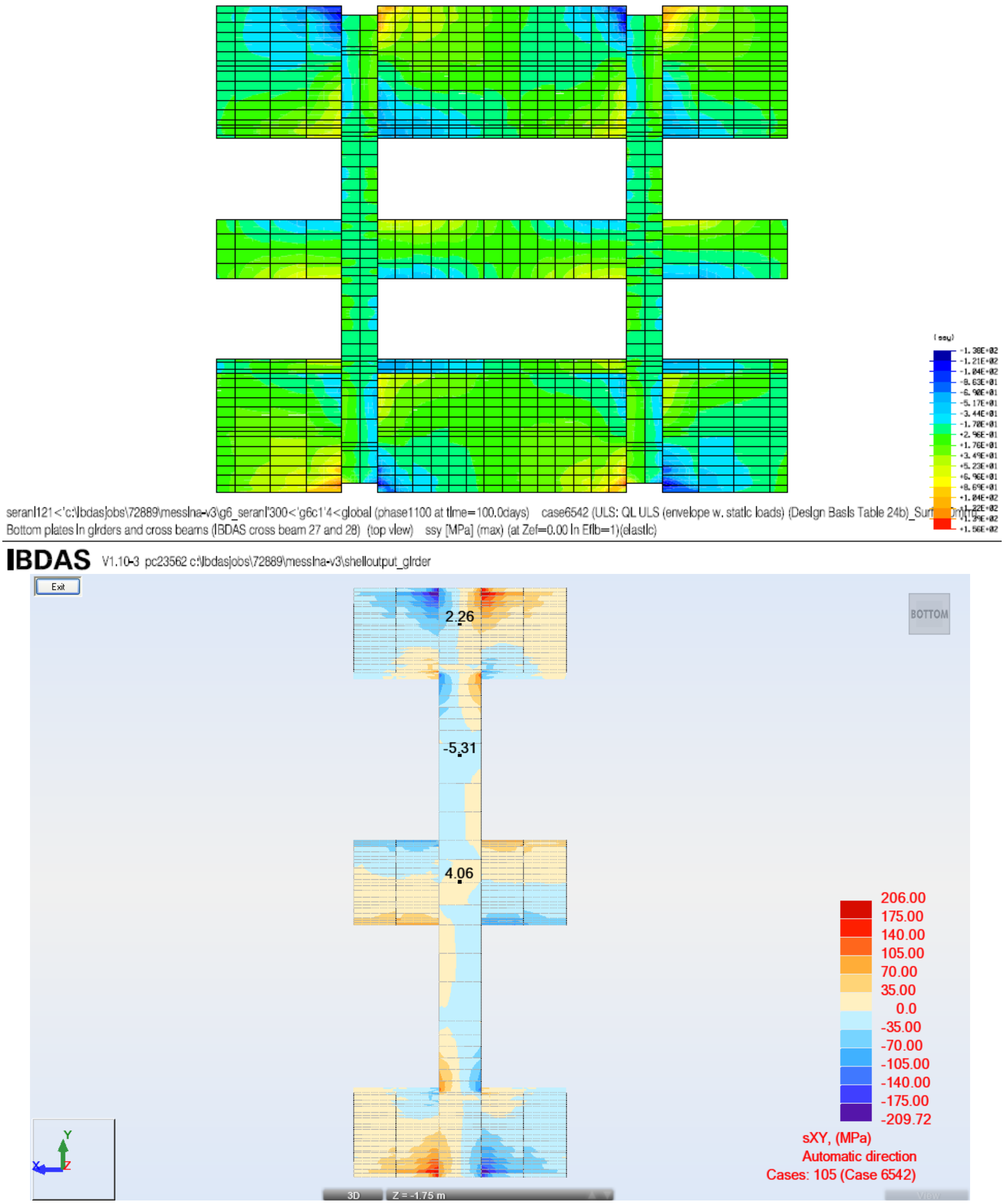


*Figure 2-25 Bottom plates, 6542 – stress sXY*

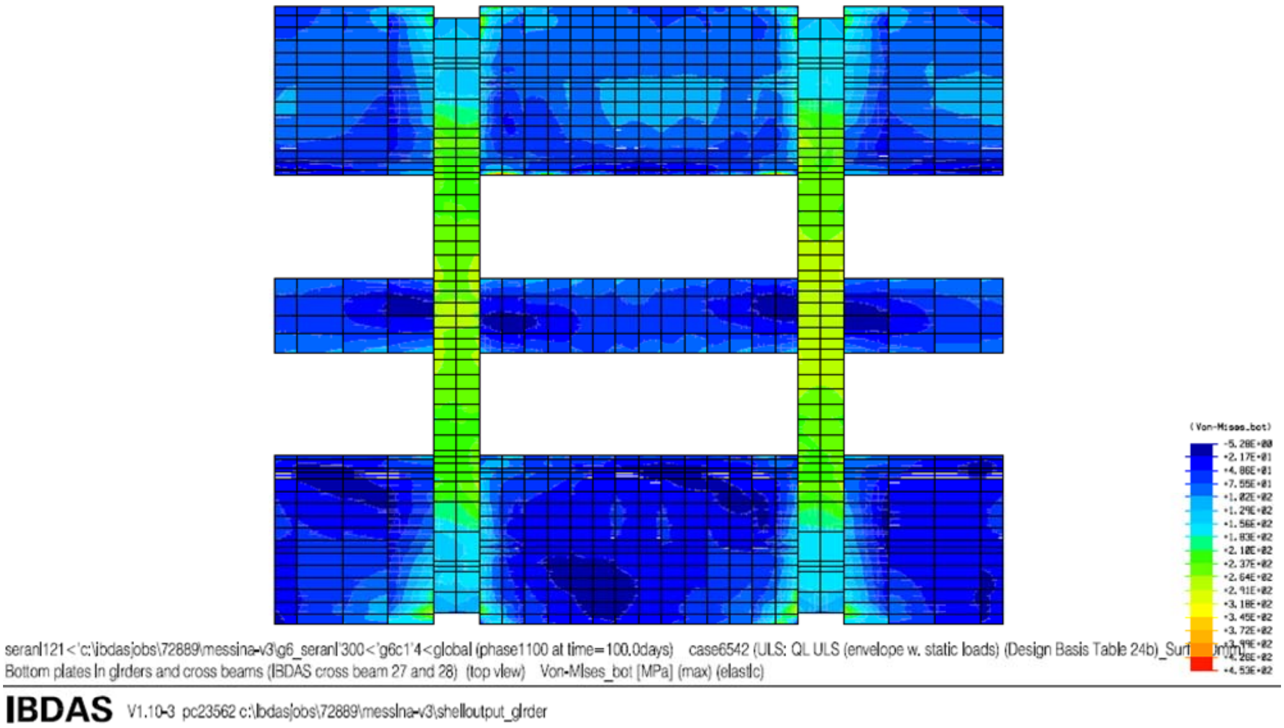


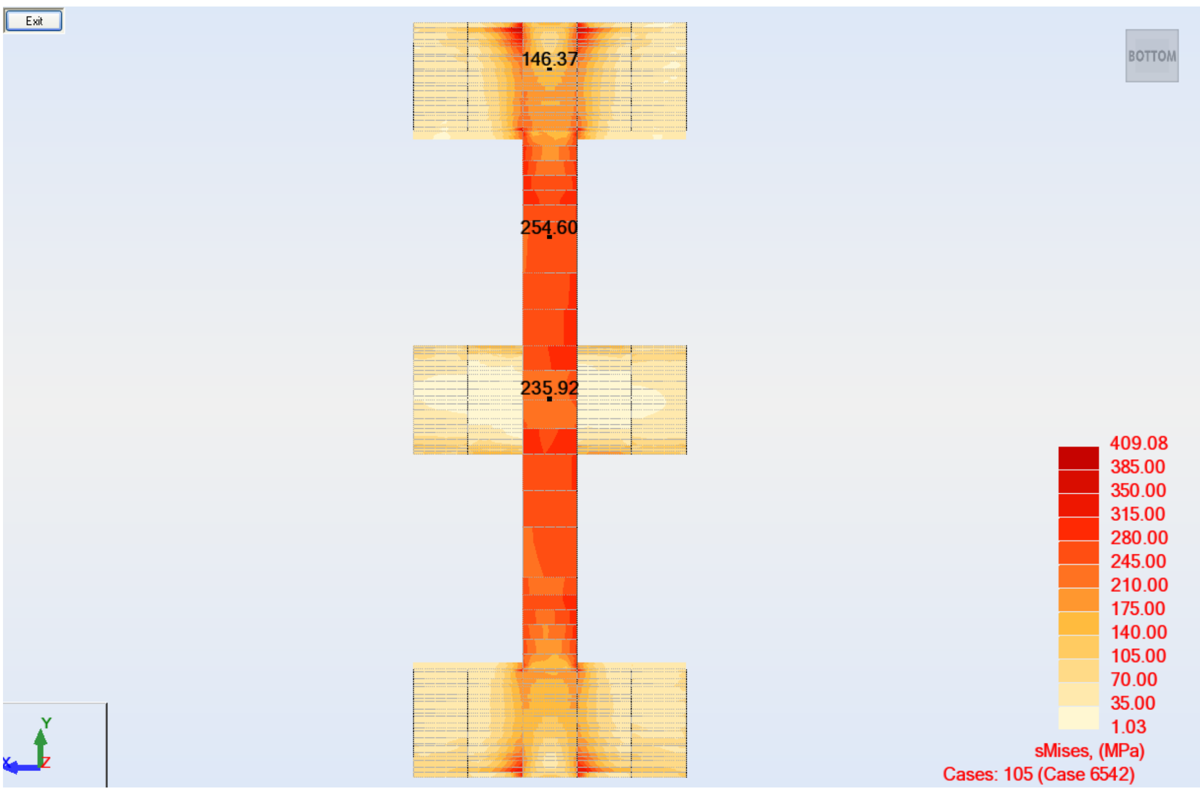


*Figure 2-26 Bottom plates, 6542 – stress von Mises*

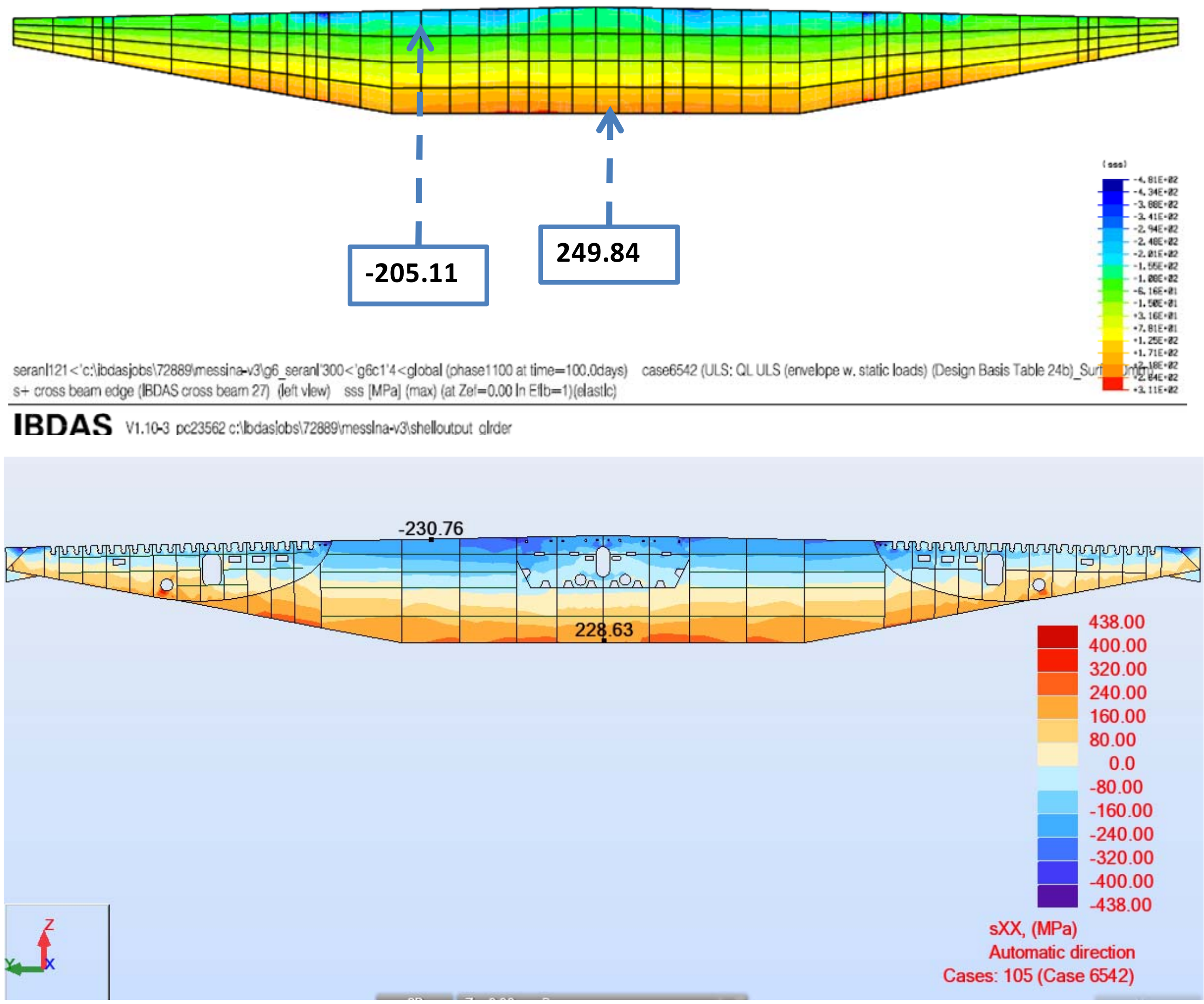


*Figure 2-27 Cross girder web, 6542 – stress sXX*

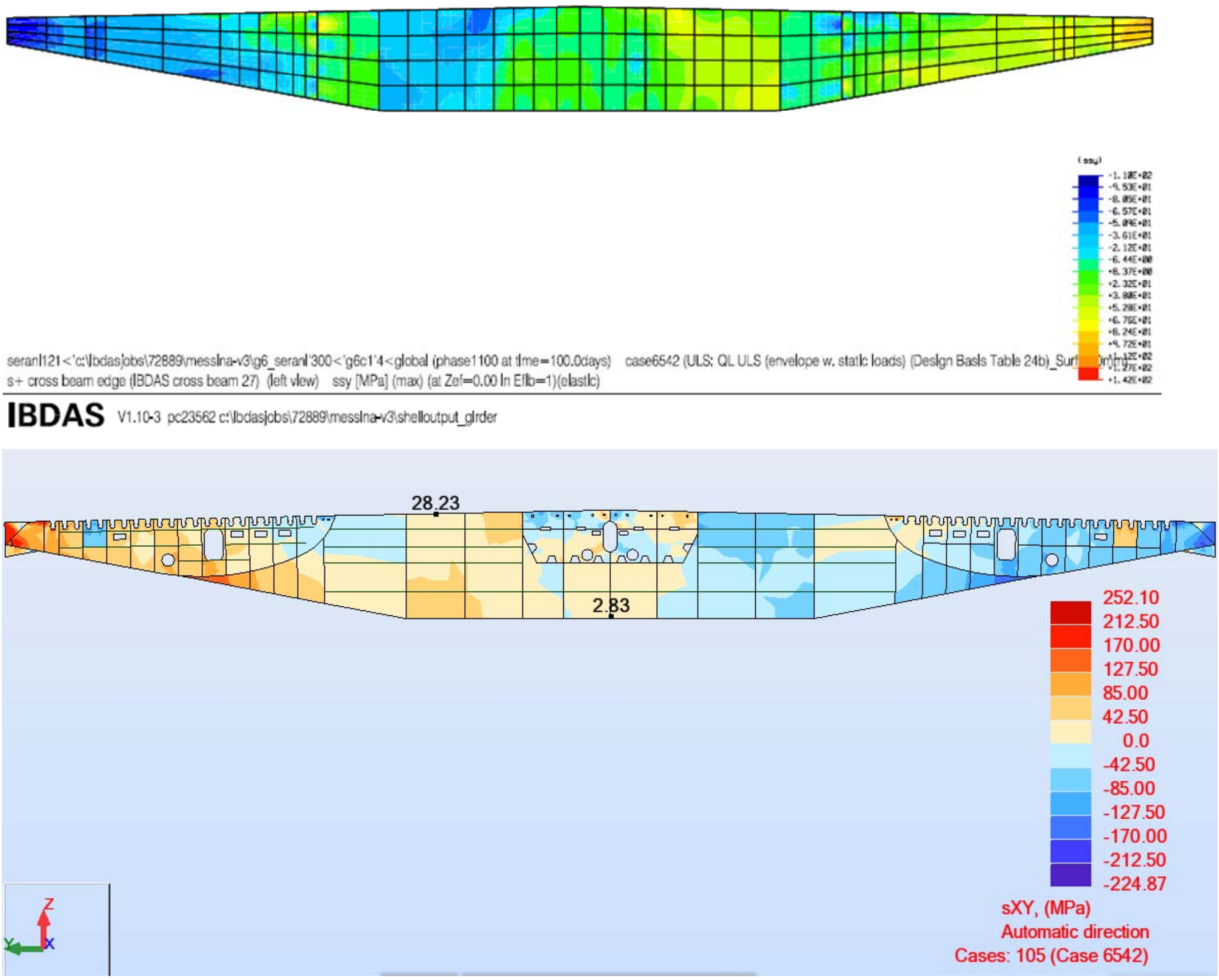


*Figure 2-28 Cross girder web, 6542 – stress sXY*

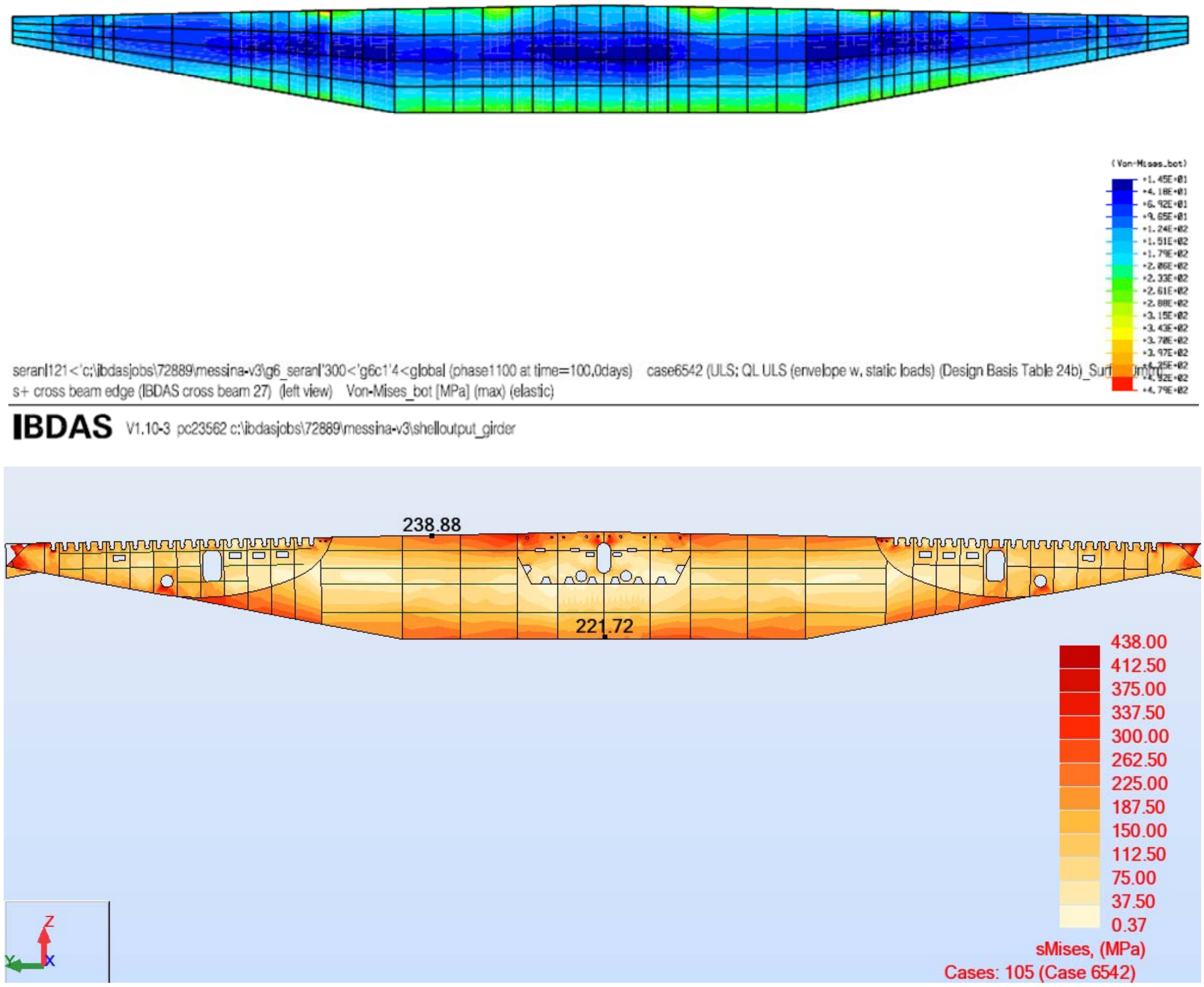


*Figure 2-29 Cross girder web, 6542 – stress von Mises*

### 2.1.3 Stress flow at cross girder intersection with longitudinal girders

In the following contour plots the cross girder webs at the intersection with the longitudinal girders are presented. The scope has been to verify the stress level at sensible location such as openings in the cross girders and generally where reduced web height can lead to yielding such as close to the hangers.

In the following a short documentation of the von Mises stresses is given. The stress limit has been limited to the design yielding stress of $f_{yk}/\gamma_{m0}$ which correspond to 460/1,05=438MPa (the steel grade of all steel elements at the location of the FE-model correspond to S460). For simplicity transition roundings at the top plates at the intersection between the longitudinal girder and the cross girder have not been modelled with the consequence of high stress concentration around the corners as seen in Figure 2-30 and Figure 2-31. Areas where the stress limit is exceeded are shown as transparent.

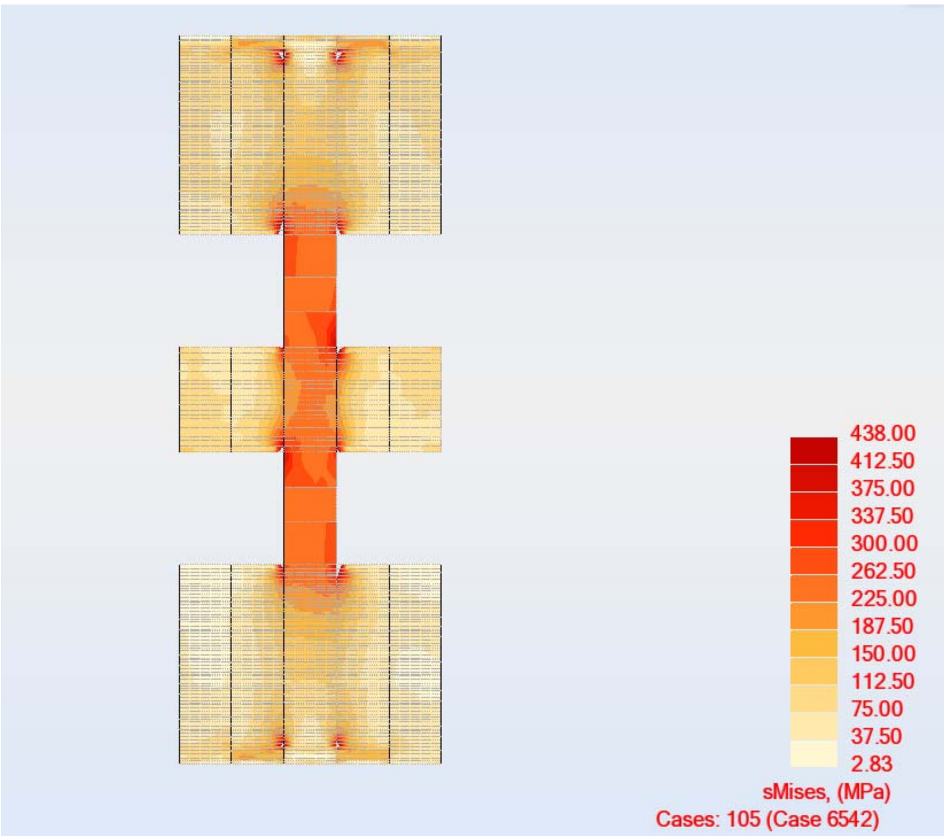


*Figure 2-30 von Mises stresses – Top plates – Case 6532 (Max sagging moment cross girder)*

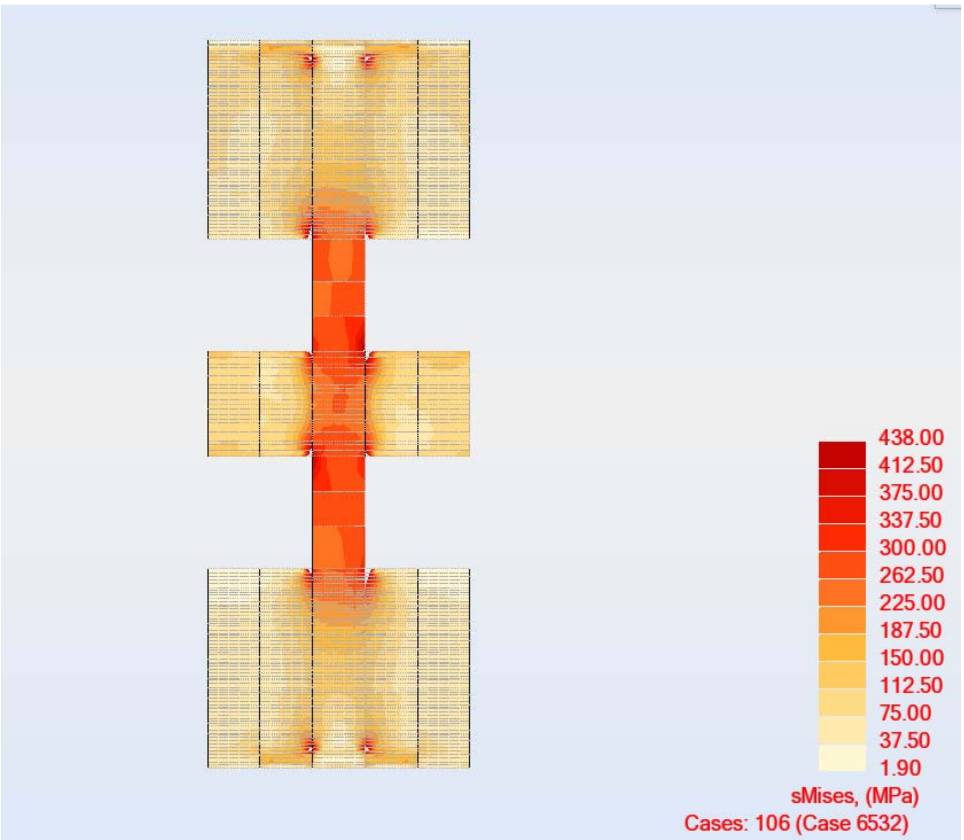


*Figure 2-31 von Mises stresses – Top plates – Case 6542 (Max tension in hanger)*

The above mentioned stress concentrations are merely a result of the detail level of the model at these locations and will not be real; they do not represent an issue for the general design.

Stress concentrations can also be seen around the cross girder manhole at the railway location. In *Figure 2-33* to Figure 2-35, it can be noticed that this detail is below yielding stress as the correct geometry of the ring stiffeners has been implemented by means of beam elements around the manhole.

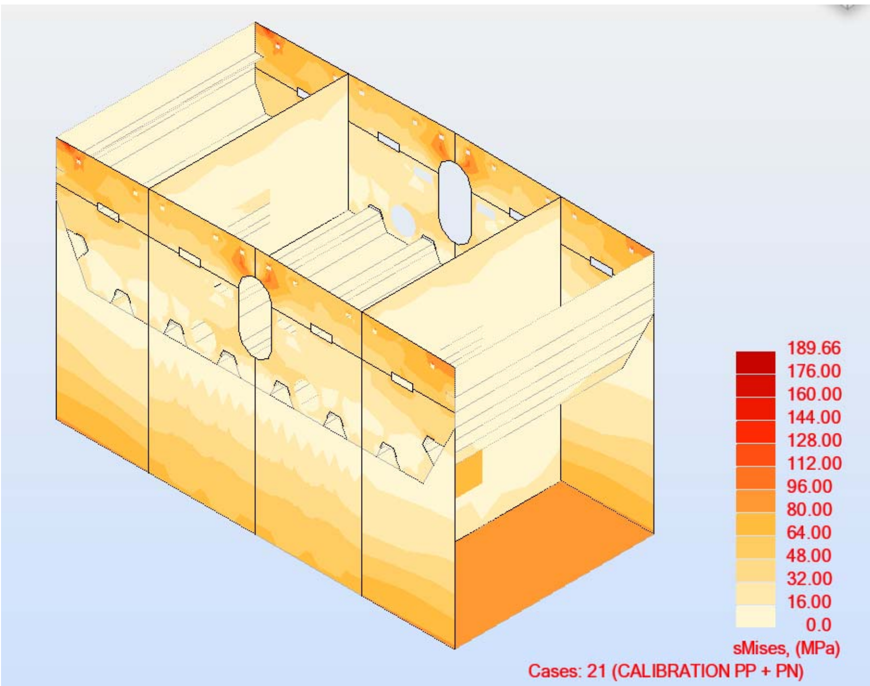


*Figure 2-32 von Mises stresses – Cross girder web at railway intersection – Case 21 (PP+PN)*

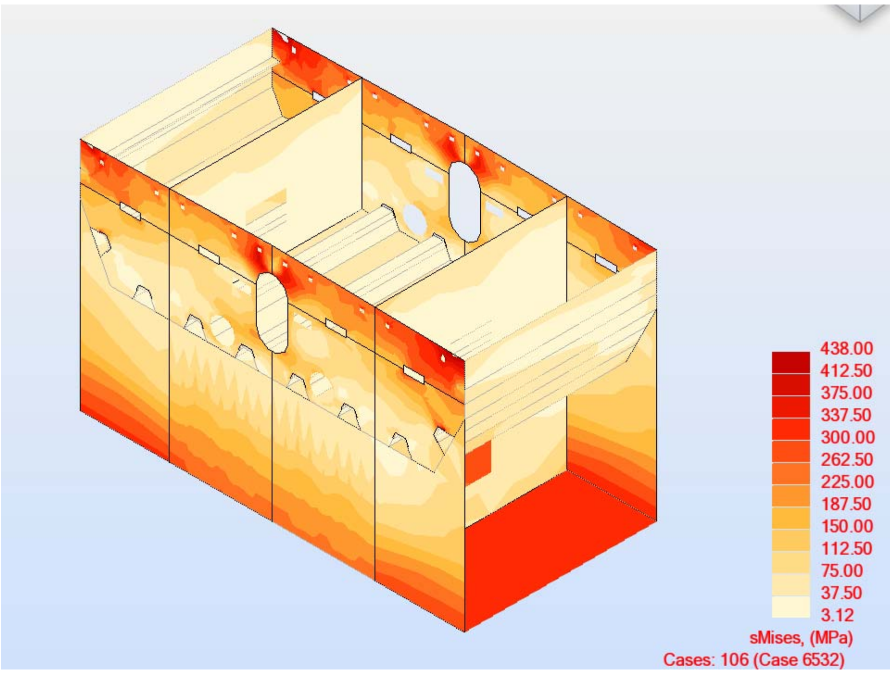


*Figure 2-33 von Mises stresses – Cross girder web at railway intersection – Case 6532 (Max sagging moment cross girder)*

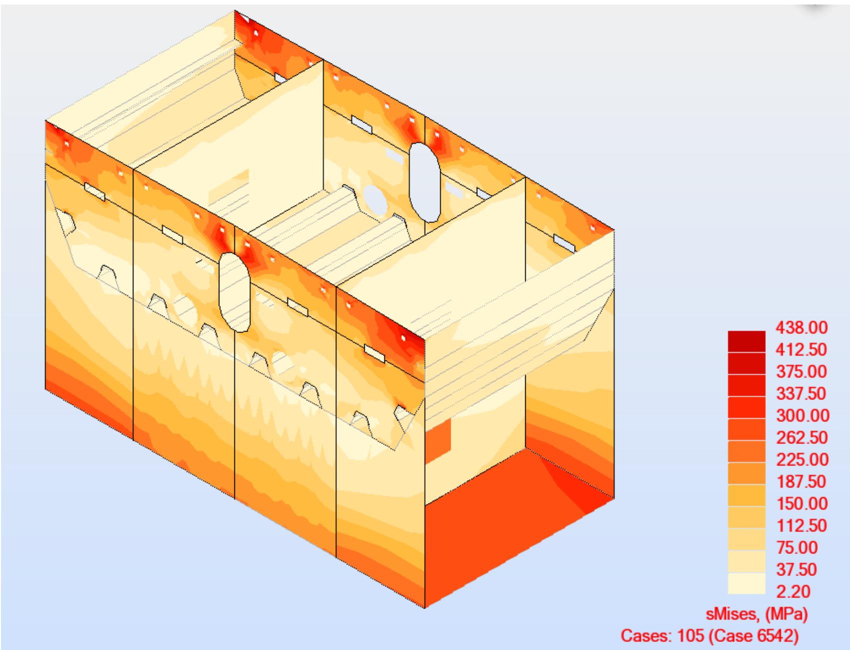


*Figure 2-34 von Mises stresses – Cross girder web at railway intersection – Case 6542 (Max tension in hanger)*

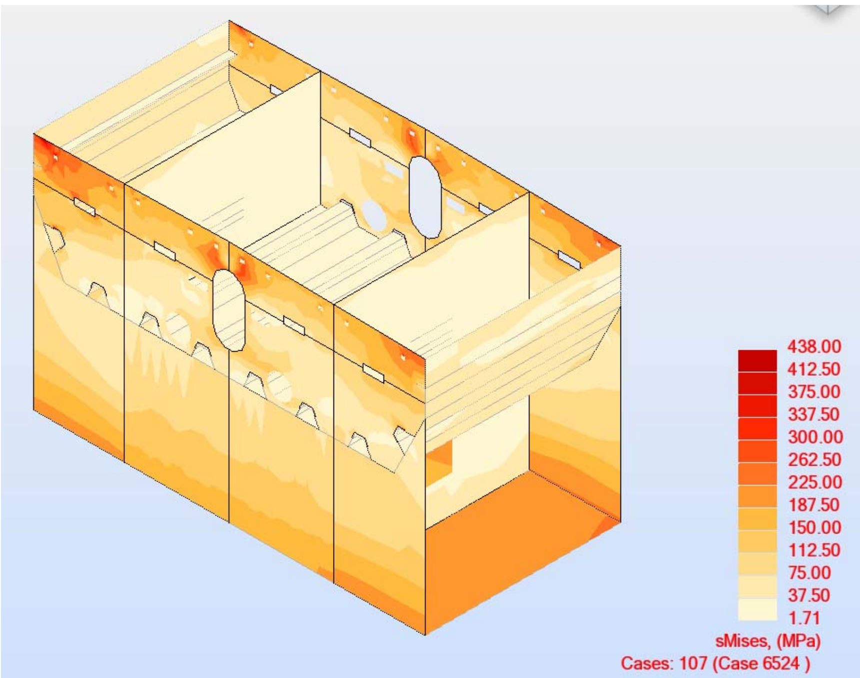


*Figure 2-35 von Mises stresses – Cross girder web at railway intersection – Case 6524 (Max torsion in the railway girder)*

Areas where the design yielding stress is exceeded occur typically at the hanger anchorage where the actual hanger force have been directly applied to the web edge as point loads, see Figure 2-36 to . This excess is a result of the detail level at this location and therefore disregarded in the verification. A more detailed local model of the hanger anchorage can be seen in section 2.4.

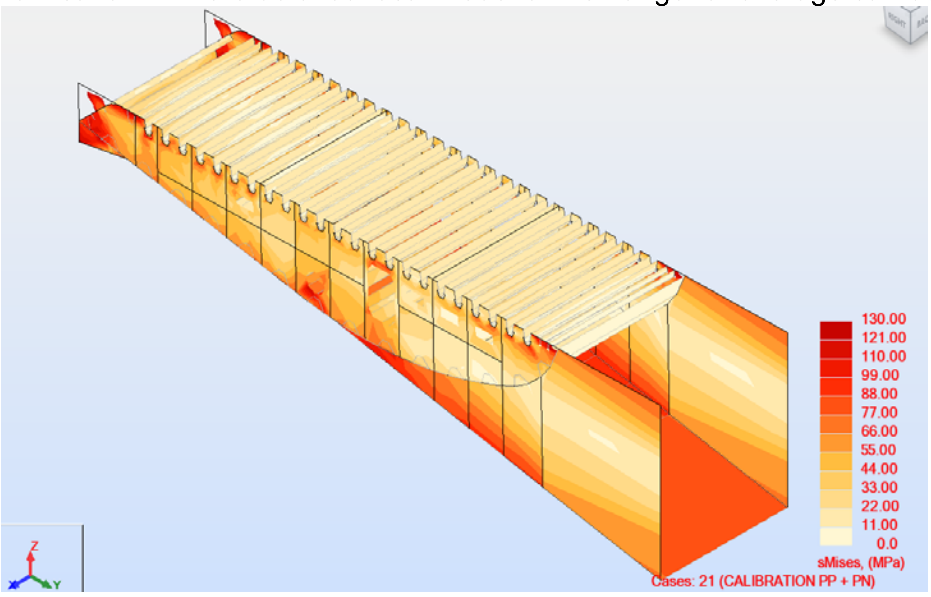


*Figure 2-36 von Mises stresses – Cross girder web at roadway intersection – Case 21 (PP+PN)*

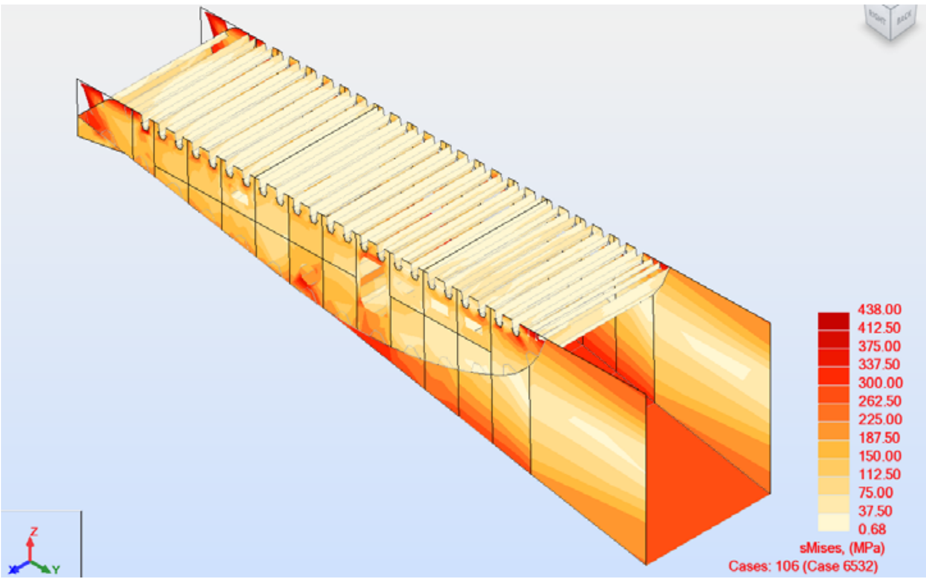


*Figure 2-37 von Mises stresses – Cross girder web at roadway intersection – Case 6532 (Max sagging moment cross girder)*

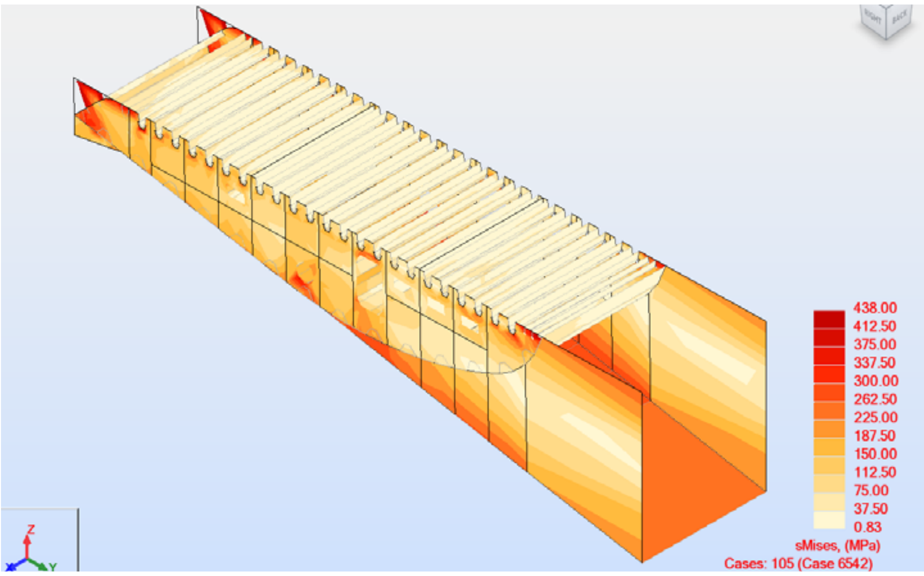


*Figure 2-38 von Mises stresses – Cross girder web at roadway intersection – Case 6542 (Max tension in hanger)*

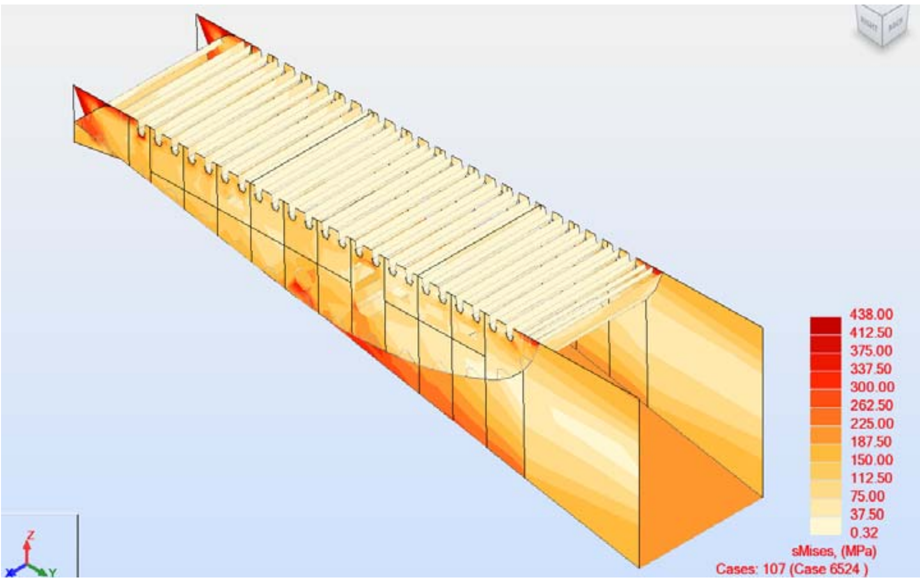


*Figure 2-39 von Mises stresses – Cross girder web at roadway intersection – Case 6524 (Max torsion in the railway girder)*

All von Mises stresses at cross girder intersection with longitudinal girders are within the design yields stresses.

### 2.1.4 Stress level in the cross girder diaphragms

The von Mises stresses in the diaphragms are shown for following load cases:

- Load combination 6532, Max sagging moment cross girder
- Load combination 6542, Max tension in hanger
- Load combination 6524, Max torsion in railway girder

As seen from Figure 2-40 to Figure 2-42  all stresses are within the design yields stresses.

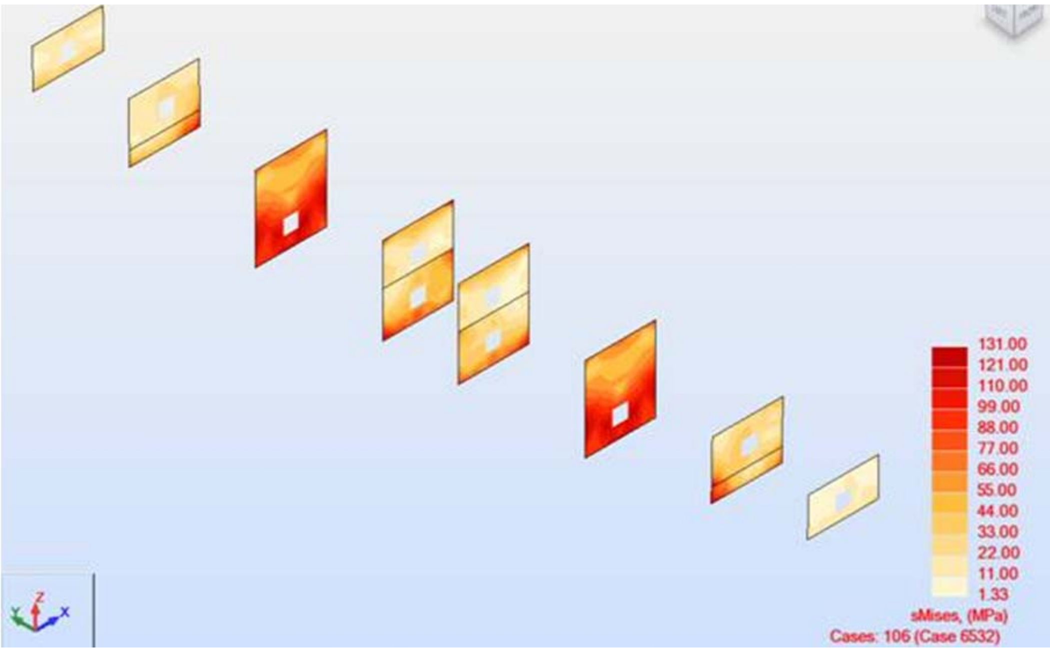


*Figure 2-40 von Mises stresses – Cross girder diaphragms – Case 6532 (Max sagging moment cross girder)*

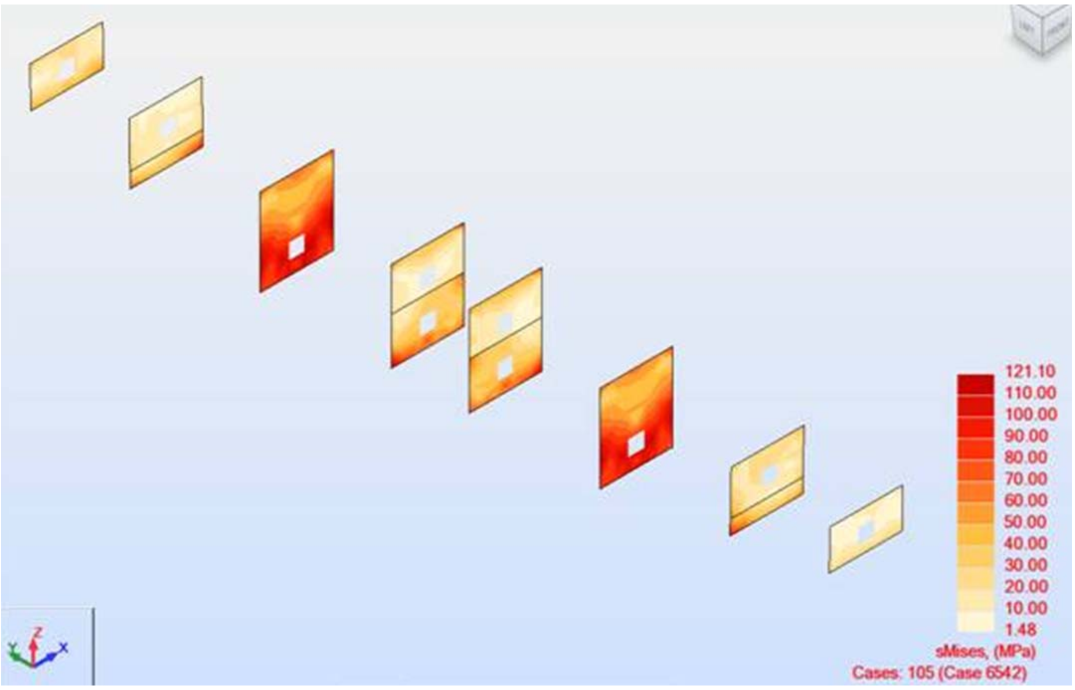


*Figure 2-41 von Mises stresses – Cross girder diaphragms – Case 6542 (Max tension in hanger)*

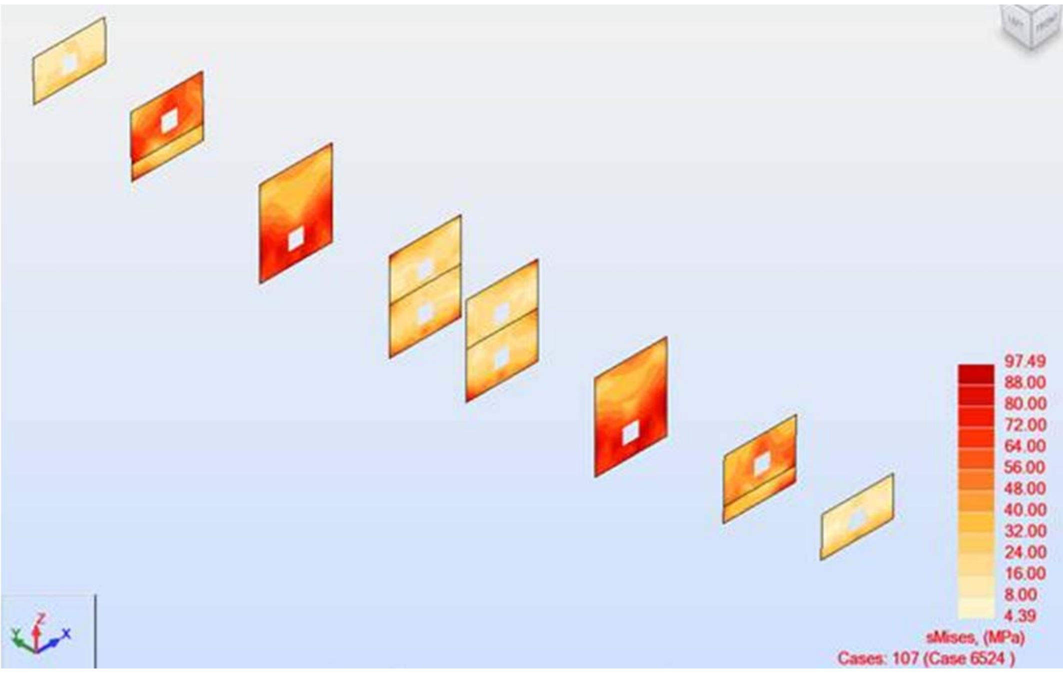


*Figure 2-42 von Mises stresses – Cross girder web at roadway intersection – Case 6524 (Max torsion in the railway girder)*

## 2.2 Local FE-Model of Roadway Girder

A detailed description of the local FE-model of the roadway girder can be found in the report "General Design Principles for Suspended Deck".

### 2.2.1 Load cases

The traffic load have been fixated for two load cases in the global IBDAS model in order to maximise the sectional forces in the centre of the span for the roadway:

- My+ (load case 6561, Maximum My in centre of the span)
- Vz+ (load case 6567, Maximum Vz in the centre of the span).

The most critical position of live load has then been applied on the local FE-model according to IBDAS influence line plots.

The only live load action on this model is the traffic, which is applied directly on the local FE-model. For the load cases 6561 and 6567 the heaviest traffic load have been applied in the traffic lane closest to the service lane, however in order to maximise the bending moment in the diaphragm (Ms+), a third load case has been introduced in the local FE-model:

- Ms+ (load case 4000, Maximum sagging moment of the diaphragm)

The stresses from the applied traffic load are therefore not superimposed with the stresses from the global section forces. Position of traffic load in load case 6561 My+ is shown in Figure 2-43.

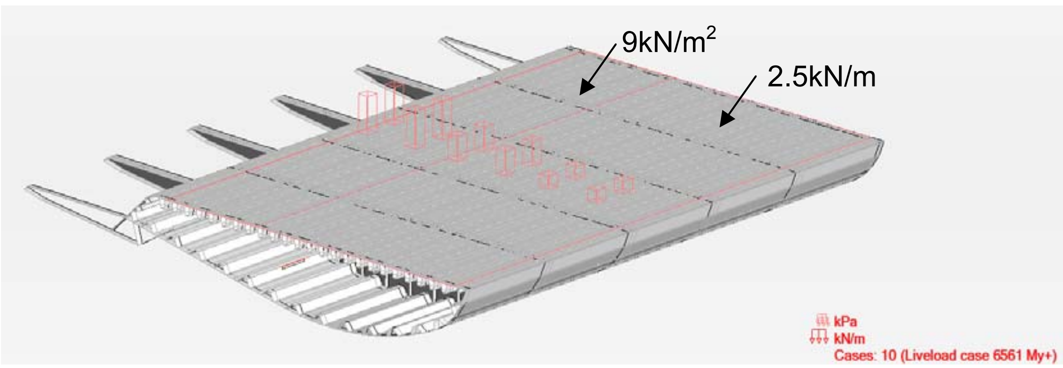


*Figure 2-43 Position of traffic load in load case 6561 (My+)*

Position of traffic load in load case 4000 Ms+ is shown in Figure 2-44.

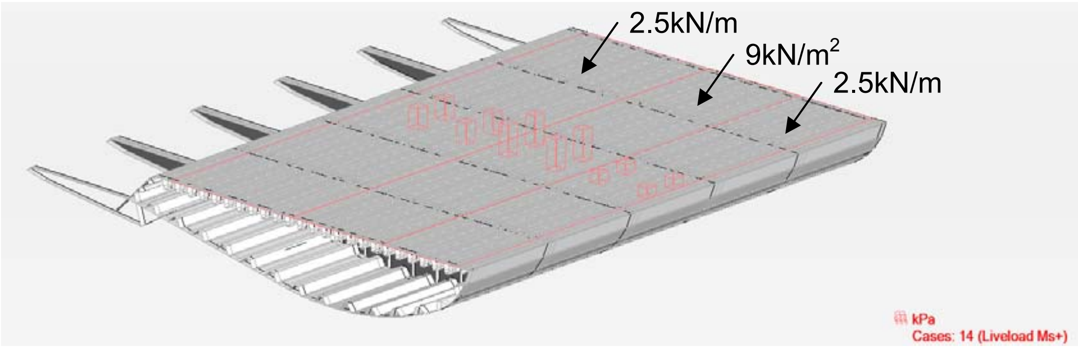


*Figure 2-44 Position of traffic load in load case 4000 (Ms+)*

Position of traffic load in load case 6567 Vz+ is shown in Figure 2-45.

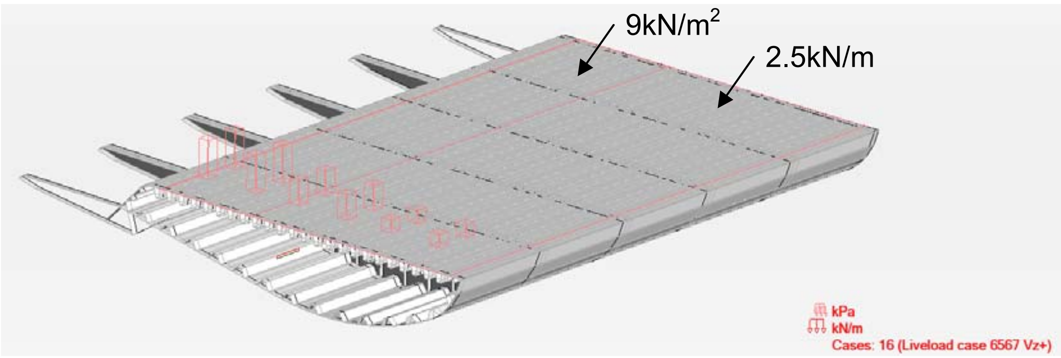


*Figure 2-45 Position of traffic load in load case 6567 (Vz+)*

### 2.2.2 Stress verification and comparison with semi-local IBDAS model

In the following the stresses in the roadway girder are presented as axial stresses and von Mises stresses. At the considered bridge stationing the section is equivalent to the geometry of CS3 with a design yielding stress of $f_{yk}/\gamma_{m0}$ which correspond to 460/1.05=438MPa.

An overview of the comparison between roadway local FE-model and IBDAS semi-local model is given in Table 2-4. The structural elements investigated, load combinations and the layer where the stresses have been calculated are presented.

The comparison has been performed for My+ (LC 6561). For this load combination the longitudinal and transverse stresses, sXX and sYY, have been compared for the deck and bottom plate, and transverse and vertical stresses are compared for the diaphragms.

Detailed description of load cases can be found in the document "General Design Principles for Suspended Deck".

*Table 2-4 Stresses used for comparison*

| | Element | Stress | Panel layer |
|---|---|---|---|
| Maximum My+ (LC6561) | Deck plate | sXX, sYY | Middle |
| | Bottom plate | sXX, sYY | Middle |
| | Diaphragm | sXX, sYY | Middle |
| Maximum Vz+ (LC6567) | Deck plate | sXX, sYY | Middle |
| | Bottom plate | sXX, sYY | Middle |
| | Diaphragm | sXX, sYY | Middle |

In following figures, a full set of results of the above mentioned stresses are presented. Each figure are showing the IBDAS stress plot in the top of the figure, and ROBOT plot in the bottom for comparison. A colour chart of the stress magnitude is also included in the plots. A difference in the stress colour can be noticed for the two stress plots, but this does not represent a relevant difference of the stress level. The results of the main stress direction sXX and sYY are pointed out and compared for both models in three characteristic points.

A summary of the results including the percentage variation of stresses between the models can be seen in Table 2-5 for load case My+.

*Table 2-5 Summary of comparison of stresses calculated in semi-local IBDAS FE-model and local Robot FE-model*

| | Element | Section | Stress | IBDAS [MPa] | ROBOT [MPa] | Deviation from IBDAS |
|---|---|---|---|---|---|---|
| Maximum My+ (LC6561) | Deck Plate Longitudinal | 1 | sXX | 16.1 | 13.0 | -23.9% |
| | | 2 | sXX | -31.5 | -36.1 | 12.7% |
| | | 3 | sXX | -68.7 | -78.4 | 12.4% |
| | Deck Plate Transverse | 1 | sYY | -0.1 | 0.9 | 111.1% |
| | | 2 | sYY | -16.7 | -16.5 | -1.2% |
| | | 3 | sYY | -5.1 | -5.8 | 12.2% |
| | Bottom Plate Longitudinal | 1 | sXX | 155.7 | 147.6 | -5.5% |
| | | 2 | sXX | 242.5 | 246.6 | 1.7% |
| | | 3 | sXX | 15.1 | 12.7 | -18.9% |
| | Bottom Plate Transverse | 1 | sYY | 7.2 | 7.8 | 7.7% |
| | | 2 | sYY | 41.8 | 42.0 | 0.5% |
| | | 3 | sYY | 3.5 | 1.8 | -94.4% |
| | Diaphragm | 1 | sXX | -20.6 | -20.1 | -2.5% |
| | | 2 | sXX | -4.3 | -5.0 | 14.0% |
| | | 3 | sXX | 12.9 | 16.2 | 20.4% |
| | | 4 | sXX | -16.0 | -16.3 | 1.8% |
| | | 5 | sXX | -11.2 | -11.1 | -0.9% |

Table 2-5 shows relatively high deviations for this stress comparison. Taking the relative stresses into consideration, the results of the comparison are very reasonable.

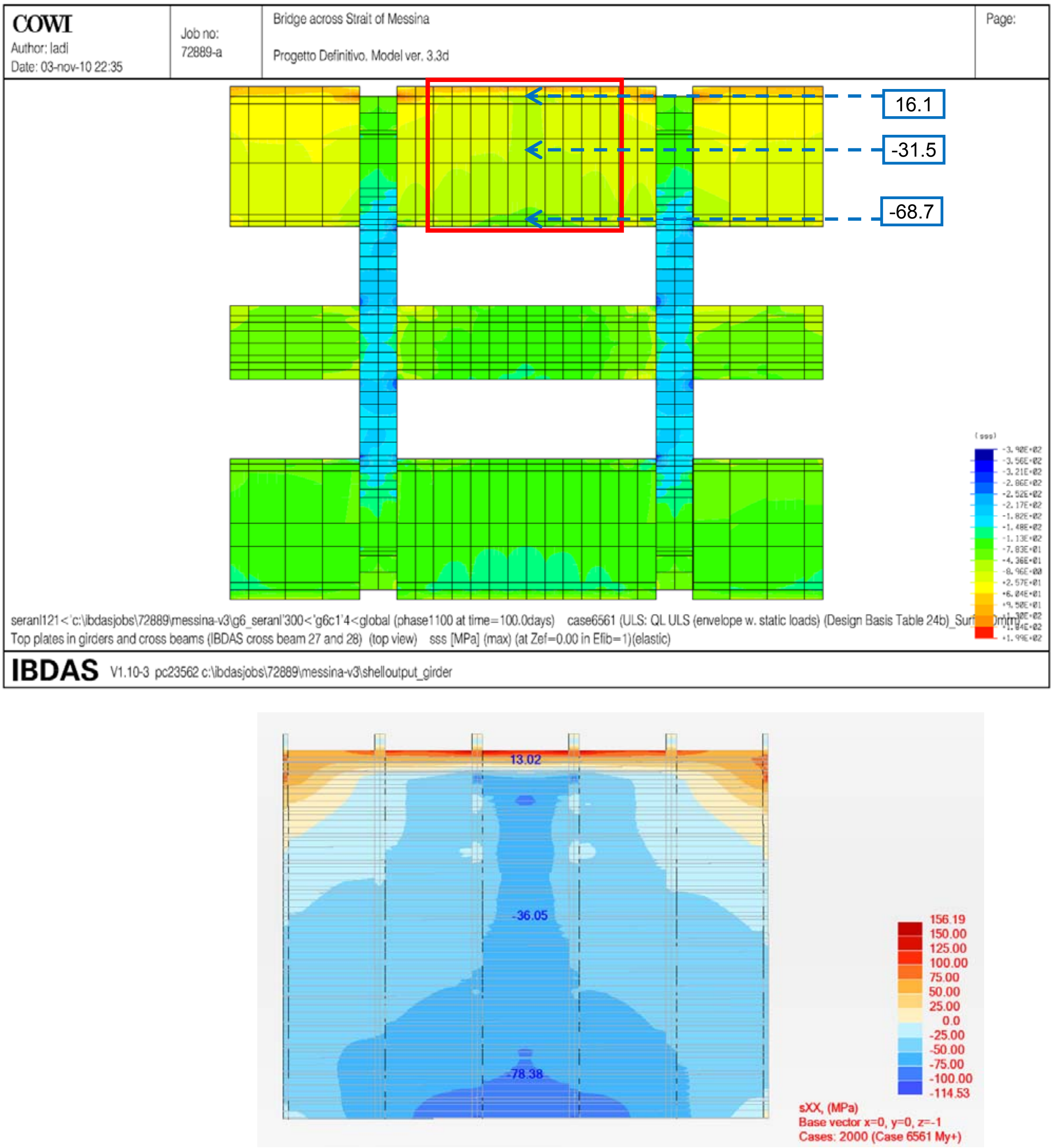


*Figure 2-46 Longitudinal stresses – Deck plate – Case 6561 (My+)*

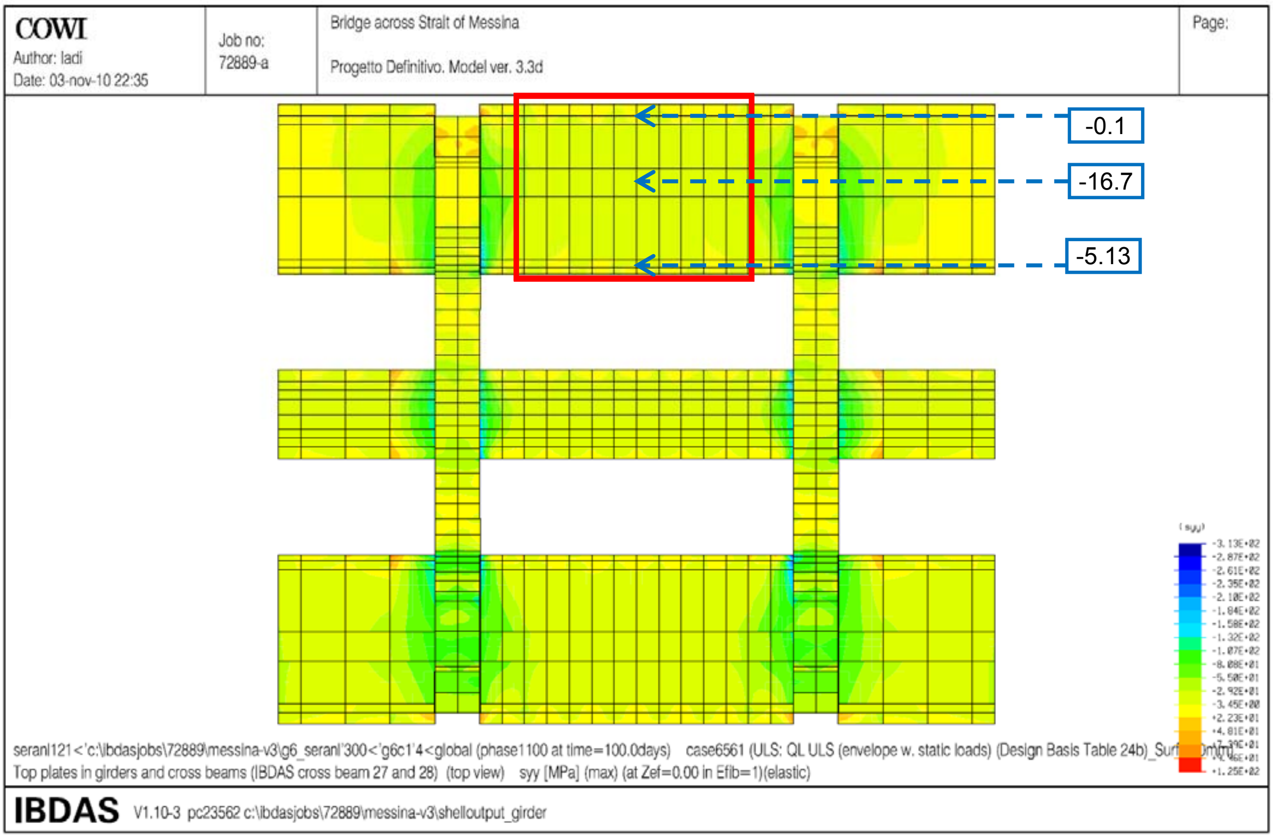


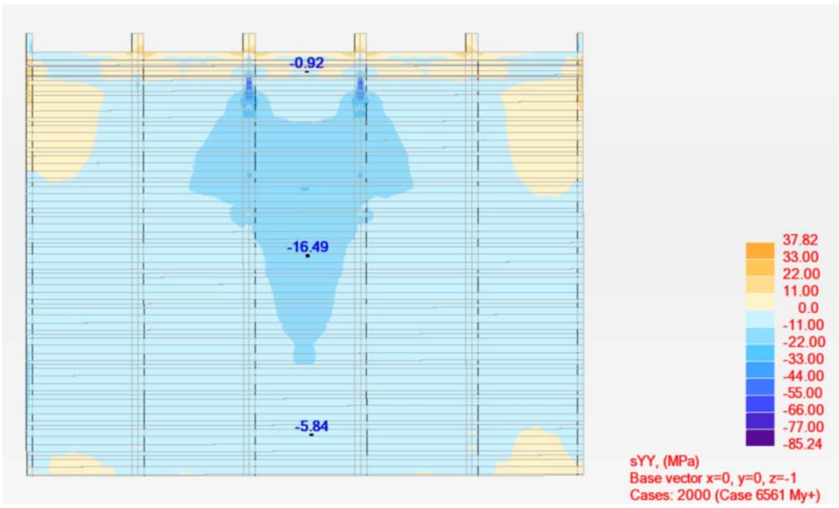


*Figure 2-47 Transverse stresses – Deck plate – Case 6561 (My+)*

The distribution shown in Figure 2-47 for the local FE-model does not appear with exactly the same contour in the plot from the semi-local IBDAS model, but as seen the stress level in the selected points correspond very well.

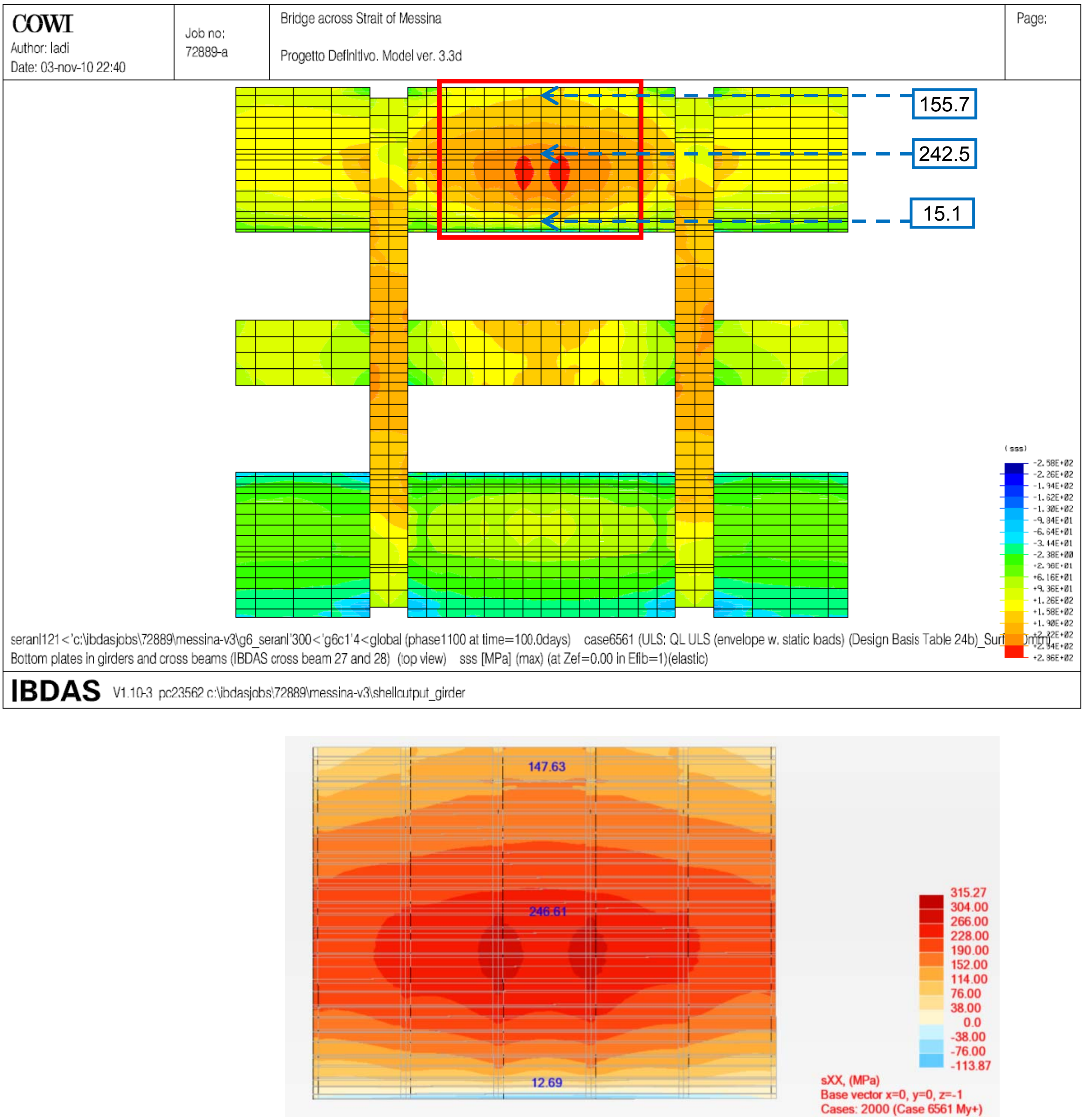


*Figure 2-48 Longitudinal stresses – Bottom plate – Case 6561 (My+)*

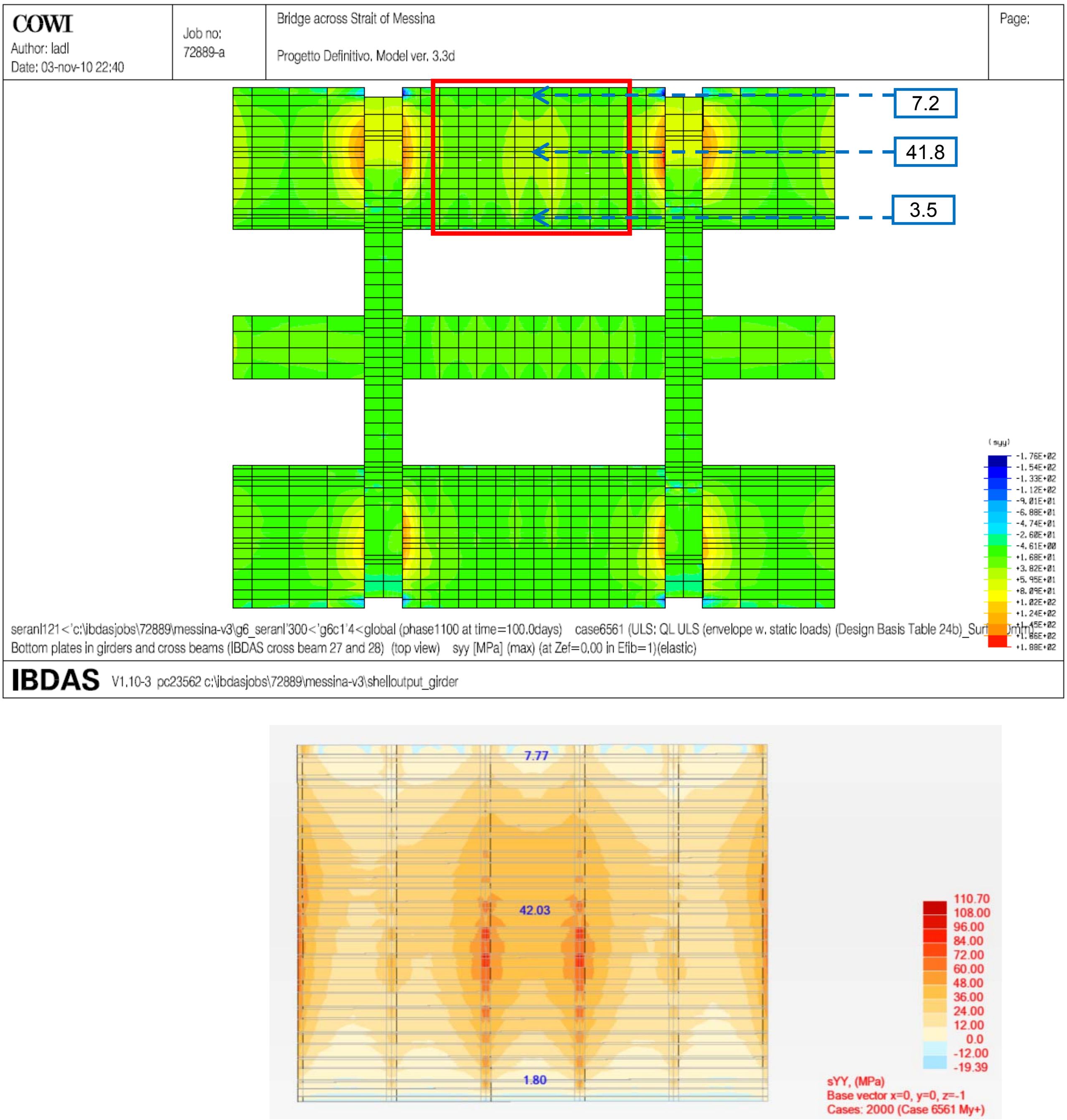


*Figure 2-49 Transverse stresses – Bottom plate – Case 6561 (My+)*

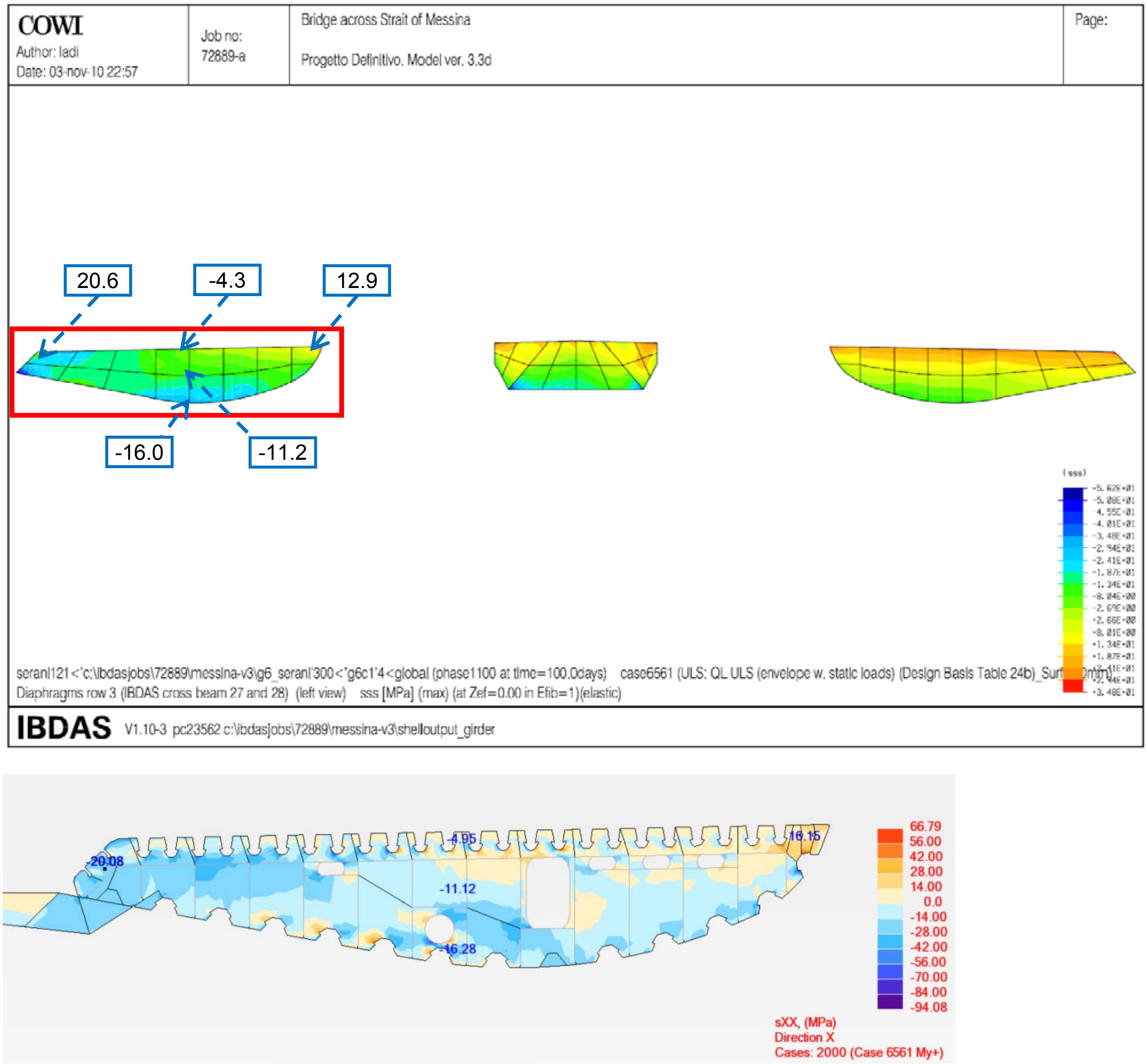


*Figure 2-50 Transverse stresses – Diaphragm – Case 6561 (My+)*

The difference in the stress distribution from the eastern to the westeren roadway girder is caused by difference in the position of the local traffic load in the two girders for this local case.

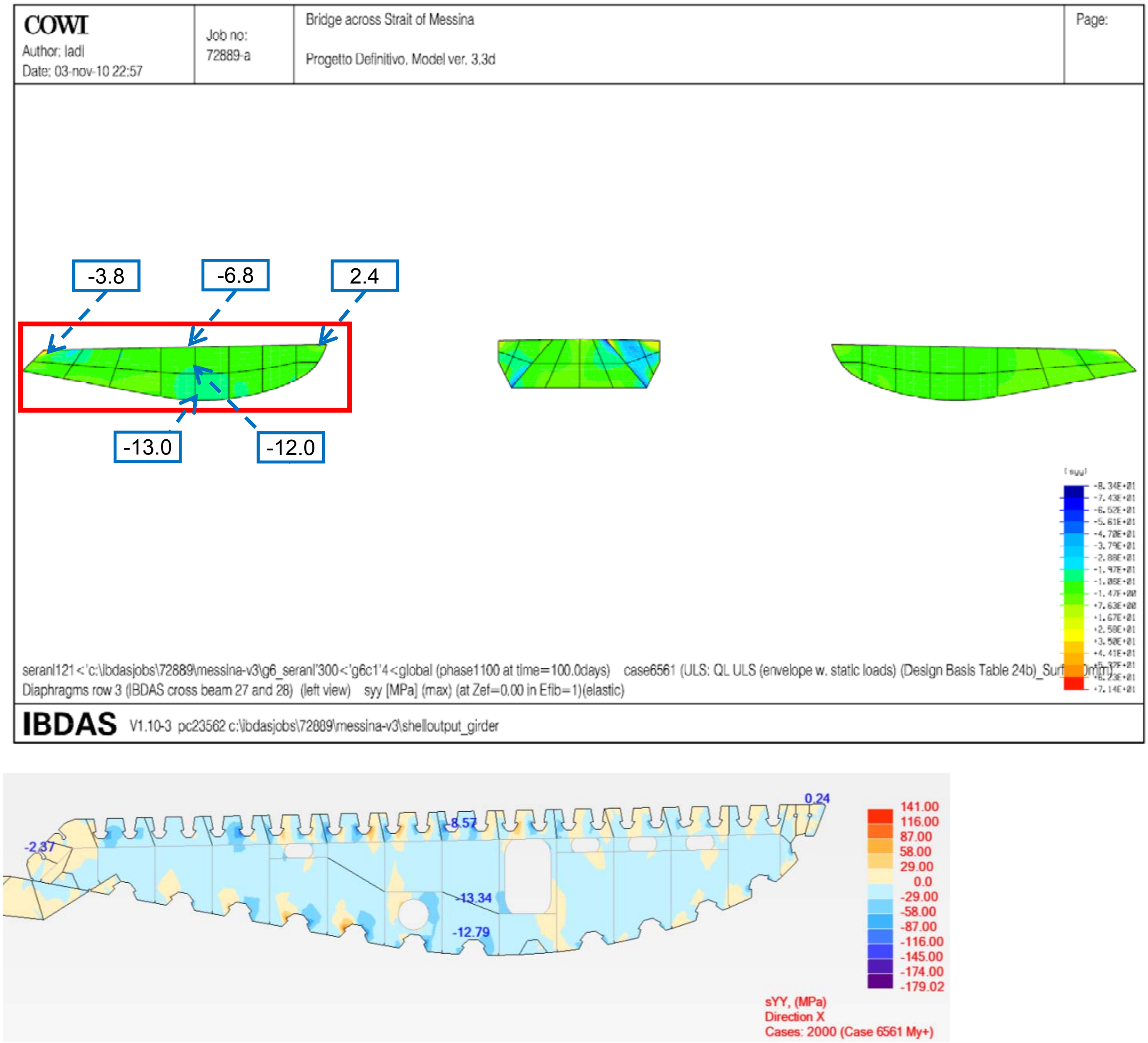


*Figure 2-51 Vertical stresses – Diaphragm – Case 6561 (My+)*

The stress distribution in Figure 2-50 and Figure 2-51 for the global IBDAS model appears more even distributed compared with the stress distribution from the local FE-model. This is caused by openings and stiffeners in the local FE-model.

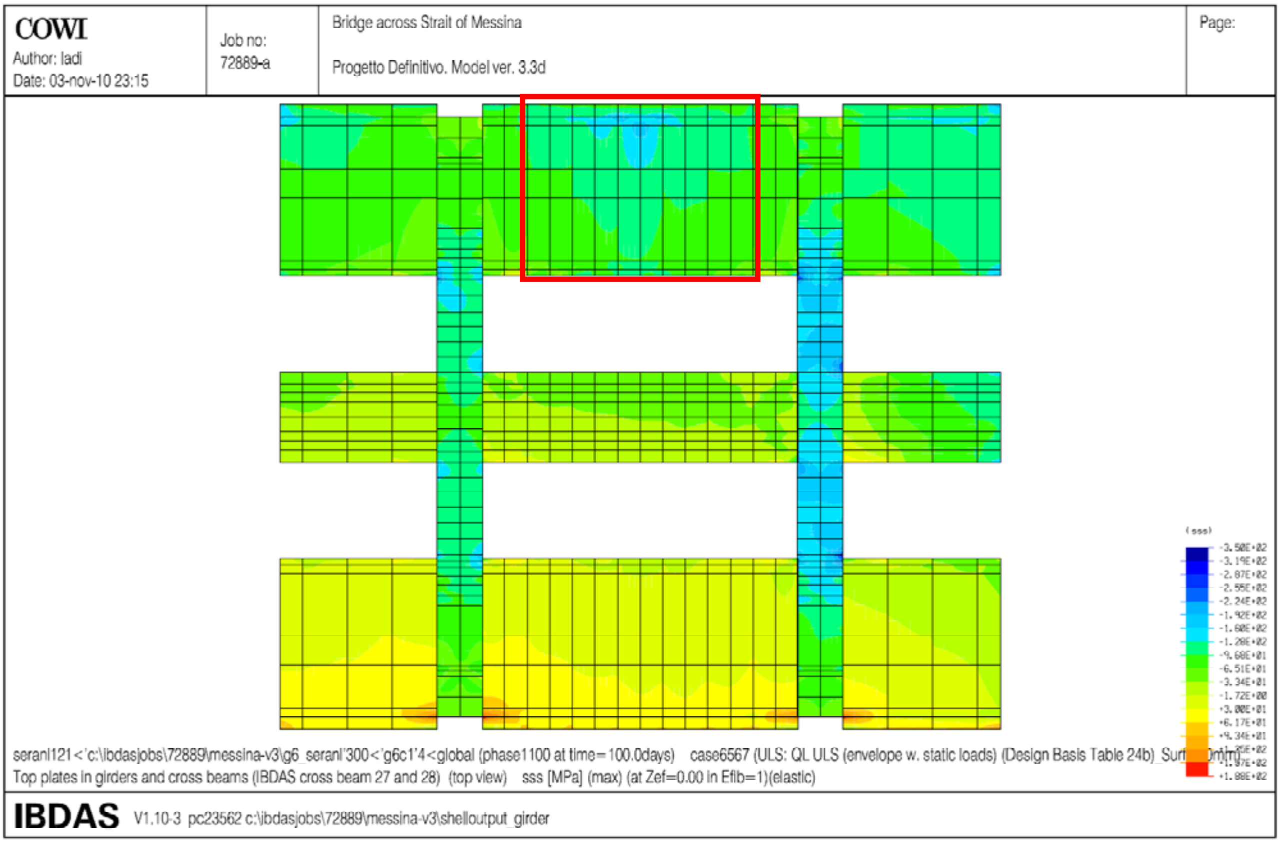


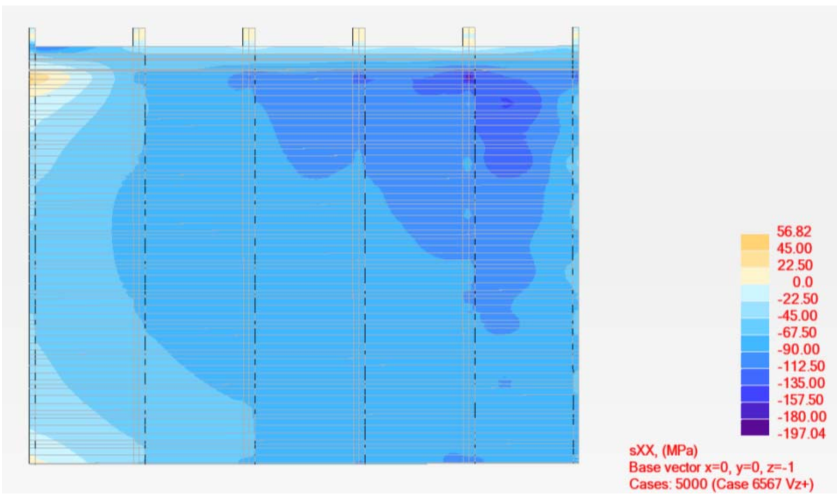


*Figure 2-52 Longitudinal stresses – Deck plate – Case 6567 (Vz+)*

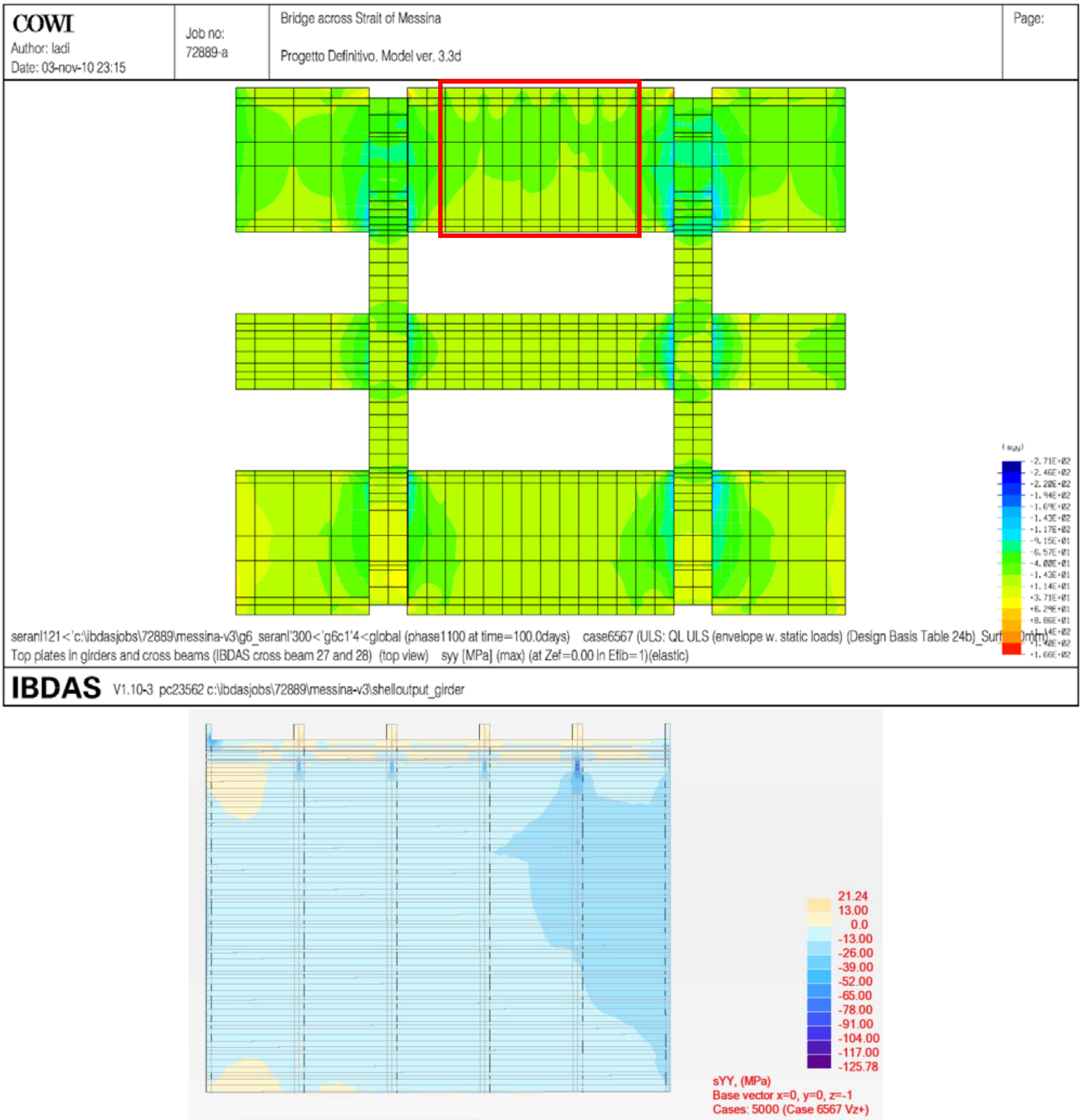


*Figure 2-53 Transverse stresses – Deck plate – Case 6567 (Vz+)*

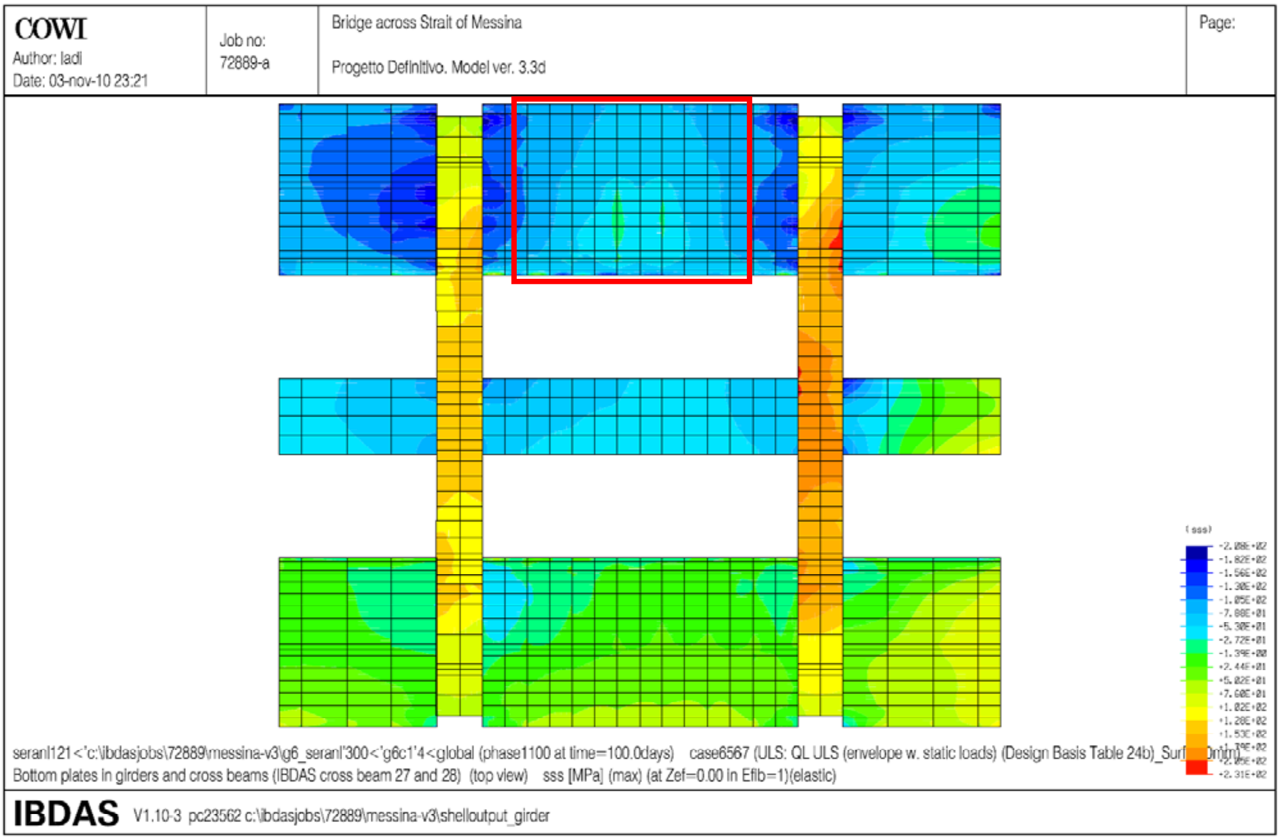


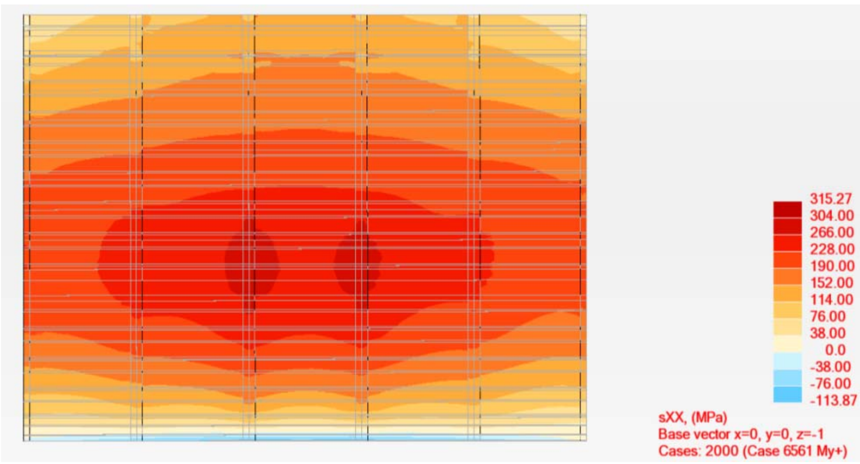


*Figure 2-54 Longitudinal stresses – Bottom plate – Case 6567 (Vz+)*


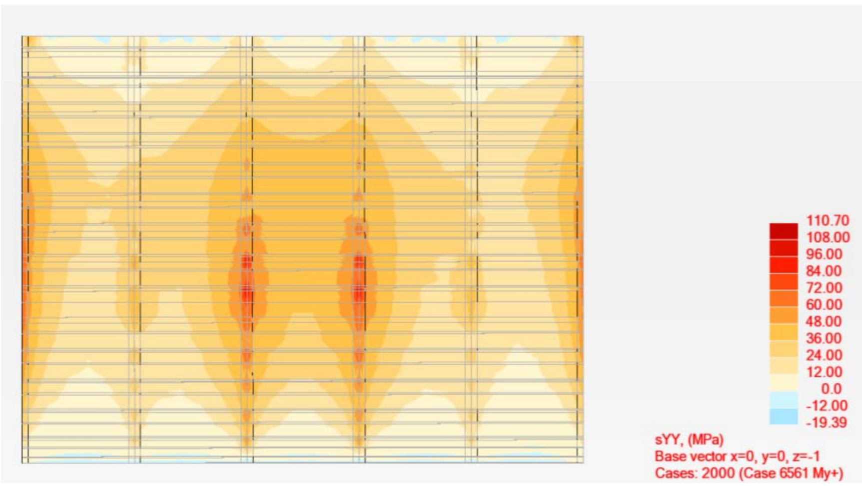


*Figure 2-55 Transverse stresses – Bottom plate – Case 6567 (Vz+)*

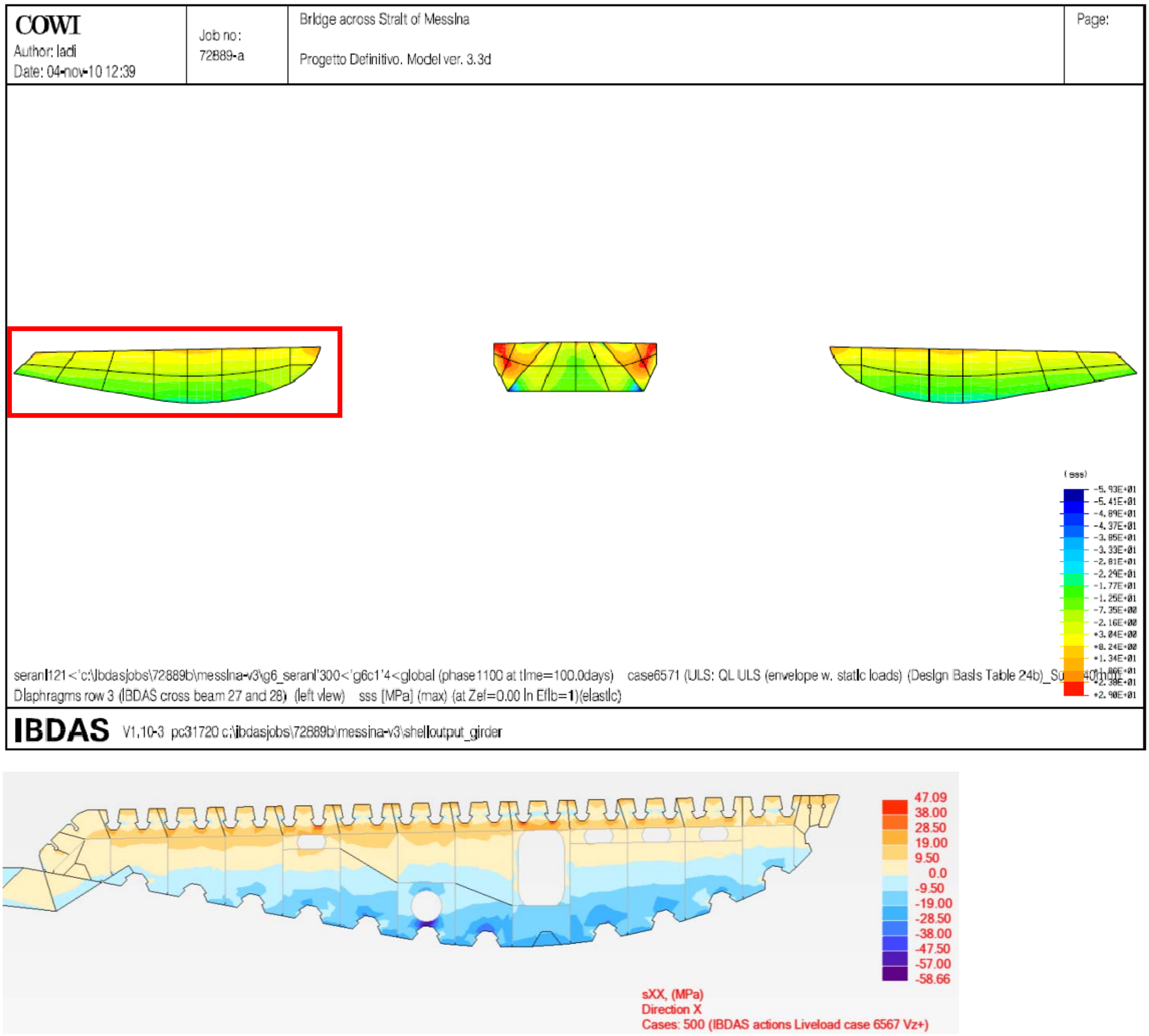


*Figure 2-56 Transverse stresses – Diaphragm – Case 6567 (Vz+)*

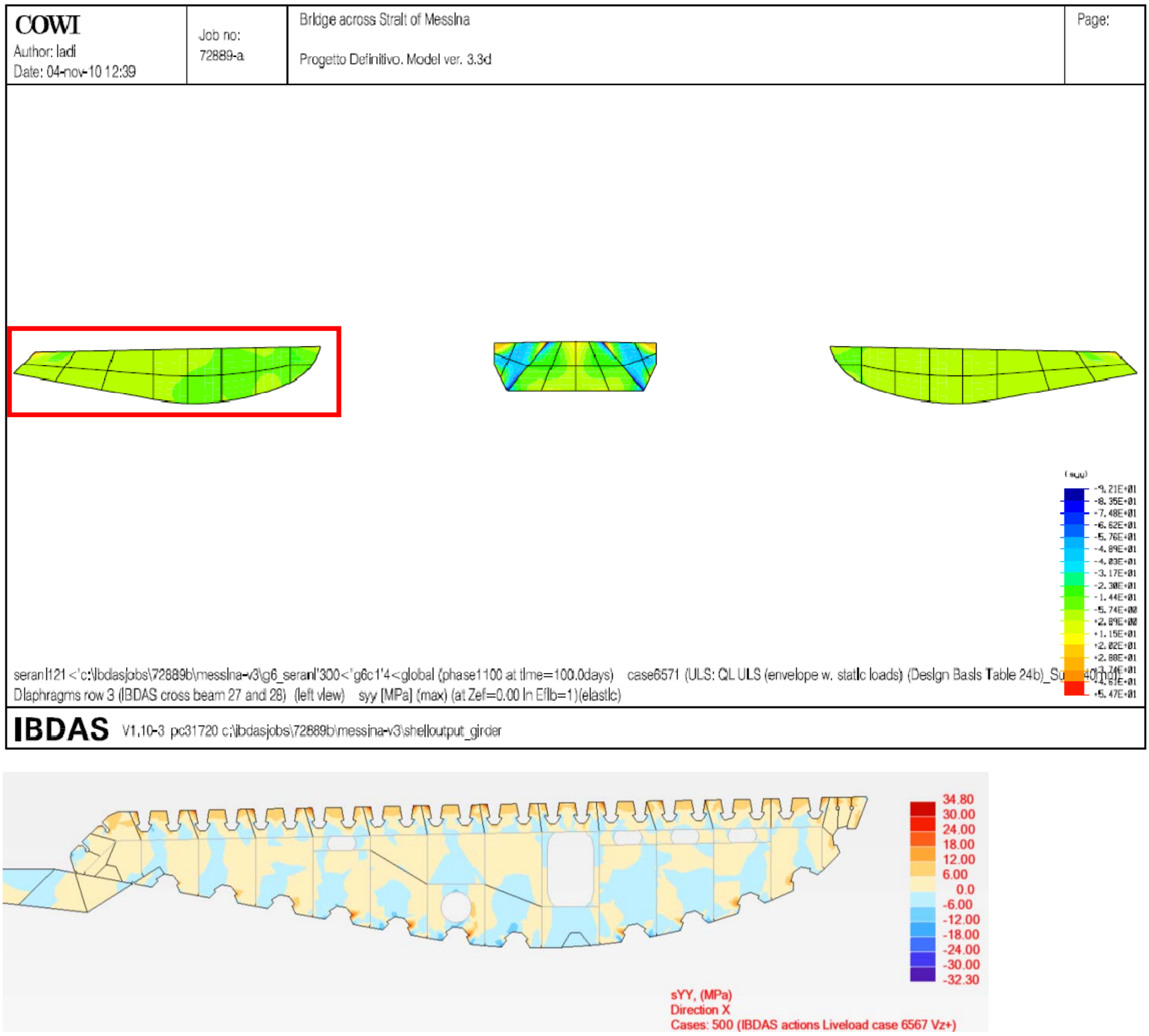


*Figure 2-57 Vertical stresses – Diaphragm – Case 6567 (Vz+)*

### 2.2.3 Verification of von Mises stresses in roadway girder

As shown in following figures the von Mises stresses are less than design yielding stress of $f_{yk}/\gamma_{m0}$ which correspond to 460/1,05=438MPa for all analysed load cases. For load case 4000 also the longitudinal and transverse stresses are shown.

**Load case: Ms+ (load case 4000, Maximum sagging moment of the diaphragm)**

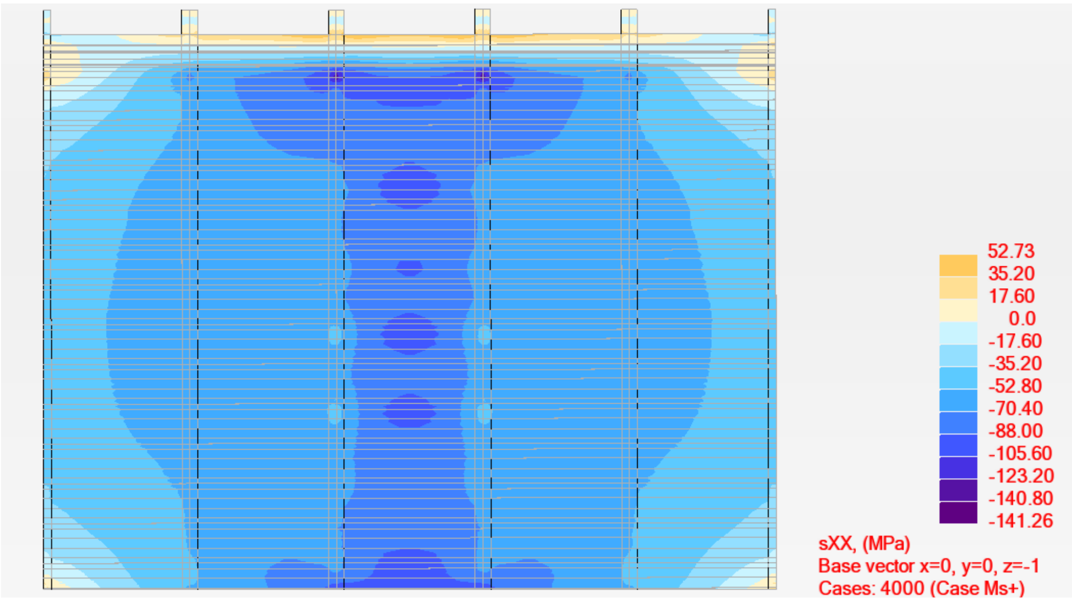


*Figure 2-58 Longitudinal stresses – Deck plate – Case 4000 (Ms+)*

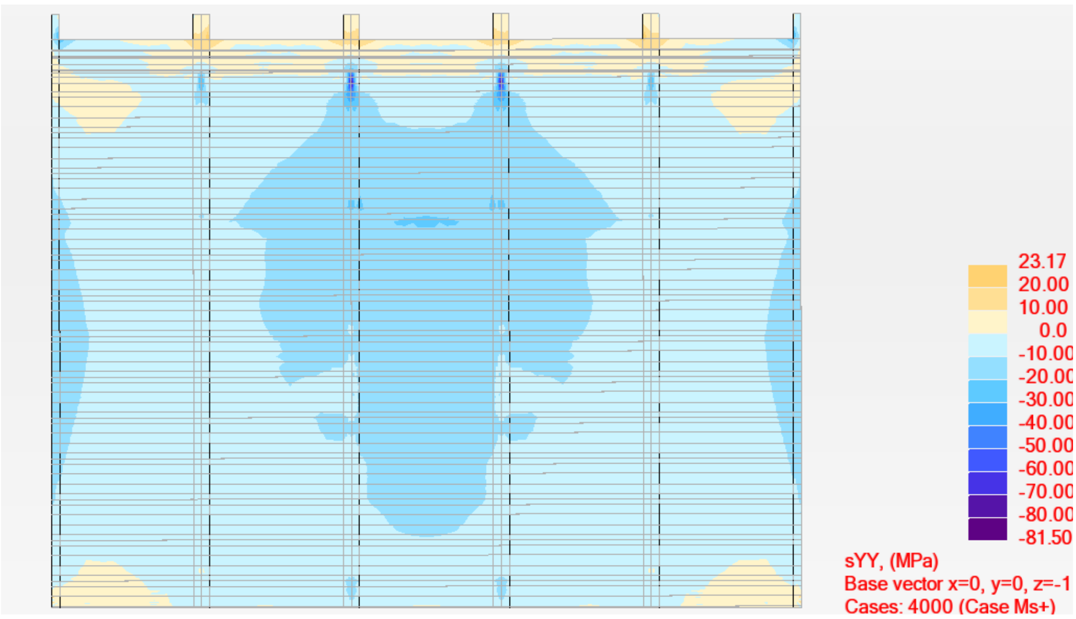


*Figure 2-59 Transverse stresses – Deck plate – Case 4000 (Ms+)*

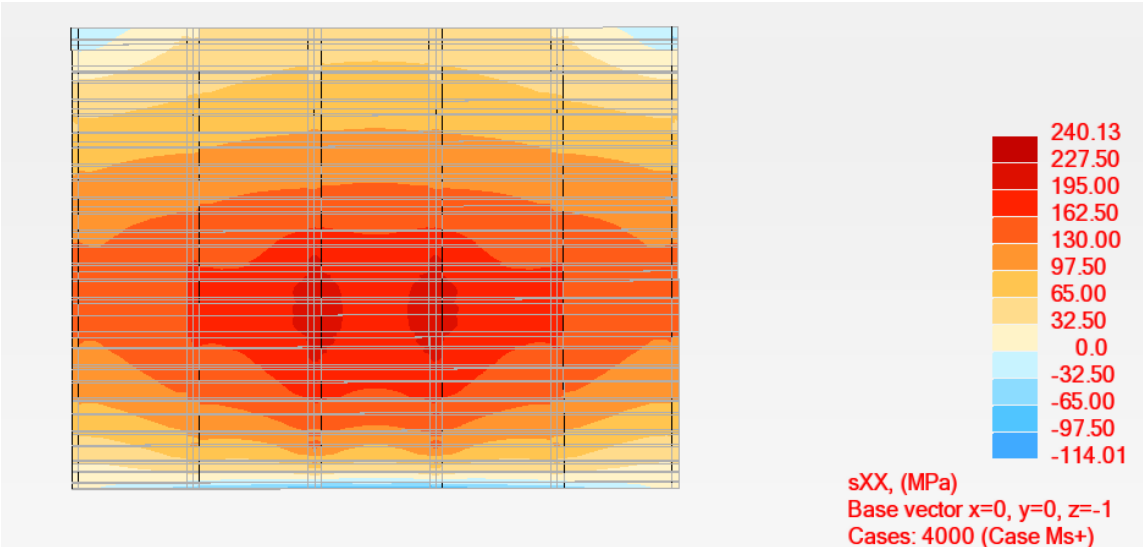


*Figure 2-60 Longitudinal stresses – Bottom plate – Case 4000 (Ms+)*

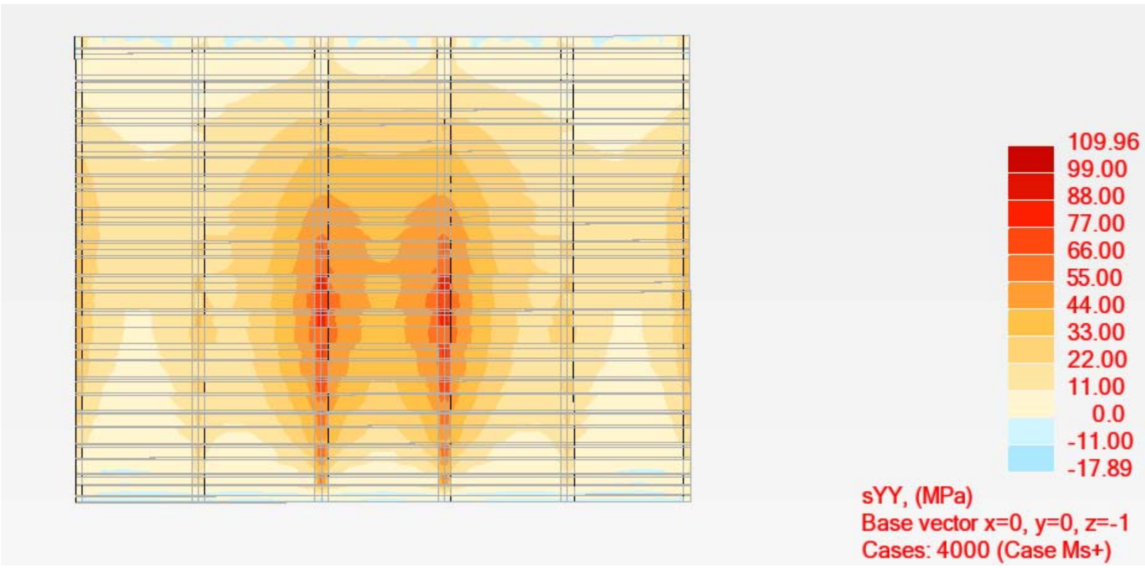


*Figure 2-61 Transverse stresses – Bottom plate – Case 4000 (Ms+)*

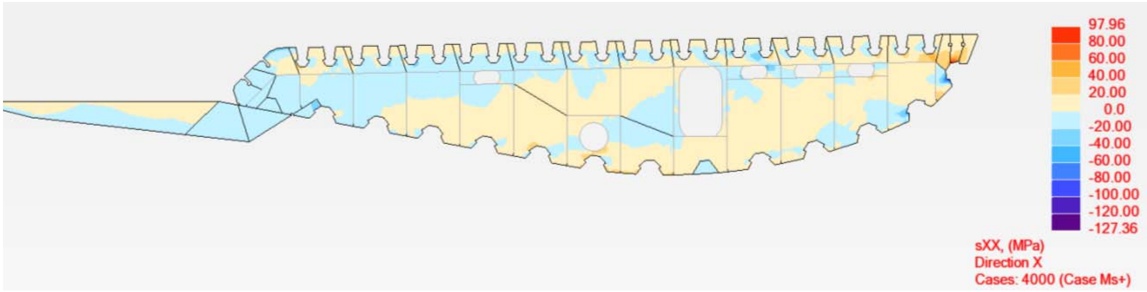


*Figure 2-62 Transverse stresses – Diaphragm – Case 4000 (Ms+)*

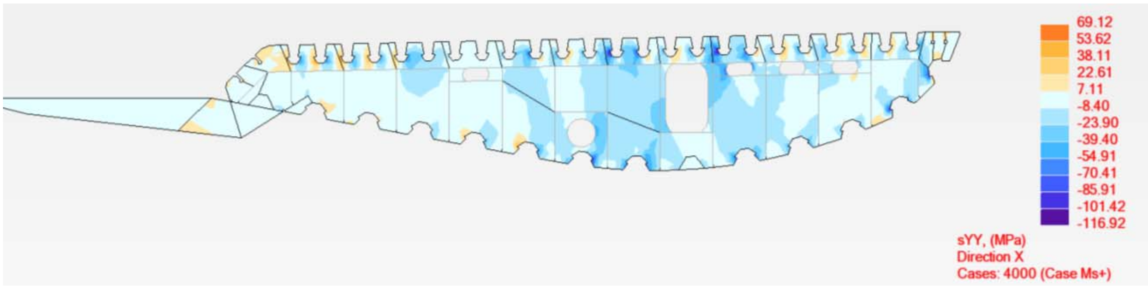


*Figure 2-63 Vertical stresses – Diaphragm – Case 4000 (Ms+)*

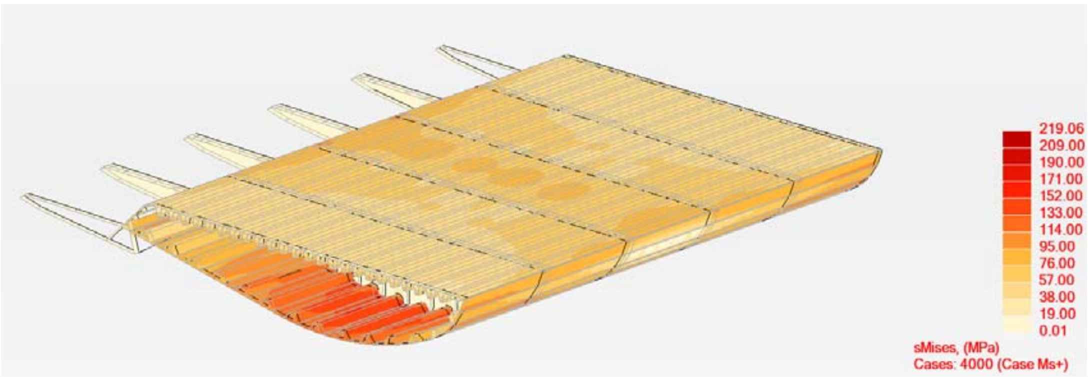


*Figure 2-64 von Mises stresses – Roadway girder overall – Case 4000 (Ms+)*

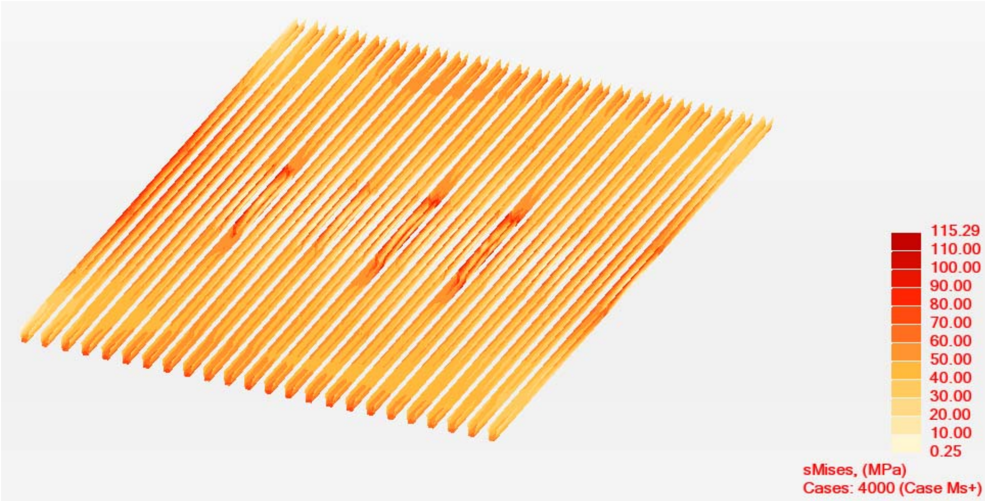


*Figure 2-65 von Mises stresses – Roadway girder stiffeners – Case 4000 (Ms+)*

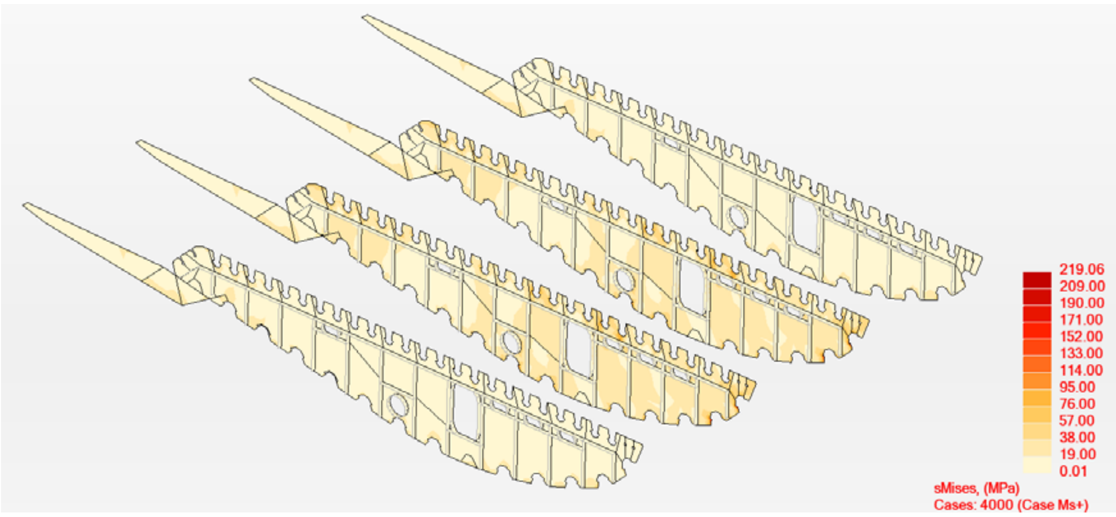


*Figure 2-66 Von Mises stresses – Diaphragms – Case 4000 (Ms+)*

**Load case: My+ (load case 6561, Maximum My in centre of the span)**

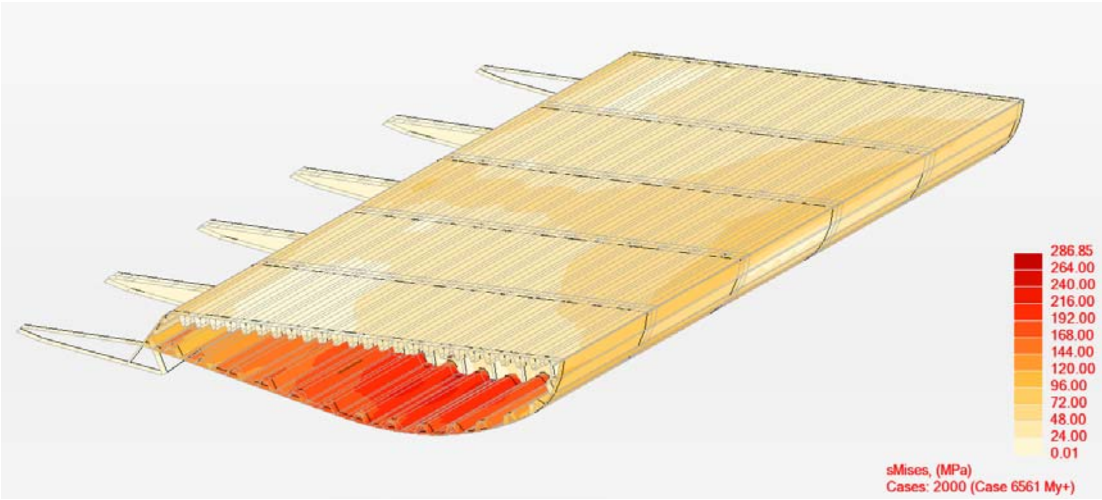


*Figure 2-67 von Mises stresses – Roadway girder overall – Case 6561 (My+)*

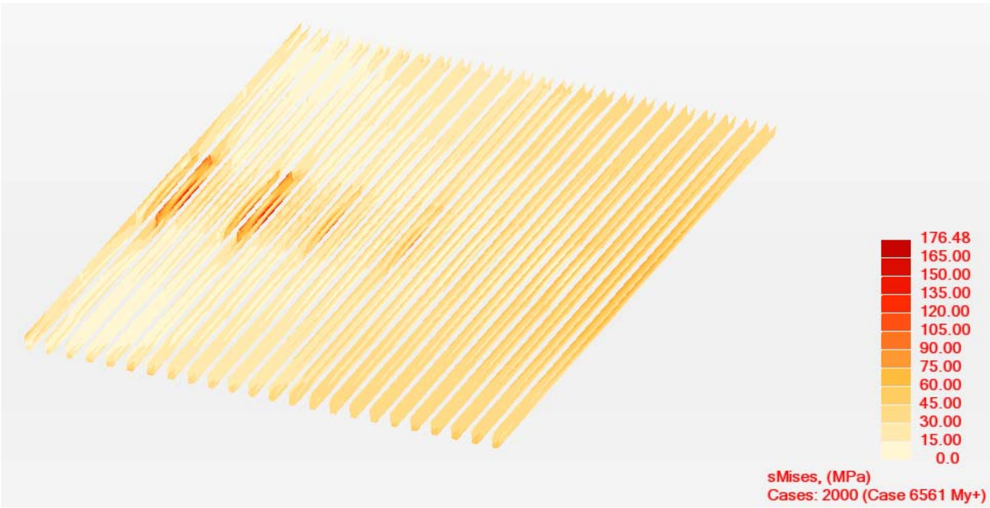


*Figure 2-68 von Mises stresses – Roadway girder stiffeners – Case 6561 (My+)*

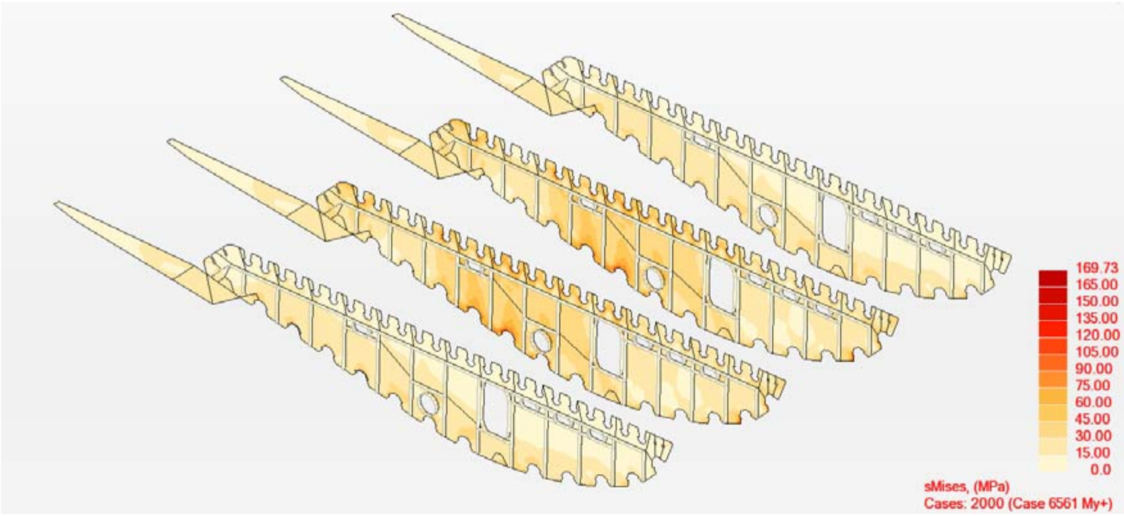


*Figure 2-69 von Mises stresses – Diaphragms – Case 6561 (My+)*

**Load case: Vz+ (load case 6567, Maximum Vz in centre of the span)**

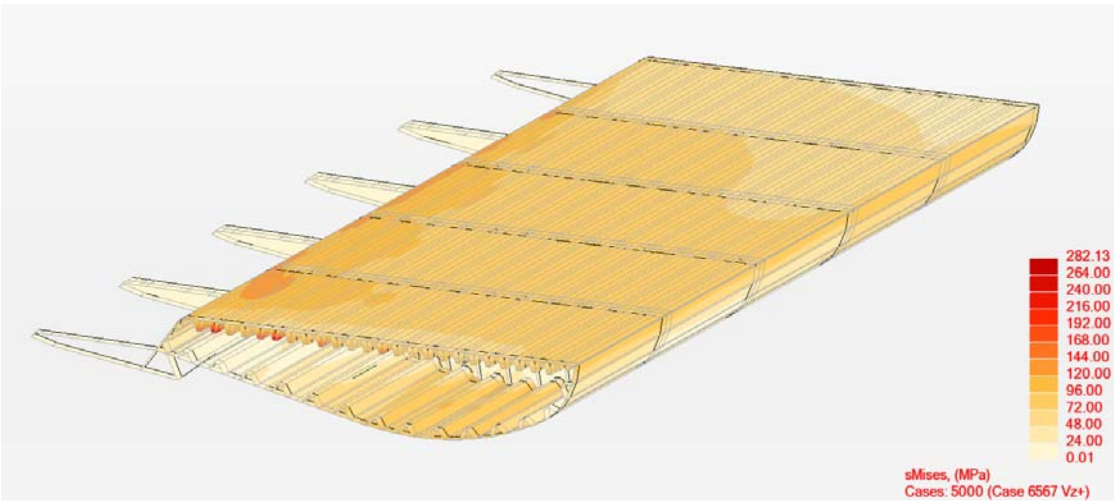


*Figure 2-70 von Mises stresses – Roadway girder overall – Case 6567 (Vz+)*

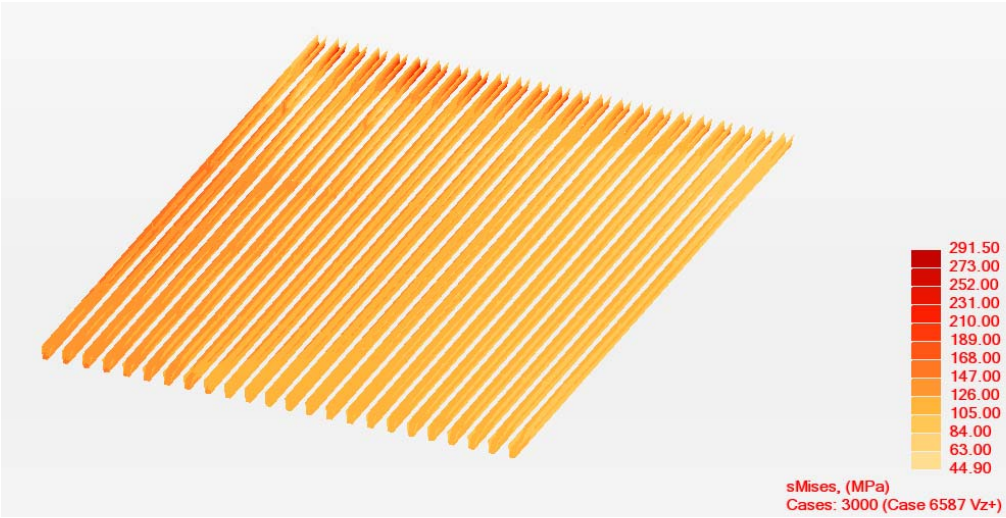


*Figure 2-71 von Mises stresses – Roadway girder stiffeners – Case 6567 (Vz+)*

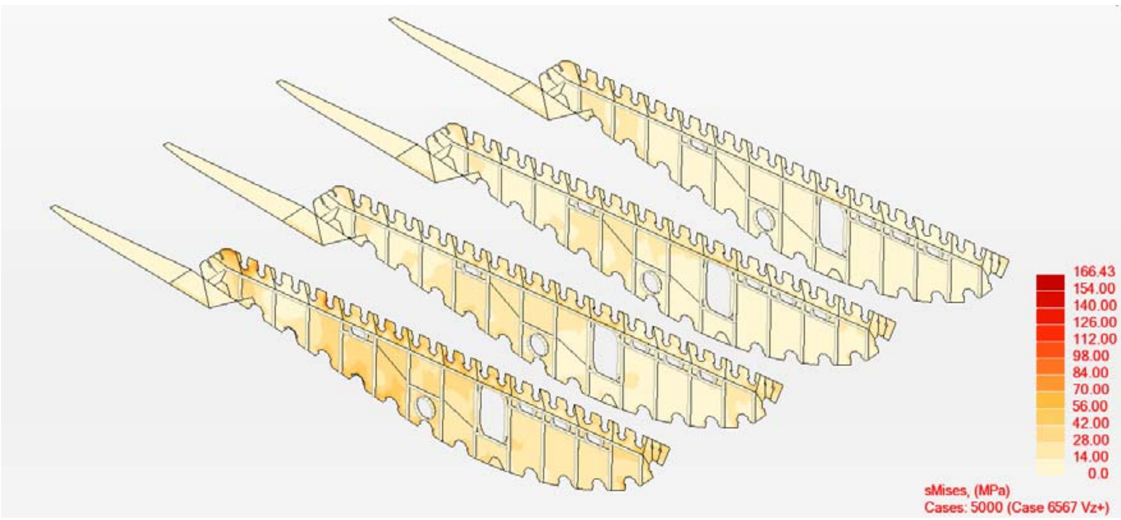


*Figure 2-72 von Mises stresses – Diaphragms – Case 6567 (Vz+)*

## 2.3 Local FE-Model of Railway Girder

A detailed description of the local FE-model of the railway girder can be found in the report "General Design Principles for Suspended Deck".

### 2.3.1 Load cases

The traffic load have been fixated for two load cases in the global IBDAS model in order to maximise the sectional forces in the centre of the span for the railway:

- My+, Maximum My in centre of the span
- Mt+, Maximum Mt in the centre of the span

The most critical live load position has then been applied on the local FE-model according to IBDAS influence line plots. The only live load action on this model is the traffic which is applied directly on the local FE-model. Plot of the applied vertical loads are shown in Figure 2-73 and Figure 2-74.

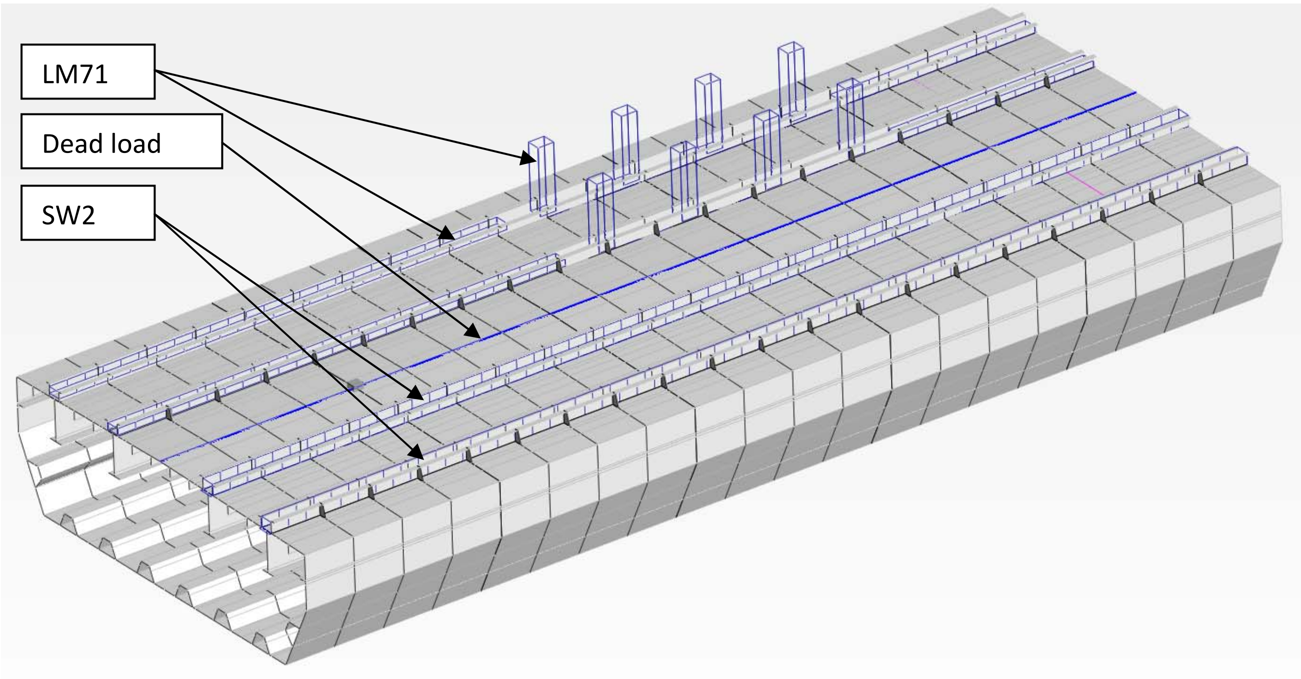


*Figure 2-73 Plot of model with applied vertical loads for load case with maximum bending moment, My+, at centre span*

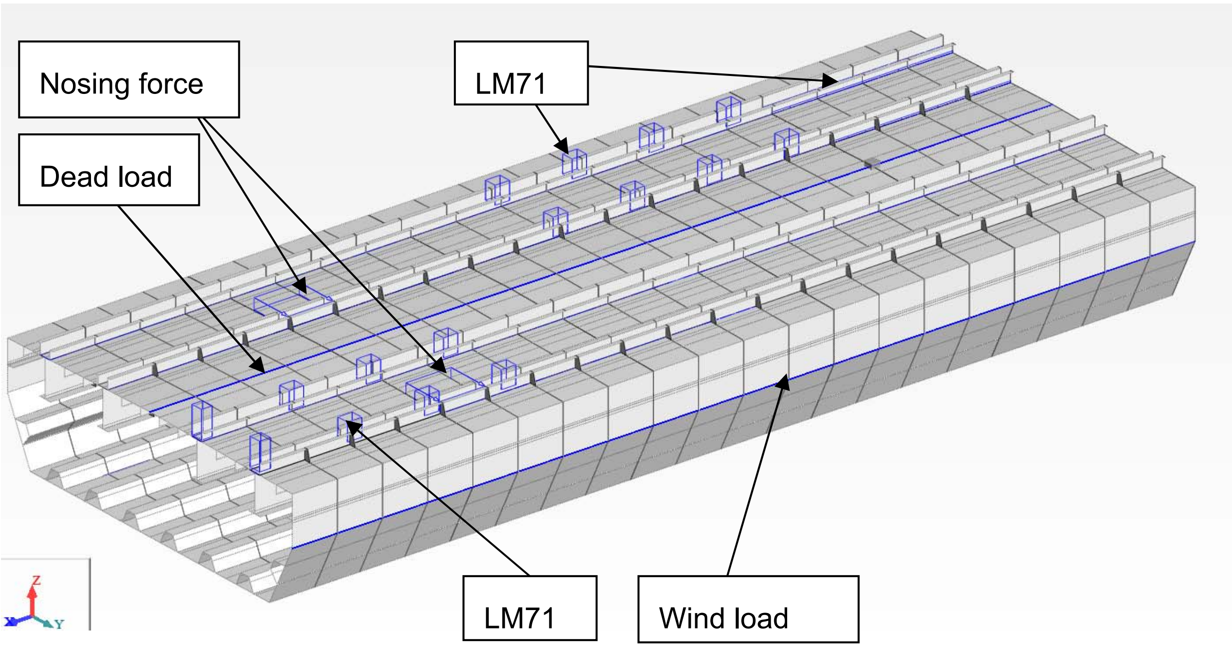


*Figure 2-74 Plot of model with applied vertical loads for load case with maximum bending moment, Mt+, at centre span*

### 2.3.2 Stress verification and comparison with semi-local IBDAS model

In the following, contour plots and stress values for both the local railway girder FE-model and the semi-local IBDAS model are presented.

The scope has been to verify that the stress distribution throughout the deck as well as the stress magnitude in three characteristic locations of the bridge elements is comparable with stresses from the semi-local IBDAS model.

The structural elements investigated are the deck plate, bottom plate and diaphragm in the railway girder and a summary of the stress object of the comparison can be found in Table 2-6 where also the load combinations and the layer where the stresses have been calculated are mentioned.

*Table 2-6 Stresses used for comparison*

| | Element | Stress | Panel layer |
|---|---|---|---|
| Maximum My+ | Top flanges | sXX, sYY | Middle |
| | Bottom flanges | sXX, sYY | Middle |
| | Diaphragm | sXX, sYY | Middle |

In the figures below a full set of results of the above mentioned stresses are presented showing the IBDAS plot in the top and the ROBOT plot in the bottom of the figures. A difference in the stress colour can be noticed, however this does not represent a relevant difference of the stress level, hence a colour chart of the stress magnitude is also included in the plots. The results of the main stress direction sXX and sYY are pointed out and compared for both models in three characteristic points in the centre of the deck plate and bottom plate. Furthermore 5 points are pointed out for the diaphragms for both stress directions.

A summary of the results including the percentage variation of stresses between the models can be seen in Table 2-7.

*Table 2-7 Summary of comparison of stresses calculated in semi-local IBDAS FE-model and local Robot FE-model*

| | Element | Section | Stress | IBDAS [MPa] | ROBOT [MPa] | Deviation from IBDAS |
|---|---|---|---|---|---|---|
| Maximum My+ | Deck Plate | 1 | sXX | -116.91 | -147.90 | 26.5% |
| | | 2 | sXX | -113.59 | -143.75 | 26.6% |
| | | 3 | sXX | -113.52 | -125.36 | 10.4% |
| | Bottom Plate | 1 | sXX | 214.66 | 185.82 | -13.4% |
| | | 2 | sXX | 206.59 | 190.17 | -7.9% |
| | | 3 | sXX | 216.61 | 206.81 | -4.5% |
| | Diaphragm | 1 | sXX | 5.27 | 24.84 | - |
| | | 2 | sXX | 27.53 | 26.64 | -3.23% |
| | | 3 | sXX | 5.25 | 4.77 | -9.14% |
| | | 4 | sXX | -21.55 | -21.67 | 0.56% |
| | | 5 | sXX | -10.86 | -22.1 | - |

Table 2-7 shows that two stress points in the deck plate deviates from the semi-local IBDAS model with 26%. The deviation can be a result of the different location of the two models, namely s=-975 for the ROBOT model and s=-810 for the semi-local IBDAS model with the consequence of not fully comparable boundary conditions.

It shall be considered that the IBDAS FE-model is not modelled with manholes and holes for utilities which most likely have an effect on the stress distribution.

The compared stresses from both models can be seen in Figure 2-75 to Figure 2-80. Besides the small deviations as explained above, it can be seen from the plots that the stress distribution is roughly similar for the two models indicating similar loading arrangement and structural behaviour of the two FE-models. The stresses are also acceptable with respect to ULS load combinations.

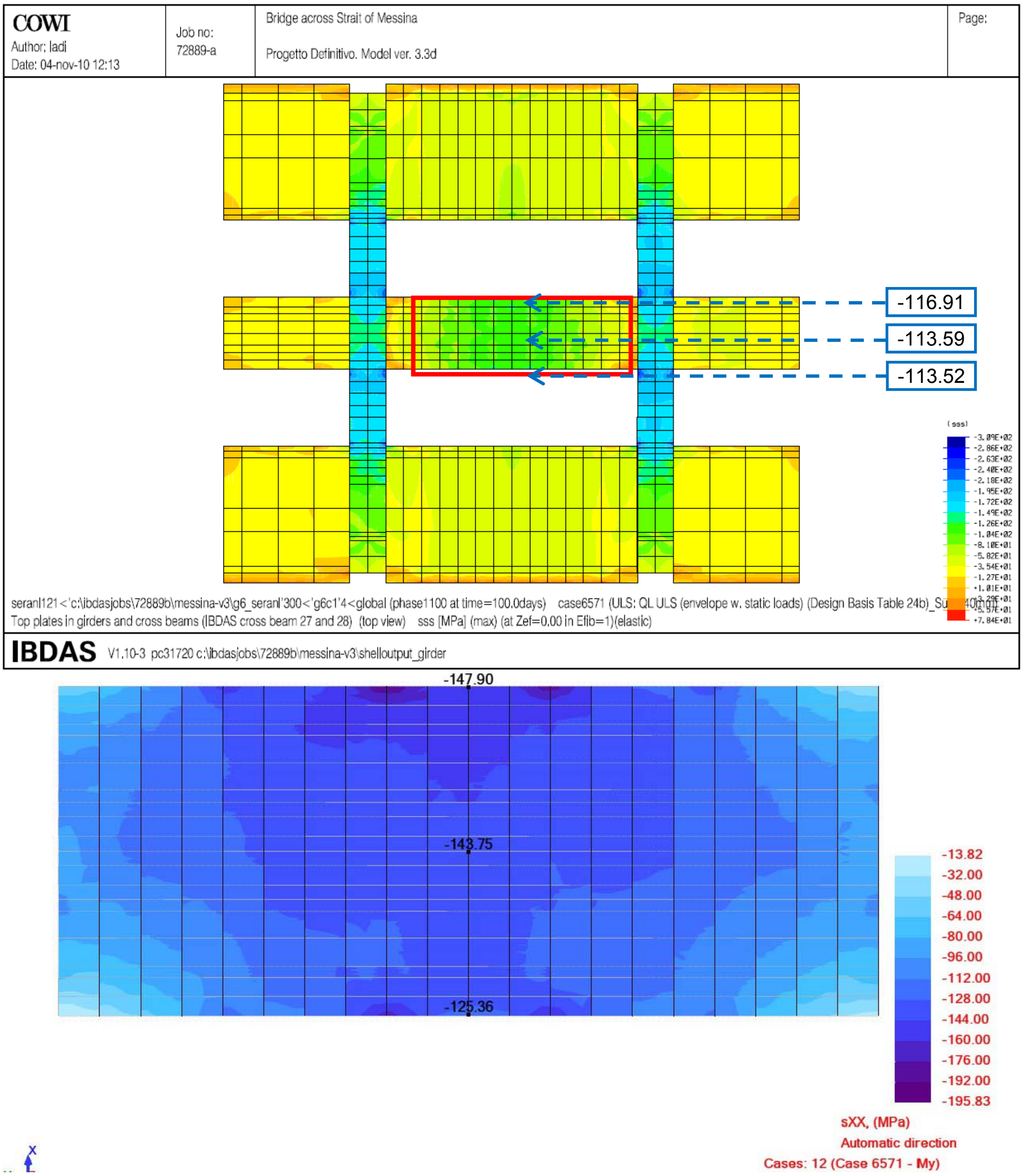


*Figure 2-75 Top plate, stresses sXX, maximum bending moment My+*

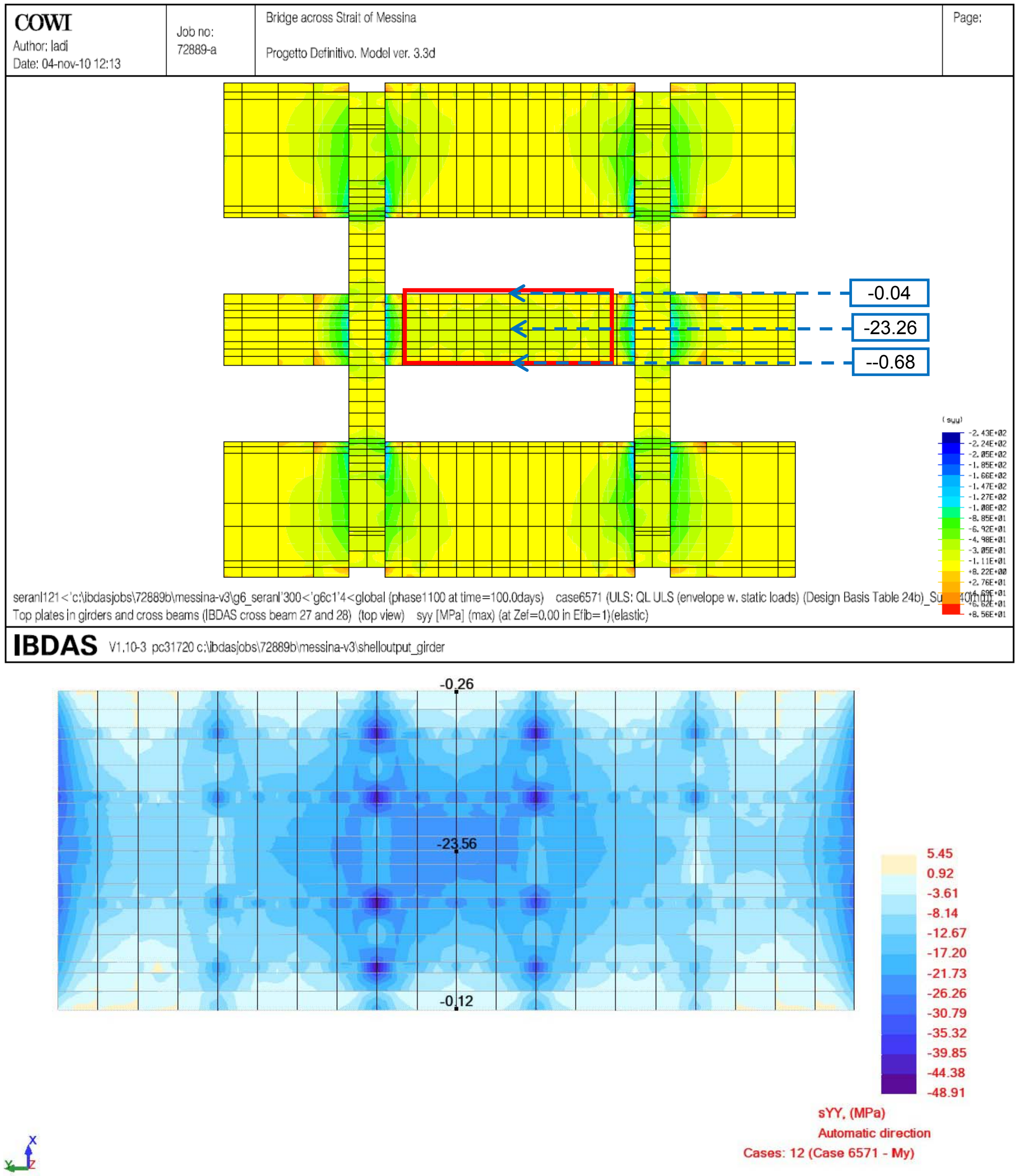


*Figure 2-76     Top plate, stresses sYY, maximum bending moment My+*

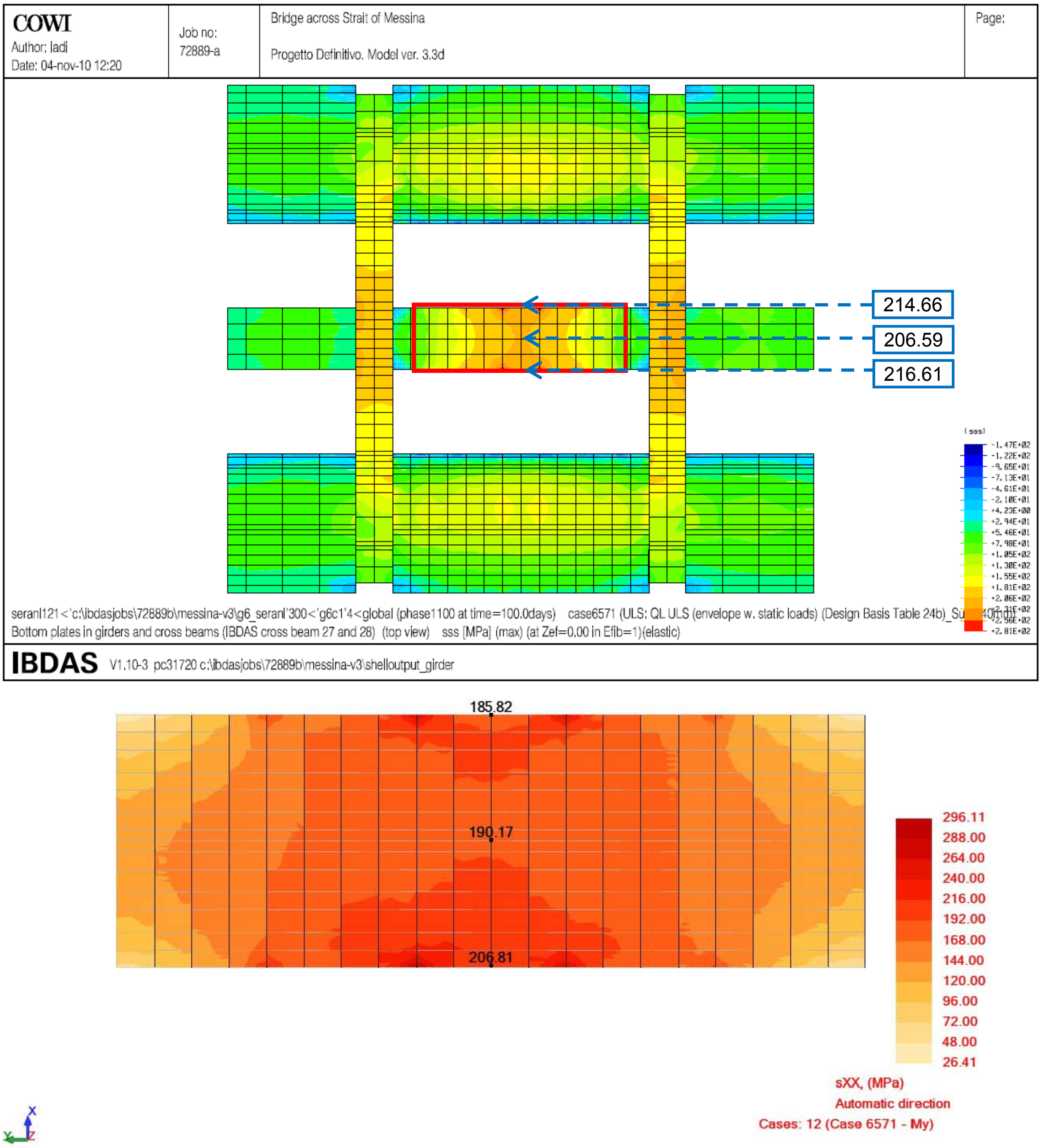


*Figure 2-77 Bottom plate, stresses sXX, maximum bending moment My+*

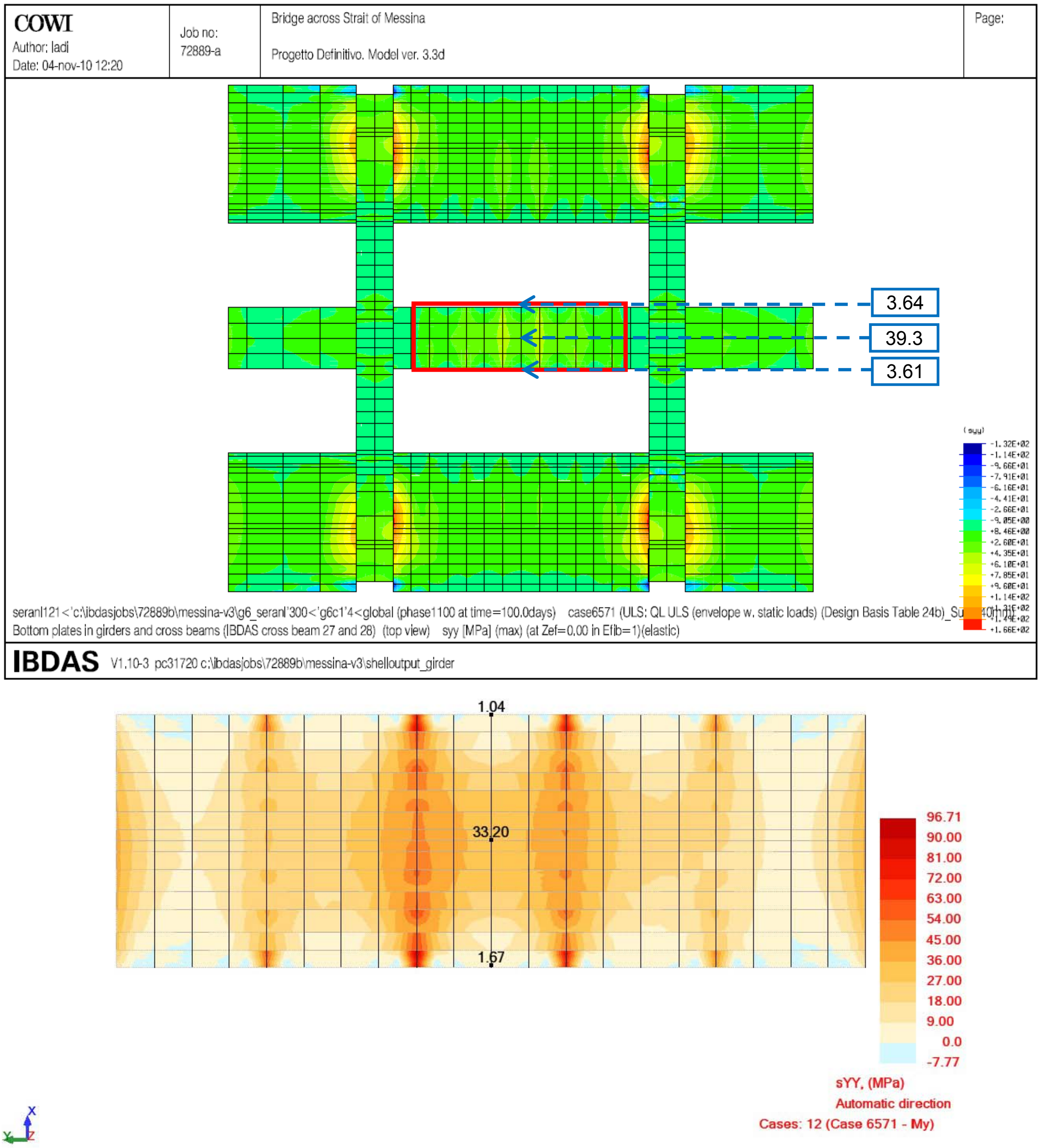


*Figure 2-78 Bottom plate, stresses sYY, maximum bending moment My+*

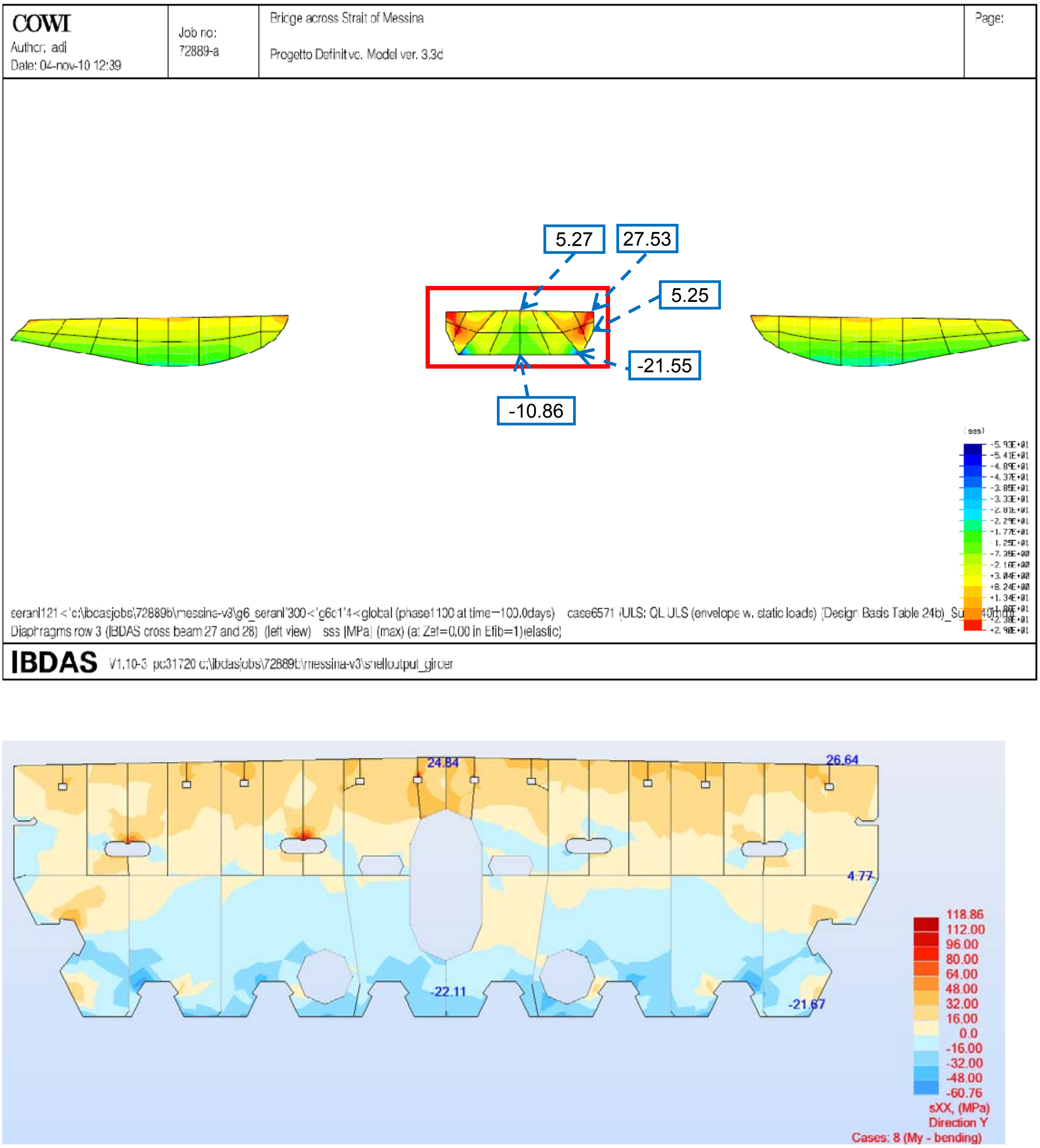


*Figure 2-79     Diaphragm, stresses sXX, maximum bending moment My+*

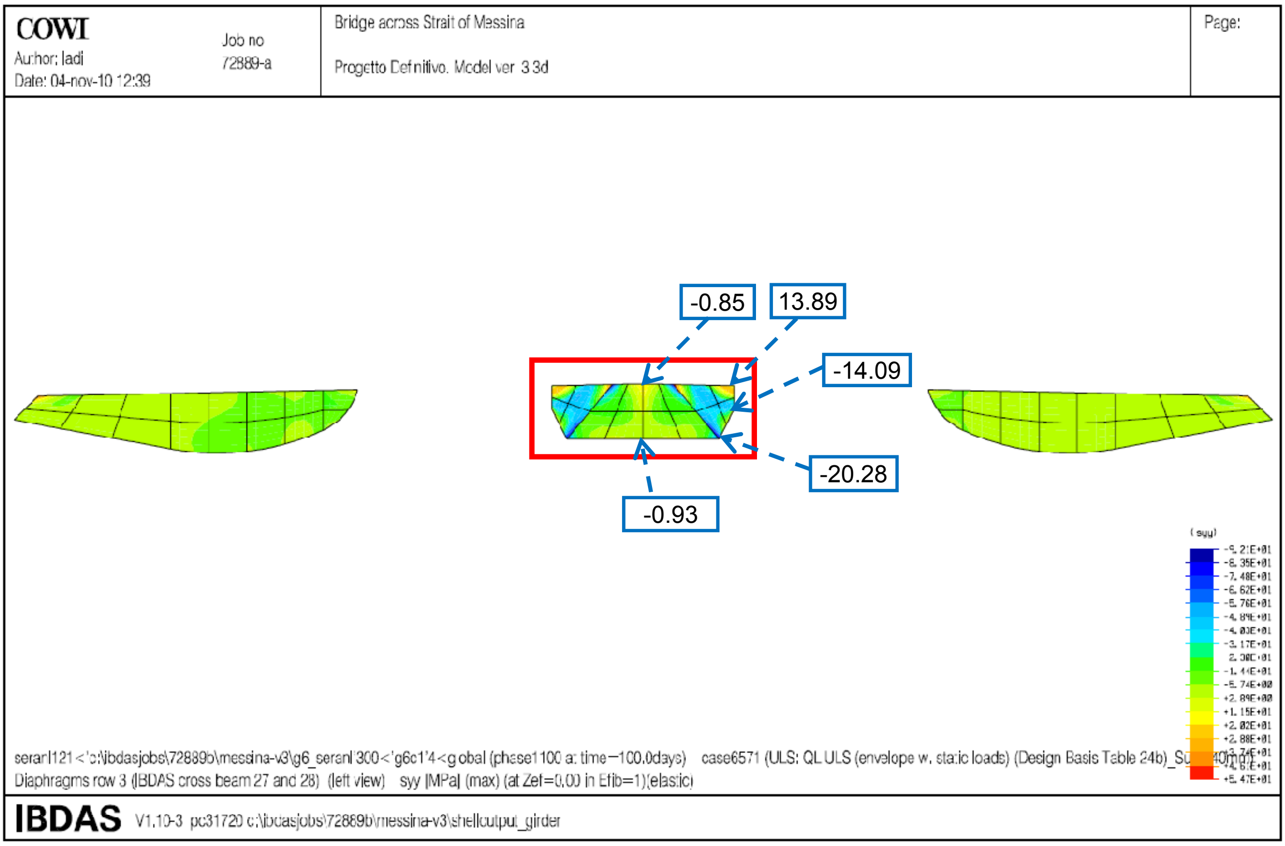


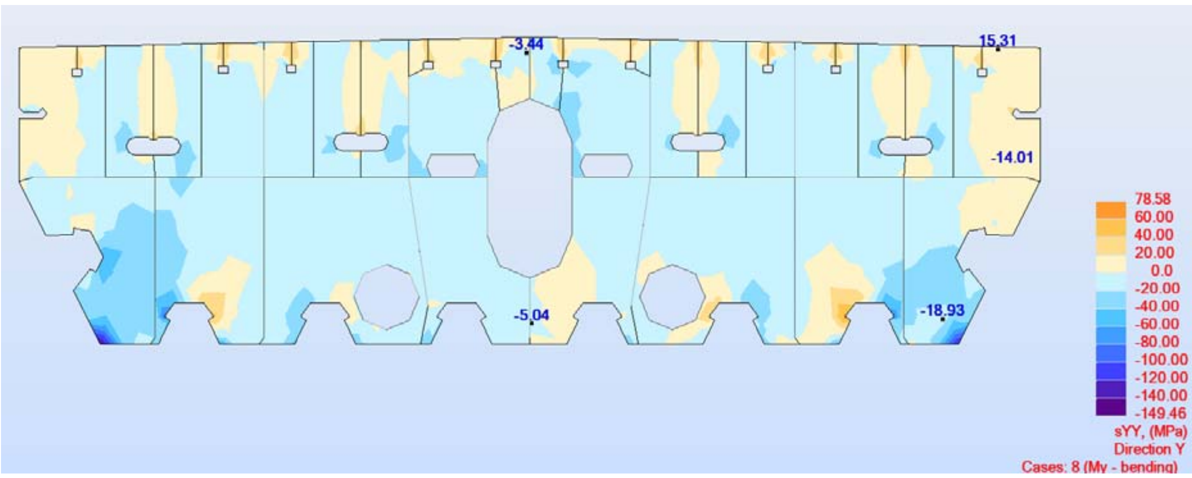


*Figure 2-80 Diaphragm, stresses sYY, maximum bending moment My+*

### 2.3.3 Verification of von Mises stresses in railway girder

As shown in following figures the von Mises stresses are less than design yielding stress of $f_{yk}/\gamma_{m0}$ which correspond to 355/1,05=338MPa for all analysed load cases.

**Load case: My+ (Maximum My in centre of the span)**

In Figure 2-81 and Figure 2-82, the von Mises stress is shown for the local FE-model of the railway girder for load combination My+. Figure 2-83 shows the von Mises for the longitudinal stiffeners. Figure 2-84 shows a von Mises stress plot of the diaphragm for load combination My+.

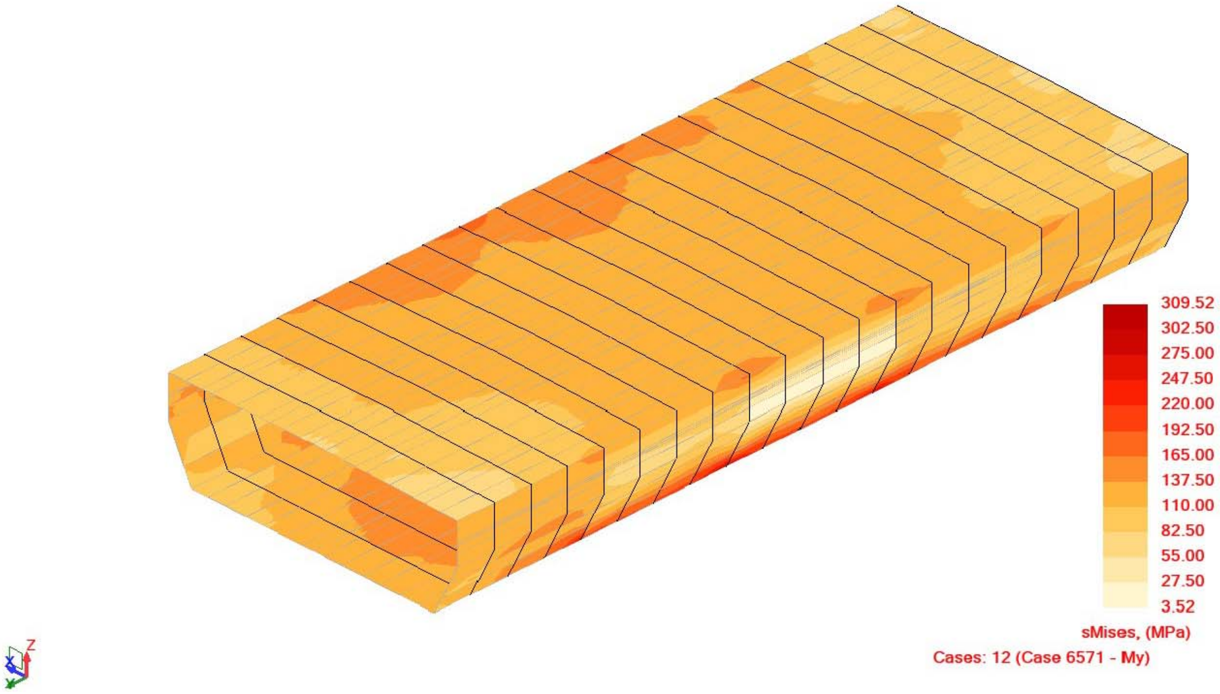


*Figure 2-81 von Mises stresses for load combination My+ for longitudinal steel*

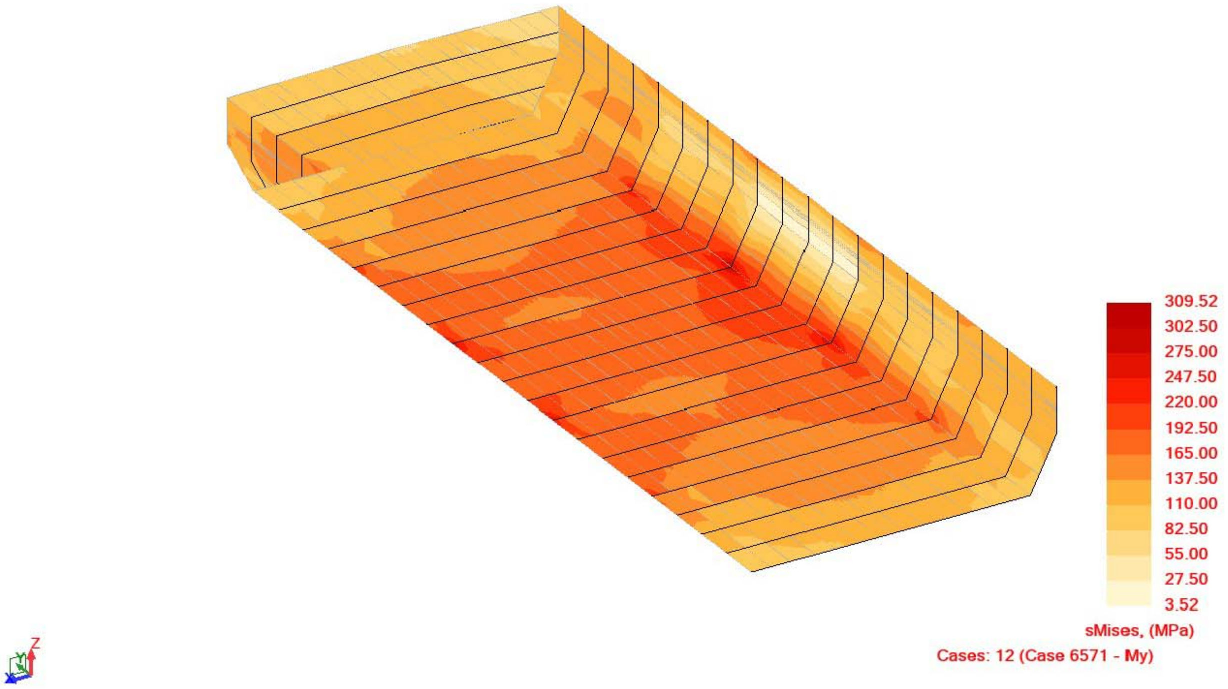


*Figure 2-82 von Mises stresses for load combination My+ for longitudinal steel*

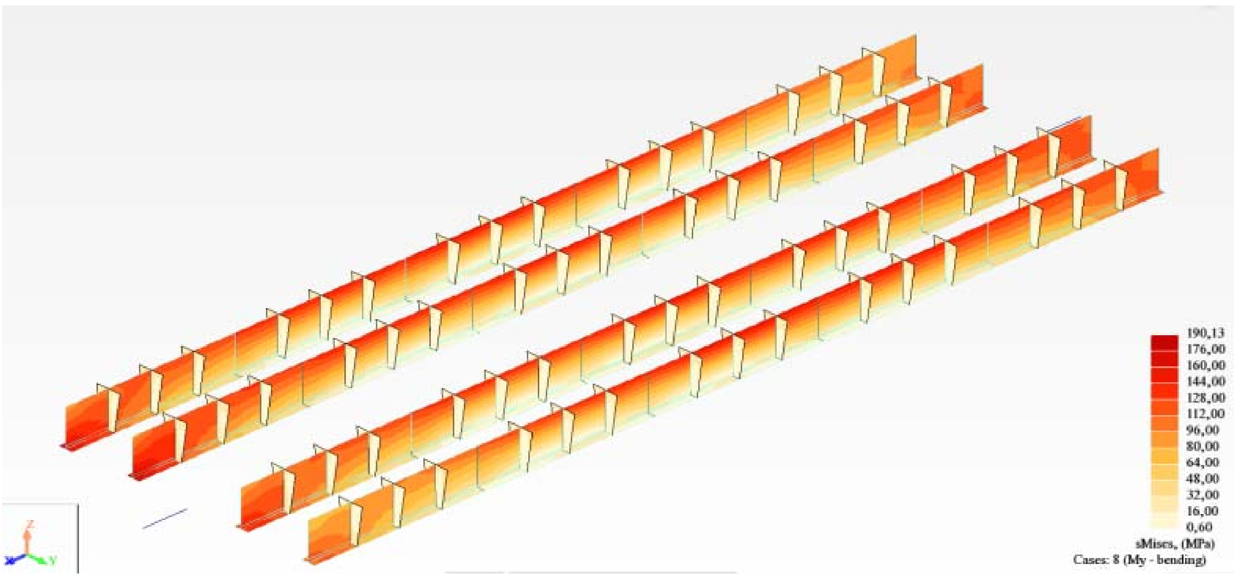


*Figure 2-83 von Mises stresses for load combination My+ for longitudinal stiffeners in top plate*

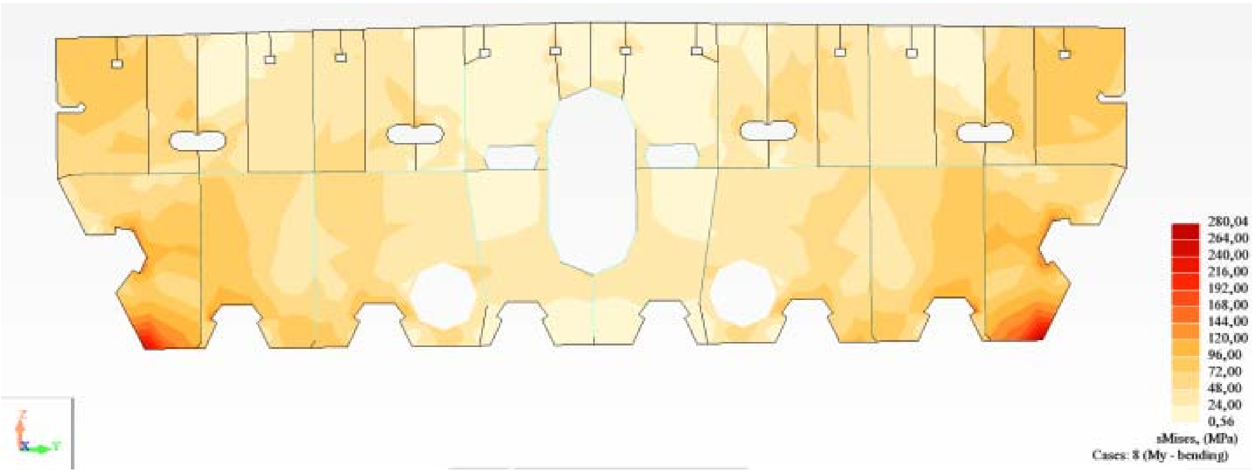


*Figure 2-84 von Mises stresses in combination My+ for the local FE-model of diaphragm*

The maximum stress for load combination My+ is 310 MPa for the longitudinal steel and is acceptable using steel S355. For the diaphragm in Figure 2-84 it is seen that the overall stress level is acceptable for steel S355. The stress limit is exceeded in very small areas along the edge of the cut out for troughs at the inclined web plate where the stresses reach a maximum value of 342MPa. However this excess does not reflect a real issue and considering the size of the area the excess of the stress limit is considered acceptable.

**Load case: Mt+ (Maximum Mt in centre of the span)**

In Figure 2-85 and Figure 2-86, the von Mises stress is shown for the local FE-model of the railway girder for load combination Mt+. Figure 2-87 shows the von Mises for the longitudinal stiffeners and Figure 2-88 shows von Mises stress of a the diaphragm for load combination Mt+.

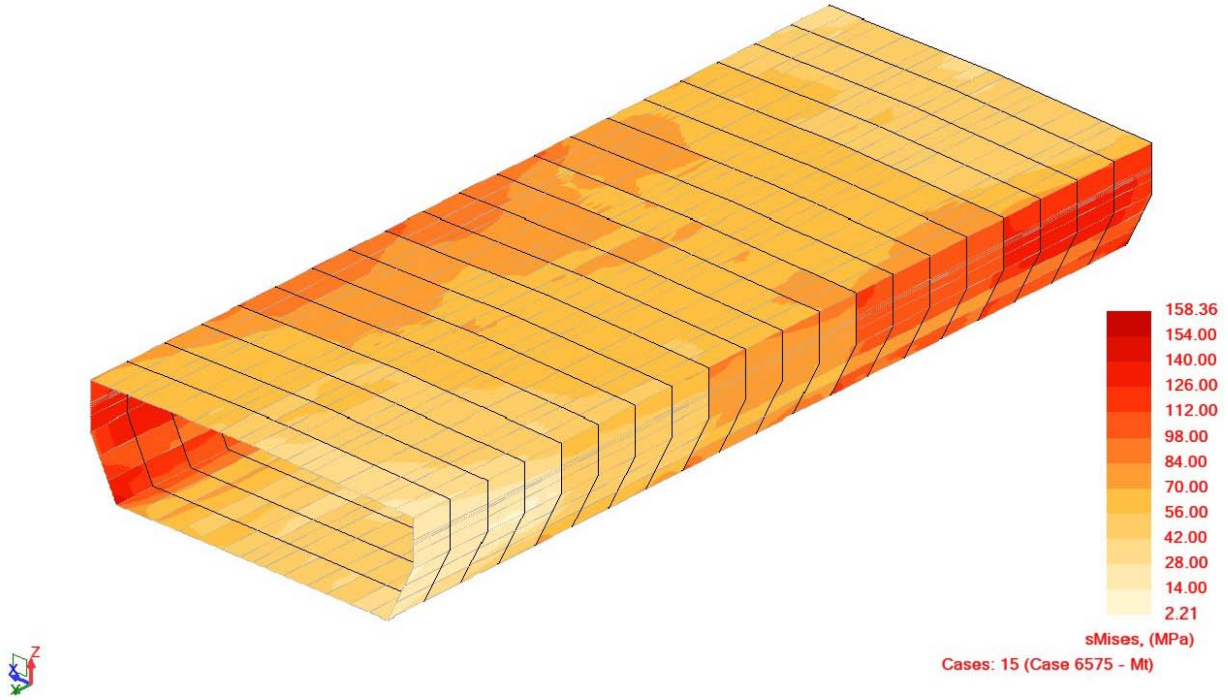


*Figure 2-85 von Mises stresses for load combination Mt+ for longitudinal steel*

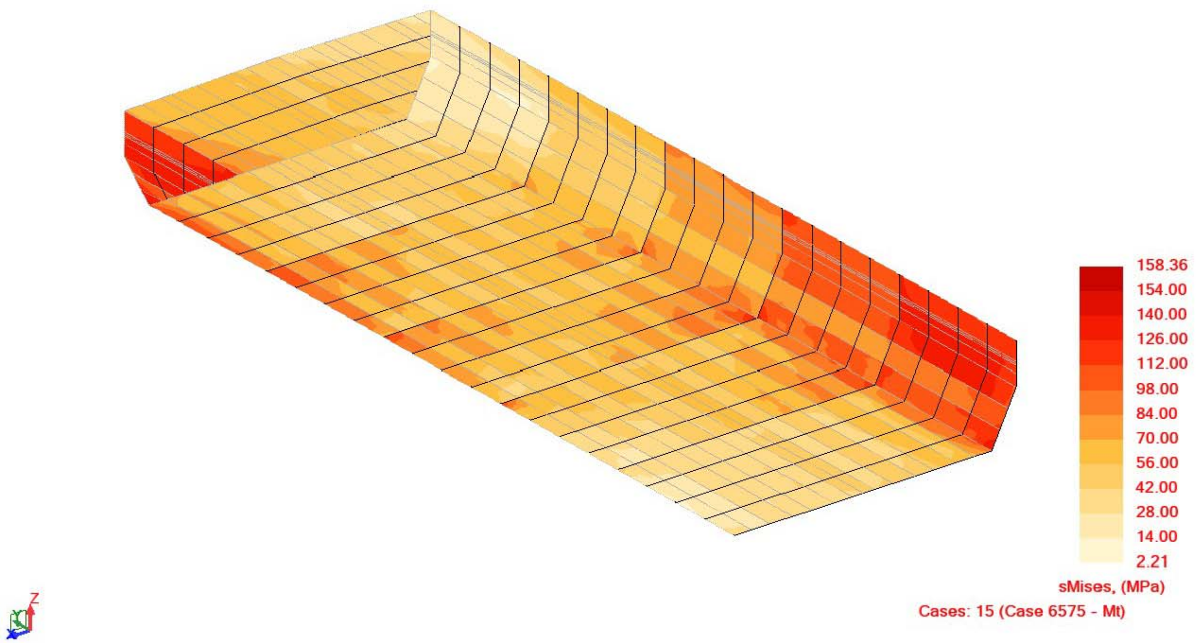


*Figure 2-86 von Mises stresses for load combination Mt+ for longitudinal steel*

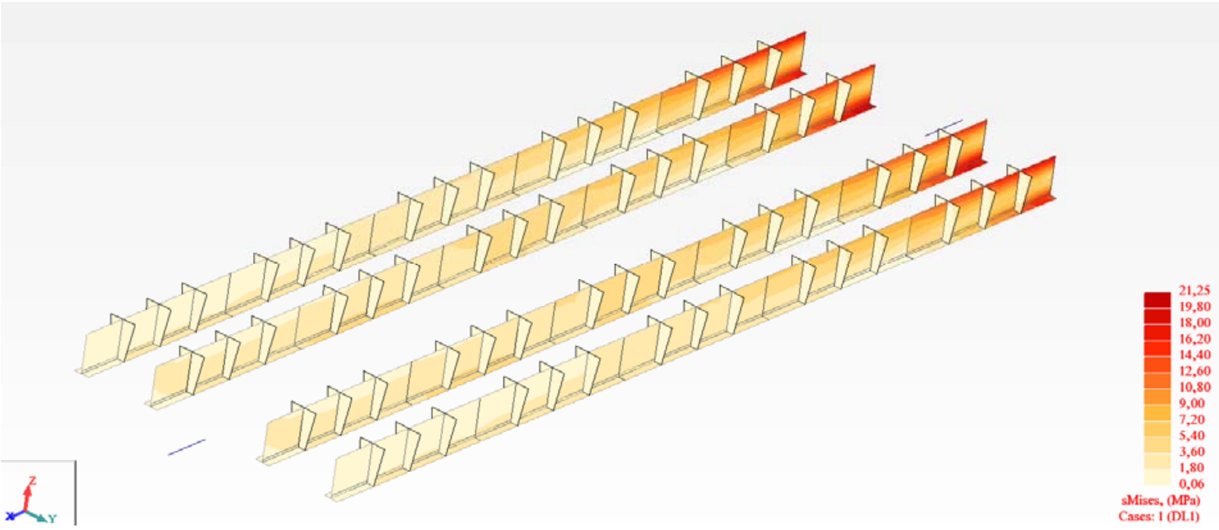


*Figure 2-87 von Mises stresses for load combination Mt+ for longitudinal stiffeners in top plate*

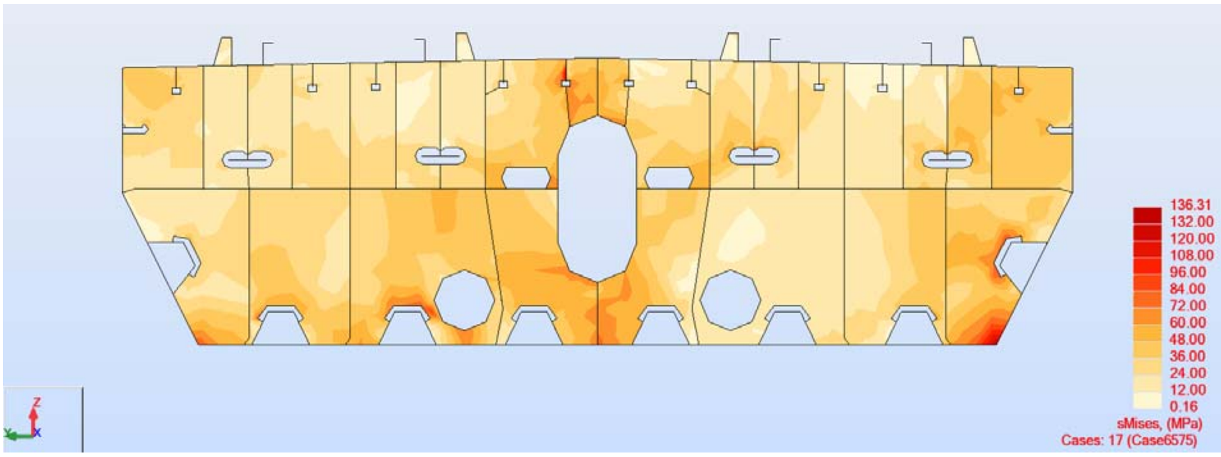


*Figure 2-88 von Mises stresses in combination Mt+ for the local FE-model of diaphragm*

The maximum stress for load combination Mt+ is 158MPa for the longitudinal steel and is acceptable using steel S355. The diaphragm in Figure 2-88 has an acceptable stress level.

## 2.4 Local FE-Model of Hanger Anchorage

### 2.4.1 General

A local verification of the pull out strength of the anchor plate and two cheek plates are presented in "Design Rapport - Support structure". In the following, the capacity of the hanger anchorages have been verified using a local FE-model, modelled entirely with shell elements. The documentation is presented with a number of stress plots of the hanger anchorage. The applied reactions from the lower hanger pin given in Table 2-9, are illustrated in Figure 2-89.

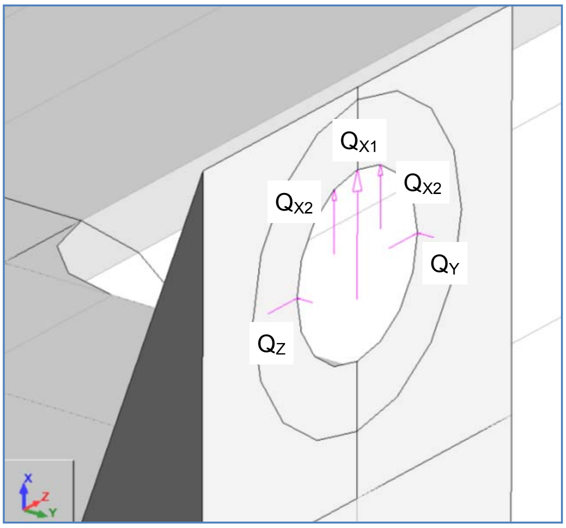


*Figure 2-89 Applied hanger loads on the hanger anchorage model*

Conversion from hanger forces and rotations to Robot coordinates is shown in Table 2-8 and Table 2-9.

*Table 2-8 ULS hanger forces and hanger rotations from IBDAS*

| **Hanger** | | | | **Maximum Ns with corresponding θy and θs** | | | **Maximum θy with corresponding Ns and θs** | | | **Maximum θs with corresponding Ns and θy** | | |
|---|---|---|---|---|---|---|---|---|---|---|---|---|
| No. | Description | s [m] | Hanger Socket | Ns [MN] | θy [deg] | θs [deg] | Ns [MN] | θy [deg] | θs [deg] | Ns [MN] | θy [deg] | θs [deg] |
| 60 | AP1 with spherical bearings and maximum rotations | 0 | P1 | 6.13 | -0.1 | 7.4 | 5.89 | -13.9 | 0.4 | 3.53 | -0.1 | 11.2 |
| 51 | AP1 with spherical | -270 | P1 | 6.08 | 2.0 | 5.1 | 5.85 | 5.7 | 0.1 | 3.51 | 1.1 | 7.9 |

| | | | | | | | | | | | | |
|---|---|---|---|---|---|---|---|---|---|---|---|---|
| | bearings | | | | | | | | | | | |
| 41 | AP2 | -570 | P2 | 6.02 | 1.5 | 3.9 | 5.79 | 3.4 | 1.9 | 3.49 | 0.9 | 5.8 |
| 20 | AP3 | -1200 | P3 | 6.04 | 0.6 | 1.2 | 5.82 | 2.8 | -0.5 | 3.51 | 0.7 | 1.5 |

*Table 2-9 Applied hanger loads on the hanger anchorage*

| | | **$Ns_{max}$ [MN]** | | | | **$\theta_{y,\,max}$ [MN]** | | | | **$\theta_{s,\,max}$ [MN]** | | | |
|---|---|---|---|---|---|---|---|---|---|---|---|---|---|
| **No.** | **Description** | $Q_{X1}$ | $Q_{X2}$ | $Q_Z$ | $Q_Y$ | $Q_{X1}$ | $Q_{X2}$ | $Q_Z$ | $Q_Y$ | $Q_{X1}$ | $Q_{X2}$ | $Q_Z$ | $Q_Y$ |
| 60 | AP1 with spherical bearings and maximum rotations | 3.04 | 1.52 | -0.01 | 0.39 | 2.86 | 1.43 | -0.71 | 0.02 | 1.73 | 0.87 | 0.00 | 0.34 |
| 51 | AP1 with spherical bearings | 3.03 | 1.51 | 0.10 | 0.27 | 2.91 | 1.46 | 0.29 | 0.00 | 1.74 | 0.87 | 0.03 | 0.24 |
| 41 | AP2 | 3.00 | 1.50 | 0.08 | 0.20 | 2.89 | 1.44 | 0.17 | 0.09 | 1.74 | 0.87 | 0.03 | 0.18 |
| 20 | AP3 | 3.02 | 1.51 | 0.03 | 0.06 | 2.91 | 1.45 | 0.14 | -0.03 | 1.75 | 0.88 | 0.02 | 0.05 |

In the following the linear stresses in the hanger anchorages are presented as von Mises stresses. The stress limit has been limited to the design yielding stress of $f_{yk}/\gamma_{m0}$ which correspond to 460/1.05 = 438 MPa. From the plots given in Figure 2-90 to Figure 2-101 it can be seen that the stress level in general is below the yielding criteria. This is verifying the capacity of the detail. Areas where the stress limit is exceeded are shown as transparent. As shown in Figure 2-90 to Figure 2-101 the areas that exceeds the design yielding stress are the cheek plates with the concentrated point loads applied. Local verification of cheek and anchor plates is shown in "Design Rapport - Support Structure".

### 2.4.2 Stress verification of hanger anchorage AP1 with maximum rotation

This model represents the hanger anchorage in cross girder no. 52 to 68.

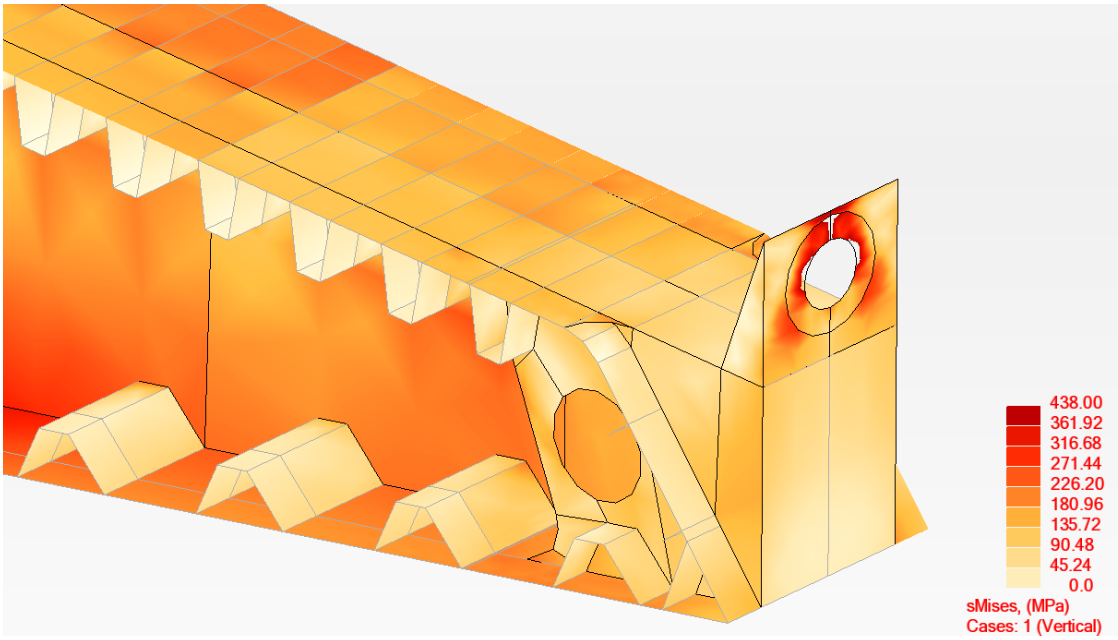


*Figure 2-90 von Mises stresses for AP1 with maximum rotations for vertical hanger reaction*

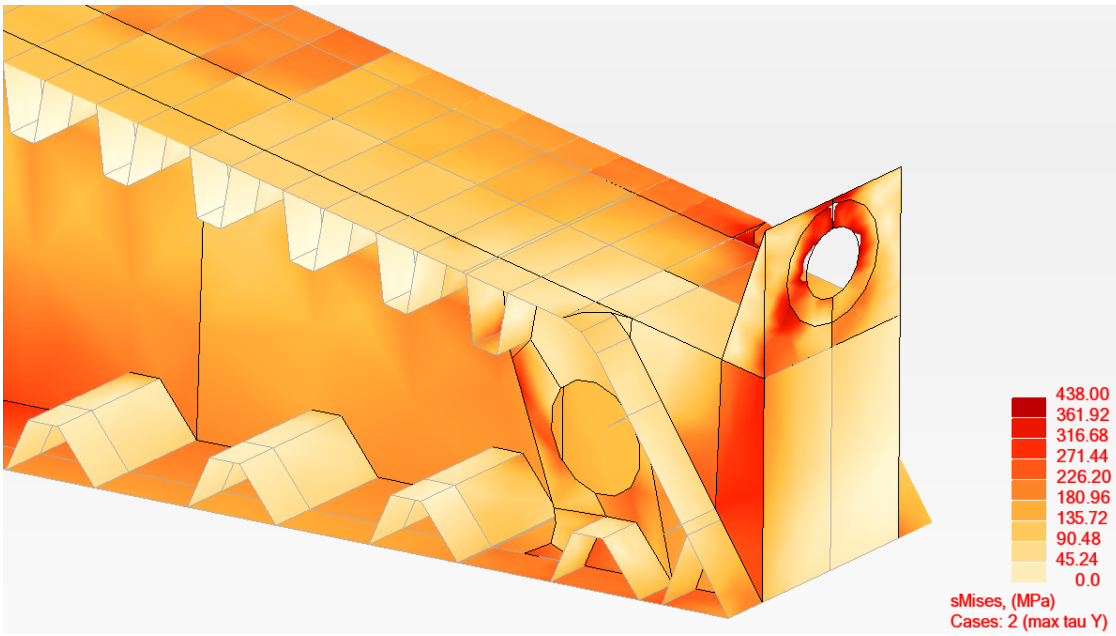


*Figure 2-91 von Mises stresses for AP1 with maximum rotations for max $\theta_Y$ rotation*

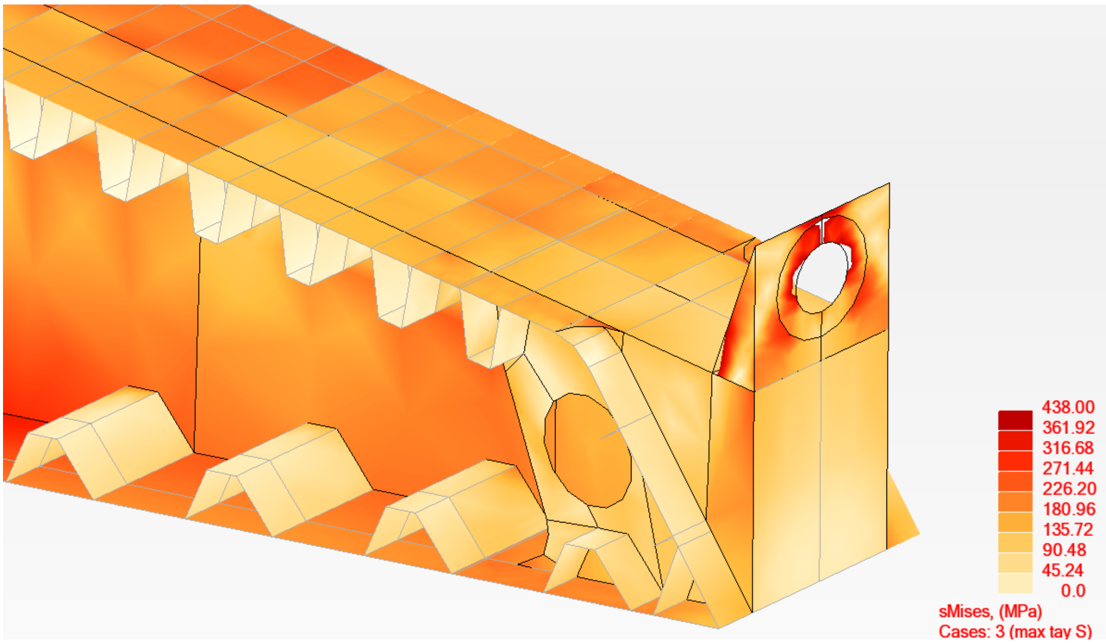


*Figure 2-92 von Mises stresses for AP1 with maximum rotations for max $\theta_S$ rotation*

### 2.4.3 Stress verification of hanger anchorage AP1

This model represents the hanger anchorage in cross girder no. 42 to 51 and 69 to 78.

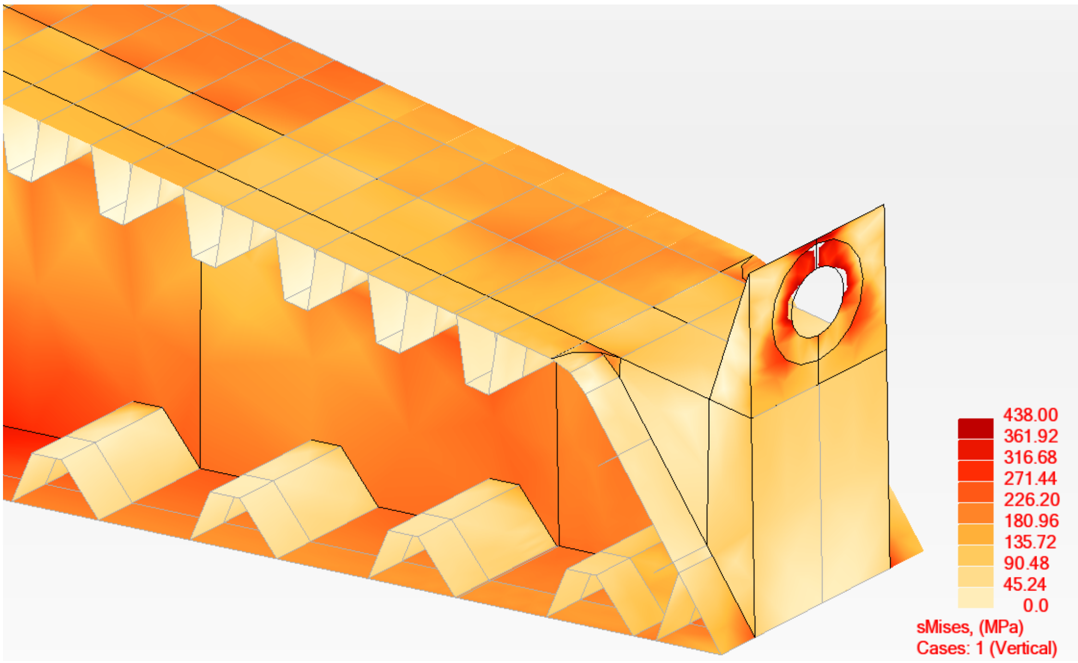


Figure 2-93 *von Mises stresses for general AP1 with vertical hanger reaction*

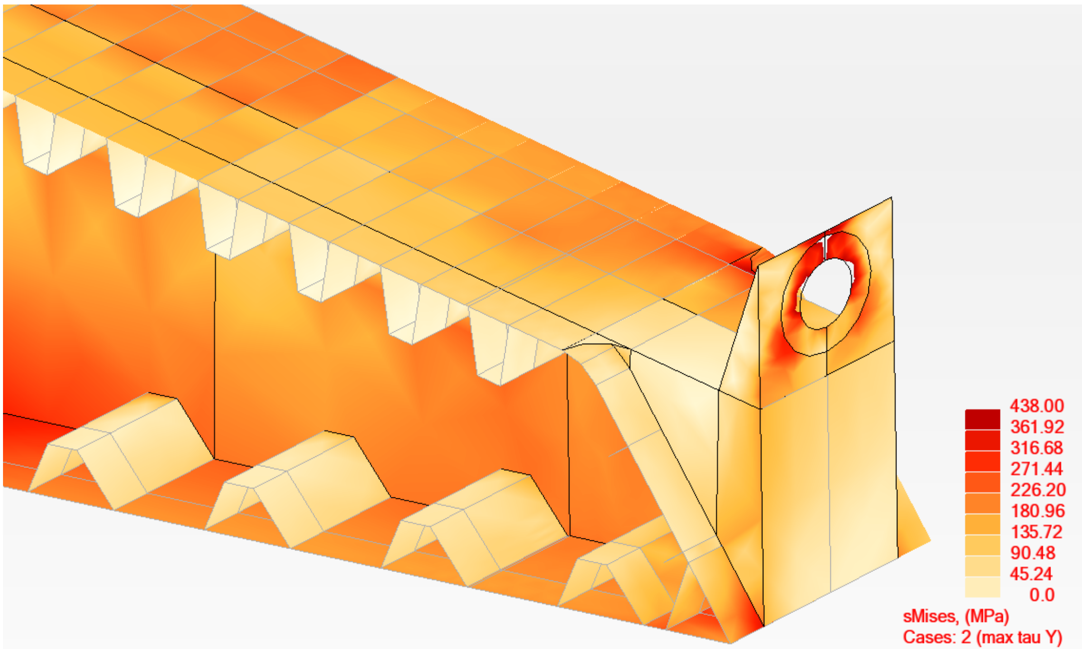


Figure 2-94 *von Mises stresses for general AP1 with max $\theta_Y$ rotation*

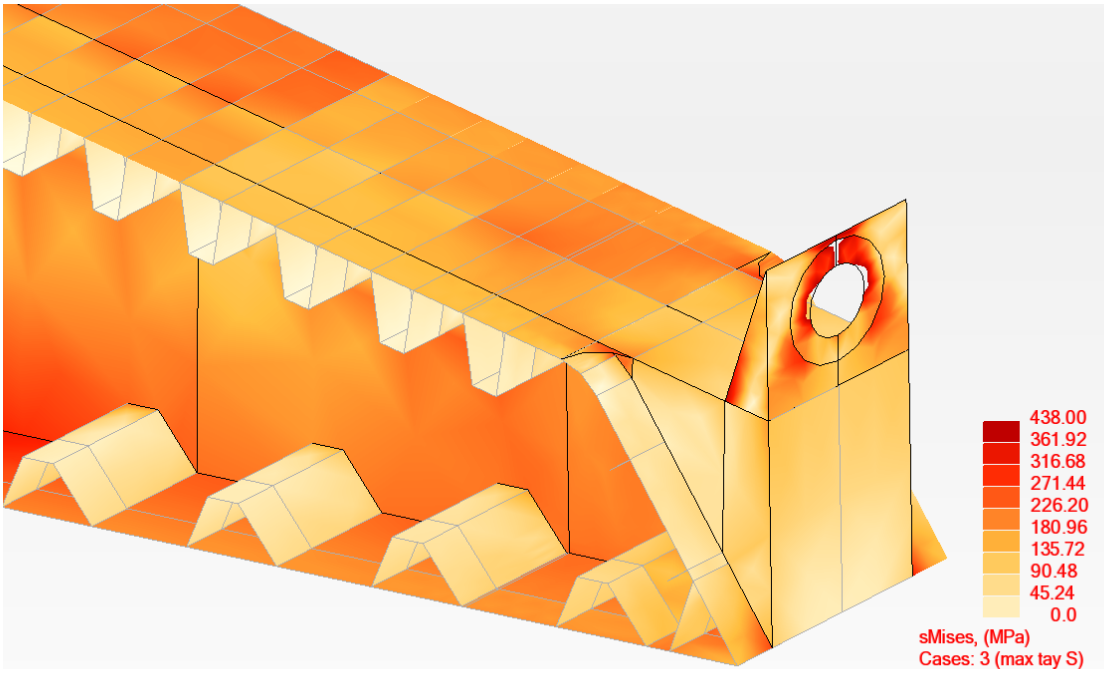


Figure 2-95 *von Mises stresses for general AP1 with max $\theta_S$ rotation*

### 2.4.4 Stress verification of hanger anchorage AP2

This model represents the hanger anchorage in cross girder no. 21 to 41 and 79 to 99.

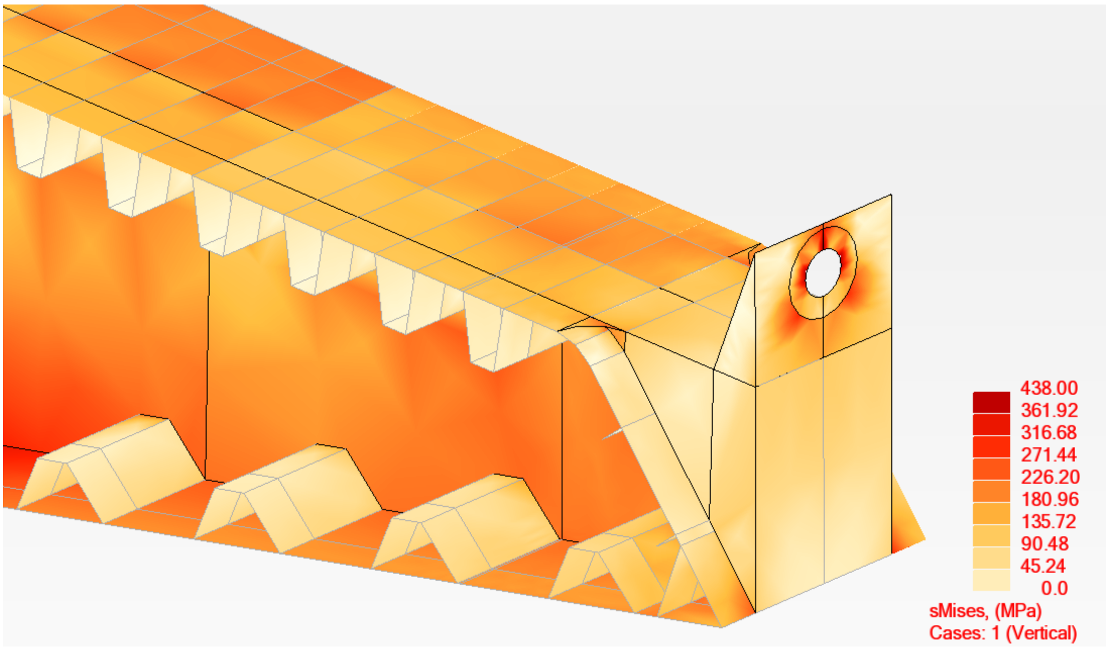


Figure 2-96 *von Mises stresses for AP2 with vertical hanger reaction*

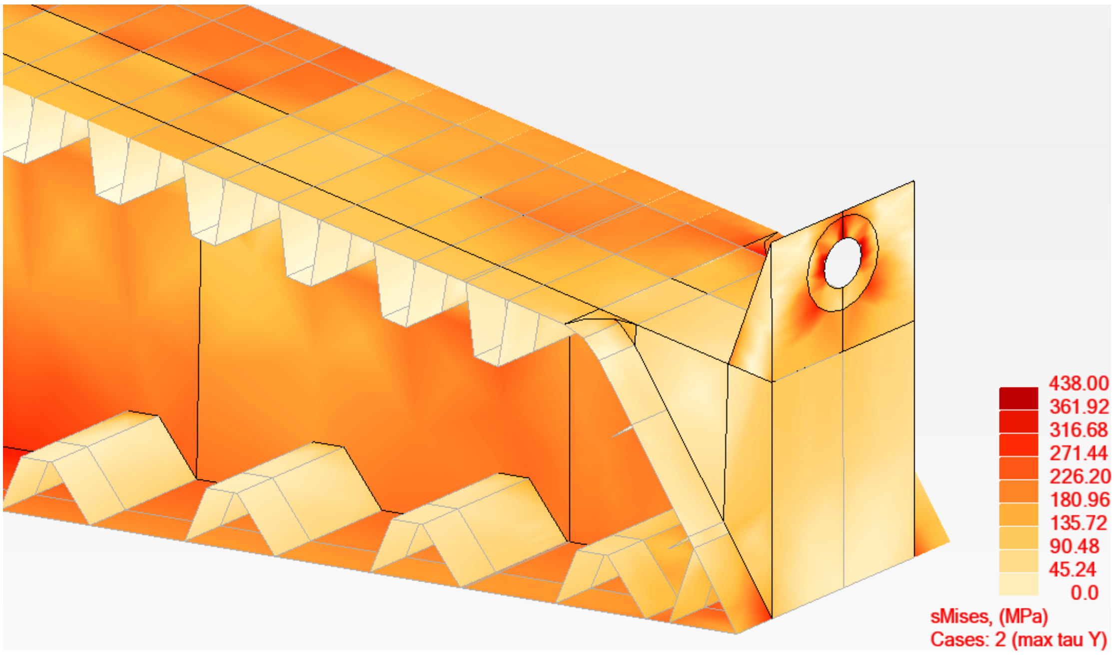


Figure 2-97 *von Mises stresses for AP2 with max $\theta_Y$ rotation*

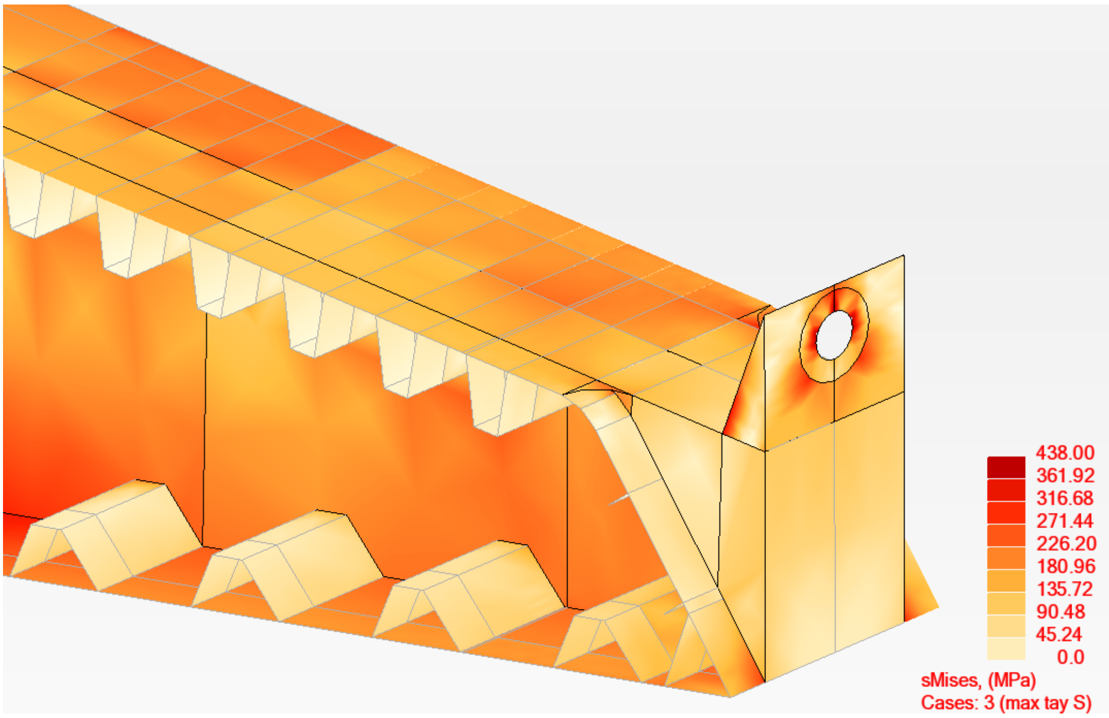


Figure 2-98 *von Mises stresses for AP2 with max $\theta_S$ rotation*

### 2.4.5 Stress verification of hanger anchorage AP3

This model represents the hanger anchorage in cross girder no. 9 to 20 and 100 to 111.

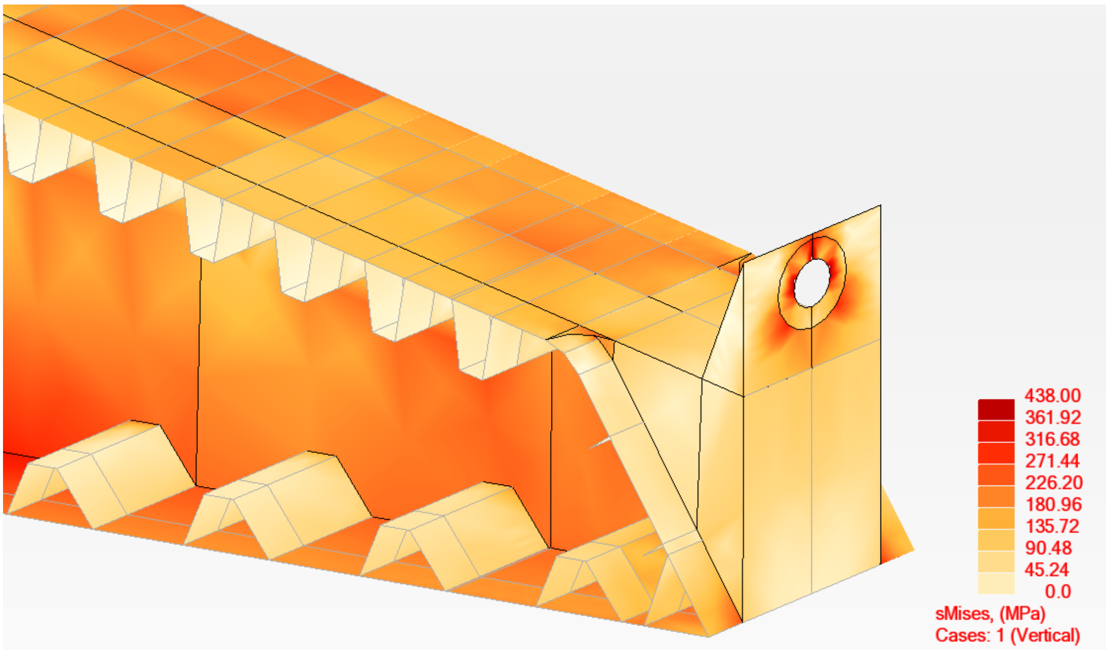


Figure 2-99 *von Mises stresses for AP3 with vertical hanger reaction*

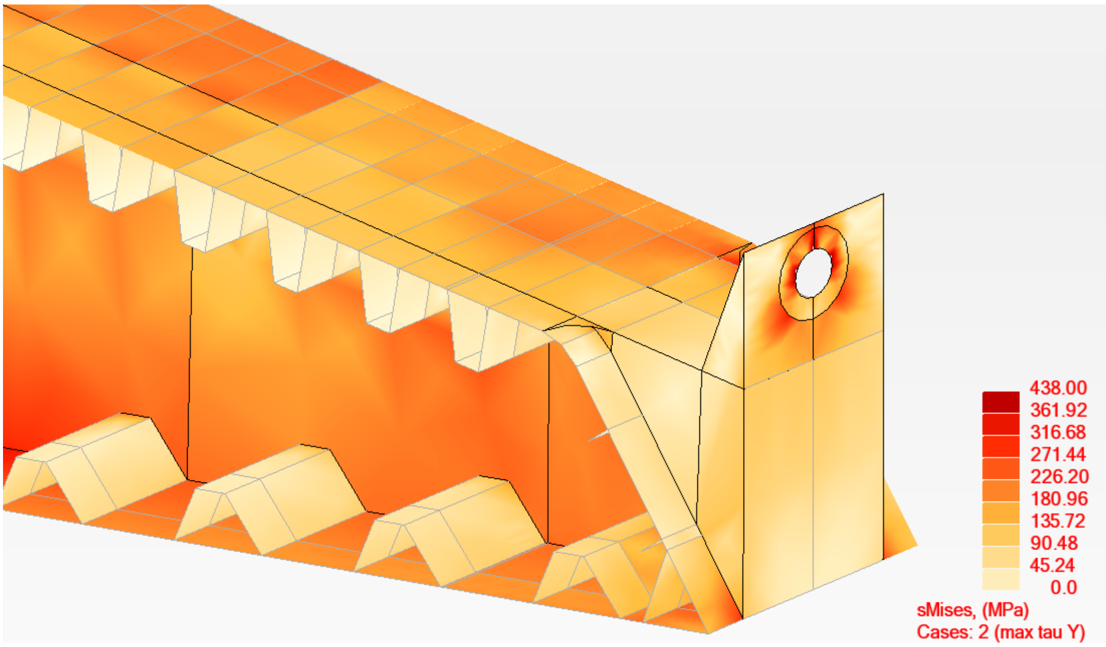


Figure 2-100 *von Mises stresses for AP3 with max $\theta_Y$ rotation*

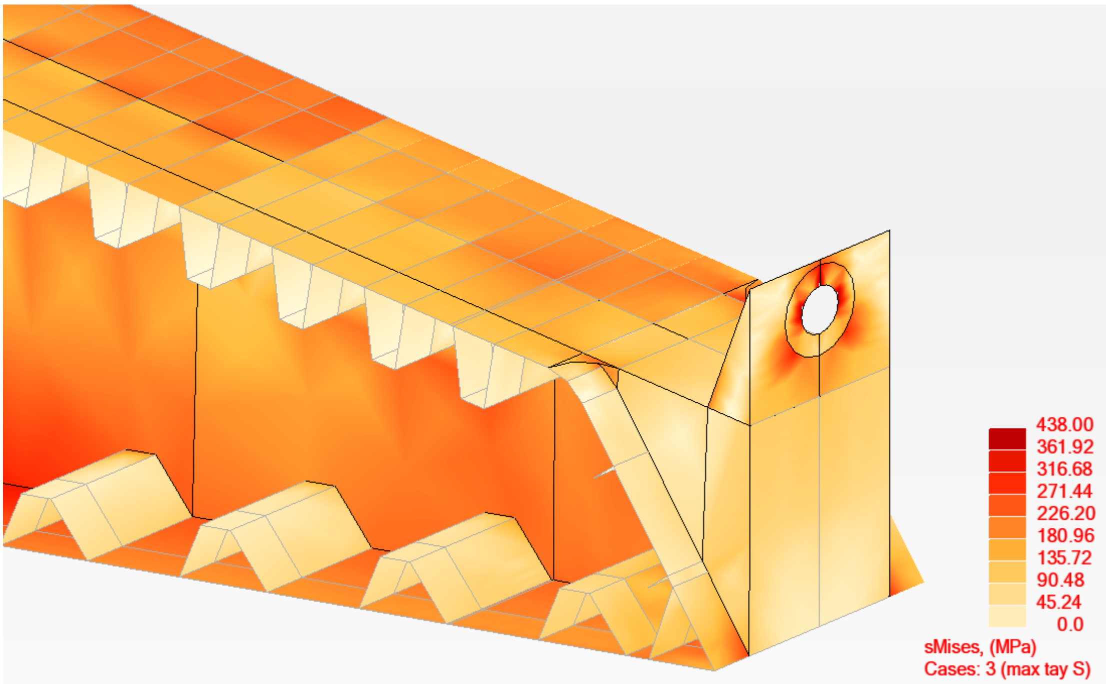


Figure 2-101 *von Mises stresses for AP3 with max $\theta_S$ rotation*